THE
PHYSICAL REVIEW
A Journal of Experimental and Theoretical Physics Established by E. L. Nichols in 1893
VOL. 52, No. 12 DECEMBER 15, 1937 SECOND SERIES

Double Scattering of Polarized X-Rays

PAUL KIRKPATRICK
Department of Physics, Stanford University, California
(Received October 8, 1937)

Formulas are derived for calculation of the intensity of twice scattered x-radiation emerging from a scattering body at 90° to an incident beam of arbitrary polarization. Spherical and cylindrical scatterers are treated, and with the latter body the cases of primary radiation incident parallel and normal to the cylinder axis are separately considered. Thomson scattering is assumed but with approximate corrections for energy losses to recoil electrons. Certain aspects of the theory are amenable to experimental testing and have been satisfactorily checked.

I. INTRODUCTION

WHEN irradiated matter gives origin to scattered x-radiation the scattered beams are invariably complex, consisting of singly scattered rays accompanied by radiation which has emerged after two or more successive deviations within the scattering matter. It is evident that the ratio of the power doubly or multiply scattered to that singly scattered will approach zero as the number of electrons in the scatterer approaches unity, but all real observations are conducted far short of this impracticable limit, so a pure singly scattered beam is an idealization.

The effects of multiple scattering upon Compton effect observations have been observed by Hulubei[1] and discussed theoretically by DuMond[2] in a paper to which later reference will be made. Appropriate corrections for such effects were applied to polarization measurements by Compton and Hagenow[3] in 1924 but have been omitted from the discussions of other experimenters in this field both before and since, through oversight or because of the undeveloped state of the theory of such effects.

The present paper presents chiefly the derivation of formulas for calculating the intensity of twice scattered radiation emerging from a scatterer at right angles to an incident beam of any degree of polarization. Spherical and cylindrical scatterers have been treated and the latter case has been carried out for two differing orientations of the cylinder relative to the incident beam. The selection of ninety degree scattering and of these particular geometric forms has been dictated jointly by the necessities for mathematically tractable expressions and for theoretical conditions applicable to polarization experiments. At the same time it is deemed that the specialization of conditions has not been such as to destroy the pertinence of these results to scattering investigations of other types and even to some problems of the medical radiologist.

[1] H. Hulubei, Comptes rendus **195**, 1249 (1932); Ann. de physique **1**, 5 (1934).
[2] J. W. M. DuMond, Phys. Rev. **36**, 1685 (1930).
[3] A. H. Compton and C. F. Hagenow, J. O. S. A. and R. S. I. **8**, 487 (1924).

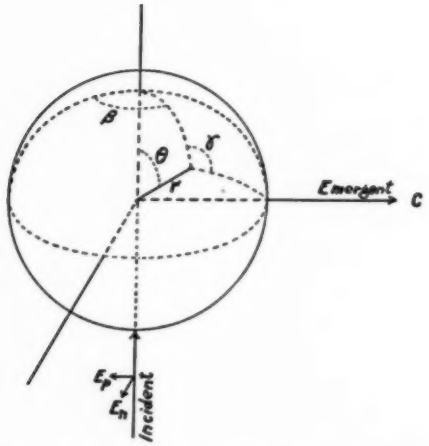

FIG. 1. Coordinate system as related to directions of incident and emergent rays with spherical scatterer.

II. THEORY OF THE SPHERICAL SCATTERER

Central primary electron

We consider first a spherical coordinate system with radius r, colatitude θ and longitude β whose origin coincides with the center of a spherical scatterer of radius L and linear absorption coefficient μ. A single electron at the origin is illuminated by plane polarized radiation propagated along the polar axis of the coordinate system in the direction $\theta=0$. The electric vector lies in the origin plane of β, and the electric intensity at the central primary electron will be designated by E_p. Subsequently the complementary polarized component, E_n, will be discussed. In either case we shall be concerned with the radiation emerging from the scatterer after being primarily scattered in a random direction by the original electron and secondarily scattered in a direction parallel to the line $\theta=\pi/2$, $\beta=\pi$ by an electron of the scattering sphere having the random position coordinates r, θ, β. The situation is illustrated in Fig. 1. In an analysis similar to that first presented by DuMond[2] we shall evaluate the electric intensity of the doubly scattered beam from two electrons at a point C distant r_3 from the origin in the designated direction of second scattering, r_3 being large as compared to L. The expression obtained will be integrated over the volume of the spherical scatterer to obtain the total double scattered intensity arising from the primary irradiation of a single electron by the given component of the incident radiation. It will be economical to speak of the electrons which scatter incident primary radiation as primary electrons, and those re-scattering the once scattered radiation as secondary electrons.

The assumption of Thomson scattering involves errors at particular angles but these errors go far toward canceling each other in cases where, as at present, integration over all scattering angles is to be performed. The integrated Thomson scattering is in error through failure to take account of the energy of recoil electrons but this defect may be approximately rectified by application of the Breit-Dirac correction factor after rather than before the integration.

E_p may be resolved into a component $E_p \cos\beta$ lying in the plane of θ, the angle of primary scattering, and a component $E_p \sin\beta$ normal to that plane. The primary scattering of these components gives rise to two components of electric intensity in the once scattered ray which at a distance r are, respectively,

$$X=E_p(M/r)\cos\beta\cos\theta,$$
$$Y=E_p(M/r)\sin\beta,$$

where $M\equiv e^2/mc^2$. The electric vector whose components are X and Y is scattered out in the direction of C (Fig. 1) by the electron at r, θ, β, but before evaluating this twice scattered intensity it is desirable to resolve the vector whose components are X and Y in directions conveniently related to the plane of the second scattering angle, θ_2. The resolved components in and normal to the plane of the second scattering angle are, respectively,

$$H=X\cos\gamma+Y\sin\gamma,$$
$$Q=X\sin\gamma-Y\cos\gamma,$$

where γ is now defined as the dihedral angle between the planes of the first and second scattering angles. The scattering of the vectorial components H and Q by the secondary electron produces doubly scattered radiation with electric components

$$R=(HM/r_3)\cos\theta_2,$$
$$S=QM/r_3,$$

and the total *radiation* intensity at C produced by the cooperation of these two electrons is measured by R^2+S^2.

In preparing these expressions for integration we eliminate undesired angles by means of the geometrical relations[4]

$$\cos\theta_2=-\sin\theta\cos\beta,$$
$$\cos\gamma=\cos\theta\cos\beta/(1-\sin^2\theta\cos^2\beta)^{\frac{1}{2}};$$

and obtain

$$S^2=0,$$
$$R^2=(E_p^2M^4/r^2r_3^2)\sin^2\theta\cos^2\beta(1-\sin^2\theta\cos^2\beta).$$

If ρ denote the volume density of electrons in the scatterer we have as the total radiation intensity at C due to scattering of E_p by the central electron and re-scattering by all other electrons of the sphere

$$\rho\int_0^L\int_0^\pi\int_0^{2\pi}(R^2+S^2)r^2\sin\theta\,dr\,d\theta\,d\beta = 8\pi\rho LM^4E_p^2/15r_3^2. \quad (1)$$

The corresponding analysis for the other incident component, E_n, follows the above procedure so closely that it may be summarized without discussion by the following parallel set of equations. The resolved components of E_n lying in and normal to the plane of θ are respectively $E_n\sin\beta$ and $E_n\cos\beta$.

$$X=E_n(M/r)\sin\beta\cos\theta,$$
$$Y=E_n(M/r)\cos\beta,$$
$$H=X\cos\gamma-Y\sin\gamma,$$
$$Q=X\sin\gamma+Y\cos\gamma,$$
$$R=(HM/r_3)\cos\theta_2,$$
$$S=(QM/r_3),$$
$$R^2=(E_n^2M^4/r^2r_3^2)(\sin^6\theta\sin^2\beta\cos^2\beta/\sec^2\beta-\sin^2\theta),$$
$$S^2=(E_n^2M^4/r^2r_3^2)\cos^2\theta/(1-\sin^2\theta\cos^2\beta).$$

Total radiation intensity at C due to scattering of E_n by the central electron and rescattering by all other electrons of the sphere is

$$\rho\int_0^L\int_0^\pi\int_0^{2\pi}(R^2+S^2)r^2\sin\theta\,dr\,d\theta\,d\beta = 12\pi\rho LM^4E_n^2/5r_3^2. \quad (2)$$

The *single* scattering arriving at C is due exclusively to E_n, and a comparison of (1) and (2) shows that the predominance of E_n persists in the *double* scattering also, since this component contributes $4\frac{1}{2}$ times as much as does E_p. The expressions (1) and (2) enable the calculation of the double scattering from an unpolarized or partly polarized beam since in scattering problems such beams may be represented by two mutually incoherent and perpendicular plane polarized components of suitable intensity.[5] This extension is directly applicable only in case either the maximum or minimum electric vector of the partially polarized beam lie in the plane AOC, but in other cases the computation may be achieved with only very slight inaccuracy in the following way.

The expressions (1) and (2) may be regarded as statements of the double scattered intensity issuing from a single plane polarized vector in the end-on and broadside directions, so to speak. No considerable error can result from an assumption that for intermediate directions the double scattered intensity distribution is elliptical. This assumption takes the place of a complicated and perhaps impossible series of integrations and makes the polarization orientation of the incident beam a matter of indifference since the double scattered contributions resulting from its components may readily be separately computed under the elliptical assumption.

For the special case of unpolarized incident radiation, the case with which DuMond[2] was concerned, we put $E_p=E_n$ and add (1) and (2) obtaining for the total double scattered radiation intensity $44\pi\rho LE_n^2M^4/15r_3^2$. This may be compared to the *single* scattered intensity, which is entirely due to E_n and has the magnitude $E_n^2M^2/r_3^2$. The ratio of double to single scattering is then $(44/15)\pi\rho LM^2$, which is identical with DuMond's Eq. (29) when the latter is evaluated for 90° scattering.

Effect of absorption

The ratio of double to single scattering as just given requires correction for the effects of absorption in the scatterer. The proportional effect of absorption of the *entering* ray upon the intensity measured at C is approximately the same whether the final intensity results from single scattering or from double, and this is also true of the emergence segment. In the double scattering case, however, the ray between the

[4] The derivation of relations of this kind is carried out in more detail and with illustrative figures in DuMond's paper, reference 2.

[5] See for example Kirkpatrick, Phys. Rev. **29**, 632 (1927).

two electrons suffers from an absorption which has no counterpart in the single scattering case, and this absorption we now determine. Evidently it suffices to multiply the values of R^2 and S^2 by $e^{-\mu r}$ before integration, an operation which attaches a factor $(1-e^{-\mu L})/\mu L$ to the right members of each of the equations (1) and (2). These amended expressions will be used in the next section.

Eccentric primary electrons

Up to this point only the central electron of the sphere has been considered illuminated by the primary radiation. The irradiation of any other single electron would produce a doubly scattered beam not profoundly different from that just calculated but necessarily somewhat weaker because of the increased distances between primary and secondary electrons. To a good approximation the intensities of the doubly scattered beams resulting from the primary irradiation of differently located electrons within the scatterer will be proportional respectively to $\sum 1/p^2$, where p is the distance from the primarily irradiated electron to any other electron, the summation extending over the entire scatterer. Relative to the central electron we have readily $\sum 1/p^2 \equiv \sum 1/r^2 = 4\pi\rho L$, while for an electron situated at $r=s$ it may be shown that

$$\sum 1/p^2 = 2\pi\rho L + [\pi\rho(L^2-s^2)/s] \log (L+s/L-s).$$

Then if J represents the double scattered intensity resulting from the irradiation of a single central electron (as formulated in Eqs. (1) and (2)) we have for the intensity doubly scattered as a result of the primary irradiation of a volume element dV at r the following expression:

$$J\rho/4L[2L+(L^2+r^2/r) \log (L+r/L-r)]dV.$$

Integration of this expression over the sphere yields $\pi\rho JL^3$ as the total doubly scattered intensity when the entire sphere is bathed in primary radiation. Since the total number of electrons present is $(4/3)\pi\rho L^3$ it appears that the average yield of doubly scattered radiation per primary electron is $\frac{3}{4}J$, a conclusion which was also reached by DuMond[2] by a different argument.

The double scattering which results from irradiation of a single eccentric primary electron is not only weaker than that deriving from the central primary but it possesses a different distribution in space. However, nonmathematical inspection and a certain amount of numerical checking indicates that symmetrically disposed primary electrons tend to balance off each other's individual asymmetries and produce in cooperation spatial distributions of doubly scattered radiation differing but slightly from that of the central primary.

From the present section and the two preceding we have the conclusion that the ratio of doubly to singly scattered intensity when x-rays of any degree of polarization are scattered through 90° by a spherical scatterer is

$$(\pi\rho M^2/5\mu)(1-e^{-\mu L})(2P+9), \qquad (3)$$

where $P=(E_p/E_n)^2$ is a measure of the polarization of the incident radiation.

This conclusion and others above concerning intensity find their best application to cases wherein the scattering is predominantly unmodified. For modified scattering the intensity expressions should be multiplied before integration by the Breit-Dirac factor $(1+(h\nu/mc^2)$ vers. $\phi)^{-3}$, where ϕ is the angle of scattering, but such treatment renders the integrands so discouragingly complicated that we have effected a first approximation to this usually small correction by applying the factor to the integrals instead of to the integrands, putting $\phi=90°$. The Breit-Dirac factor applies twice to double scattering expressions and only once in the case of single scattering, so the net effect upon (3) is to multiply it by $(1+\alpha)^{-3}$, where $\alpha=h\nu/mc^2$.

III. Theory of the Cylindrical Scatterer

Side irradiation

Figure 2 sufficiently illustrates the system of cylindrical coordinates appropriate to this case and the orientation of the incident and emergent rays in this system. The axis of the scatterer coincides with the axis of the coordinate system but it is not required that the scatterer be situated symmetrically with respect to the origin or even that it include the origin. Let the radius of the scatterer be L and the y coordinates of its ends be Y_2 and Y_1. Considering first E_p, the

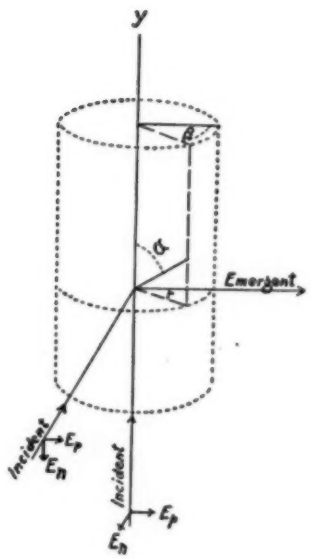

FIG. 2. Coordinate system as related to directions of incident and emergent rays with cylindrical scatterer.

electric intensity of that component of the incident beam which lies in a plane containing the emergent ray, we regard it as being scattered by a single electron at the origin of the coordinate system and the resulting radiation as being rescattered in the emergent direction by an electron at r, y, β. The distance separating these electrons is $r_2=(r^2+y^2)^{\frac{1}{2}}$. The plane containing the y axis and the second electron will be called, for brevity, the β plane. θ_2 is the second scattering angle and γ is the dihedral angle between the β plane and the plane of θ_2. The meaning of α is apparent from Fig. 2.

E_p is decomposed into a component $E_p \cos\beta$ parallel to the β plane and a component $E_p \sin\beta$ perpendicular to the β plane. That the plane containing these components is not normal to the direction of propagation need cause no concern.

Proceeding as in the case of the sphere but neglecting absorption we have the following results.

Electric intensity at secondary electron:

Component in β plane $\equiv X$
$= E_p(M/r_2)\cos\beta\cos\alpha,$

Component normal to β plane $\equiv Y$
$= E_p(M/r_2)\sin\beta,$

Component in second scattering plane $\equiv H$
$= Y\sin\gamma - X\cos\gamma,$

Component normal to 2nd scat plane $\equiv Q$
$= Y\cos\gamma + X\sin\gamma.$

Angular relations:

$\cos\theta_2=\sin\alpha\cos\beta,$
$\cos\gamma=(-\cos\alpha\cos\beta)/(1-\sin^2\alpha\cos^2\beta)^{\frac{1}{2}}.$

Electric intensity components at distance r_3:

In second scattering plane; $R=(HM/r_3)\cos\theta_2$
Normal to second scattering plane;
$S=(QM/r_3)=0.$

We have therefore

$$R^2=(M^4E_p^2/r_2^2r_3^2)\sin^2\alpha\cos^2\beta(1-\sin^2\alpha\cos^2\beta),$$

in which r_2 may be replaced through a relation given above and $\sin^2\alpha=r^2/(r^2+y^2)$. Using these substitutions we obtain the total doubly scattered radiation intensity resulting from the incidence of E_p at a distance r_3 by integrating ρR^2 over the volume of the cylinder.

$$\rho\int_0^L\int_{Y_1}^{Y_2}\int_0^{2\pi} R^2 r\,dr\,dy\,d\beta$$

$$=\frac{\pi\rho E_p^2M^4}{8r_3^2}\left[Y_2\log\left(1+\frac{L^2}{Y_2^2}\right)-Y_1\log\left(1+\frac{L^2}{Y_1^2}\right)\right.$$
$$+\frac{7}{4}L\tan^{-1}\frac{Y_2}{L}-\frac{7}{4}L\tan^{-1}\frac{Y_1}{L}$$
$$\left.+\frac{3L^2Y_2}{4(L^2+Y_2^2)}-\frac{3L^2Y_1}{4(L^2+Y_1^2)}\right]. \quad (4)$$

Inasmuch as the application of formulas deduced in this paper must often be to scatterers which do not precisely conform to the ideal geometry assumed in theory it is comforting to note that the predicted double scattering for a sphere and for an equivalent cylinder are only very slightly different. If (4) be evaluated for a cylinder whose length is equal to its diameter with a centrally located primary electron the resulting doubly scattered intensity differs by less than one percent from the prediction of (1) for a sphere of the same volume. It seems safe to suppose that the double scattering from a cube of the same volume would not differ importantly from these results.

The component E_n of the primary beam lies in the β plane and has an electric intensity $E_n(M/r_2)\sin\alpha$. Continuing the use of symbols employed above we have

$$H=E_n(M/r_2)\sin\alpha\cos\gamma, \quad R=(HM/r_3)\cos\theta_2,$$
$$Q=E_n(M/r_2)\sin\alpha\sin\gamma, \quad S=QM/r_3,$$

$$\rho\int(R^2+S^2)dV=(M^4E_n^2\rho/r_3^2)\int_0^L\int_{Y_1}^{Y_2}\int_0^{2\pi}\sin^2\alpha$$
$$\times(1-\cos^2\alpha\cos^2\beta)(r/r_2^2)dr\,d\beta\,dy$$
$$=\frac{\pi\rho M^4E_n^2}{r_3^2}\left[Y_2\log\left(1+\frac{L^2}{Y_2^2}\right)-Y_1\log\left(1+\frac{L^2}{Y_1^2}\right)\right.$$
$$\left.+\frac{7}{8}L\tan^{-1}\frac{Y_2}{L}-\frac{7}{8}L\tan^{-1}\frac{Y_1}{L}\right.$$
$$\left.-\frac{L^2Y_2}{8(L^2+Y_2^2)}+\frac{L^2Y_1}{8(L^2+Y_1^2)}\right]. \quad (5)$$

It has not been found possible to extend (4) and (5) to the practical case of primary irradiation of all electrons in the cylinder by the devices which served in the treatment of the spherical scatterer. However, extension to an axial column of primaries is achieved without difficulty by integration of (4) and (5) with respect to y and yields for radiation of arbitrary polarization the result:

$$\frac{\pi^2\rho^2(\Delta r)^2M^4E_n^2}{16r_3^2}\left\{\left[(D-b)^2\log\left(1+\frac{L^2}{(D-b)^2}\right)-(U-b)^2\log\left(1+\frac{L^2}{(U-b)^2}\right)\right.\right.$$
$$\left.-(D-a)^2\log\left(1+\frac{L^2}{(D-a)^2}\right)+(U-a)^2\log\left(1+\frac{L^2}{(U-a)^2}\right)\right](8+P) \quad (6)$$
$$\left.+\frac{7L}{2}\left[(D-b)\tan^{-1}\frac{D-b}{L}-(U-b)\tan^{-1}\frac{U-b}{L}-(D-a)\tan^{-1}\frac{D-a}{L}+(U-a)\tan^{-1}\frac{U-a}{L}\right](4+P)\right\}.$$

This expresses the doubly scattered radiation intensity at a point distant r_3 from the scatterer for 90° deviation of a beam of radiation of polarization $P=(E_p/E_n)^2$. The primary electrons occupy a cylinder of radius Δr and axial length from $y=a$ to $y=b$. The secondary electrons occupy a cylinder of radius L and axial length from $y=D$ to $y=U$.

For the important special case in which the cylinder of primary electrons is axially coextensive with the secondary column (6) becomes

$$\frac{\pi^2\rho^2(\Delta r)^2M^4E_n^2}{16r_3^2}\left[2h^2(8+P)\log\left(1+\frac{L^2}{h^2}\right)\right.$$
$$\left.+7hL(4+P)\tan^{-1}\frac{h}{L}\right], \quad (7)$$

in which $h=U-D$, the length of the cylinder.

If we put $\Delta r=L$ in (6) and (7) these equations express upper limit values of double scattering when the entire cross section of the cylinder receives primary radiation. The errors of these values, consequent upon this drastic extension of a differential quantity, depend greatly upon the dimensions of the cylinder but are typically of the order of several percent.

In some applications it is desired to know the intensity of 90° double scattering from two bodies, one of which alone is illuminated by the primary radiation. The singly scattered radiation from this body impinges upon the other, which thereby becomes a source of doubly scattered radiation. A point of interest concerning this kind of double scattering is that it can be observed and measured, whereas in the other cases discussed there is an overwhelming adulteration of singly scattered radiation.

Let the two scattering bodies be two short coaxial cylinders or disks separated by a distance y and having a common radius L and a common thickness Δy. That part of the double scattering which results from the primary action of a single central electron of the first disk is given by (4) and (5). Following the argument advanced in Section II we now make the approximately correct assertion that the ratio of the total double scattered intensity to the intensity given by (4) and/or (5) is the ratio of $\sum\sum 1/p^2$ to $\sum 1/p_0^2$. The single summation signifies the sum

of the inverse squares of distances from the central primary electron to the several secondary electrons, and has the value $\pi\rho \log (1+b)\Delta y$, where $b=L^2/y^2$. The double summation sums the inverse squares of *all* interelectronic distances separating a primary from a secondary electron.

Except when $b\gg 1$ it is found that

$$\Sigma\Sigma\frac{1}{p^2}\Big/\Sigma\frac{1}{p_0^2}=\pi\rho y^2\,dy\,f(b)/\log(1+b), \quad (8)$$

where

$$f(b)=b\log(1+b)+\frac{b(2b+1)}{(b+1)^2}\log\frac{1+(4b+1)^{\frac{1}{2}}}{2}-\frac{b+1}{4}+\frac{(5b+2)(4b+1)^{\frac{1}{2}}}{6(b+1)^2}-\frac{1+8b+5b^2}{12(b+1)}-\frac{b^2}{6(b+1)^2}.$$

A calculation of doubly scattered intensity by Eqs. (6), (7), and (8) is required in Section IV.

Axial irradiation

Consider the scatterer of Fig. 2 to receive radiation propagated in a direction parallel to the axis of the cylinder. That component of electric intensity (E_p) which lies in the direction of the emergent scattered rays will, according to the Thomson scattering formula, produce scattering effects identical with those produced by the E_p component of a primary beam incident normally to the axis of the cylinder. This case has been considered and the results, for a single axial primary electron, embodied in Eq. (4).

The other component of the axial incident beam (E_n in Fig. 2) may be resolved into a component $E_n \sin\beta$ in the plane of the first scattering angle and a component $E_n\cos\beta$ normal to that plane. Succeeding steps yield the following results:

Electric intensity components at secondary electron:

In first scattering plane,

$$X=E_n(M/r_2)\sin\beta\cos\theta,$$

Normal to first scattering plane,

$$Y=E_n(M/r_2)\cos\beta,$$

In second scattering plane,

$$H=X\cos\gamma+Y\sin\gamma,$$

Normal to second scattering plane,

$$Q=X\sin\gamma-Y\cos\gamma.$$

Angular relations for eliminating θ_2 and γ:

$$\cos\theta_2=\sin\theta\cos\beta,$$
$$\cos\gamma=-\cos\theta\cos\beta/(1-\sin^2\theta\cos^2\beta)^{\frac{1}{2}}.$$

Electric intensity components at distance r_3:

In second scattering plane,

$$R=(HM/r_3)\cos\theta_2,$$

Normal to second scattering plane,

$$S=(M/r_3)Q.$$

R^2 and S^2 have identically the forms given in Eq. (1) for the sphere, but the integrals are entirely different since the formulation of the volume element introduces a different function of the variables. Upon integrating we have

$$\rho\int_0^L\int_{Y_1}^{Y_2}\int_0^{2\pi}(R^2+S^2)r\,dr\,dy\,d\beta$$
$$=\frac{\pi\rho E_n^2M^4}{8r_3^2}\left[3Y_2\log\left(1+\frac{L^2}{Y_2^2}\right)-3Y_1\log\left(1+\frac{L^2}{Y_1^2}\right)+\frac{45}{4}L\tan^{-1}\frac{Y_2}{L}-\frac{45}{4}L\tan^{-1}\frac{Y_1}{L}+\frac{L^2Y_2}{4(L^2+Y_2^2)}-\frac{L^2Y_1}{4(L^2+Y_1^2)}\right]. \quad (9)$$

This is the total doubly scattered radiation intensity at a distance r_3 from the scatterer resulting from the irradiation of a single electron at the origin by the primary component E_n. As in (4) the longitudinal extent of the scatterer is from $y=Y_1$ to $y=Y_2$.

When Eqs. (4) and (9) are each multiplied by $\pi\rho(\Delta r)^2dy$ and integrated with respect to y between the limits given, the combination of the two results gives the radiation intensity of 90° double scattering of axially incident radiation whose polarization is $P=E_p^2/E_n^2$. The primary electrons in this case occupy a cylinder of radius Δr and length from $y=a$ to $y=b$ and the secondary electrons occupy a cylinder of radius L and length from $y=D$ to $y=U$. This intensity is

$$\frac{\pi^2\rho^2(\Delta r)^2M^4E_n^2}{8r_3^2}\{\tfrac{1}{2}(P+3)\varphi_1+(L/4)(7P+45)\varphi_2+4L^2\log\varphi_3\},$$

where φ_1, φ_2, and φ_3 are functions of the dimensions of the scattering volumes defined by

$$\varphi_1=(D-b)^2\log\left(1+\frac{L^2}{(D-b)^2}\right)-(U-b)^2\log\left(1+\frac{L^2}{(U-b)^2}\right)$$
$$-(D-a)^2\log\left(1+\frac{L^2}{(D-a)^2}\right)+(U-a)^2\log\left(1+\frac{L^2}{(U-a)^2}\right),$$

$$\varphi_2=(D-b)\tan^{-1}\frac{D-b}{L}-(U-b)\tan^{-1}\frac{U-b}{L}-(D-a)\tan^{-1}\frac{D-a}{L}+(U-a)\tan^{-1}\frac{U-a}{L},$$

$$\varphi_3=\frac{(L^2+(U-b)^2)(L^2+(D-a)^2)}{(L^2+(U-a)^2)(L^2+(D-b)^2)}.$$

This general result of course includes the simple case in which the primary and secondary volumes are coextensive.

Previous remarks about the use of the approximation $\Delta r=L$ are in effect here.

IV. Measurement of Double Scattering in a Cylinder

In view of the considerable number of approximations used in the foregoing derivations, any possible experimental confirmation will be valuable. Satisfactory general methods for making such measurements are not known but important parts of the foregoing theory have been checked by observing the double scattering in a paraffin cylinder 5.5 cm long and 1.75 cm in radius, using the arrangement shown in Fig. 3. Effectively unpolarized x-rays from a tungsten target with cathode stream at 45° to the plane of scattering passed through an absorbing grid which permitted the irradiation of uniformly spaced layers of the cylinder. A similar grid interposed between the scatterer and an ionization chamber passed to the chamber only scattered rays which had originated in *unirradiated* layers of the scatterer and which must therefore have arisen from plural scattering. Intensities thus scattered were compared with the total singly and multiply scattered intensities observed upon removal of the grids.

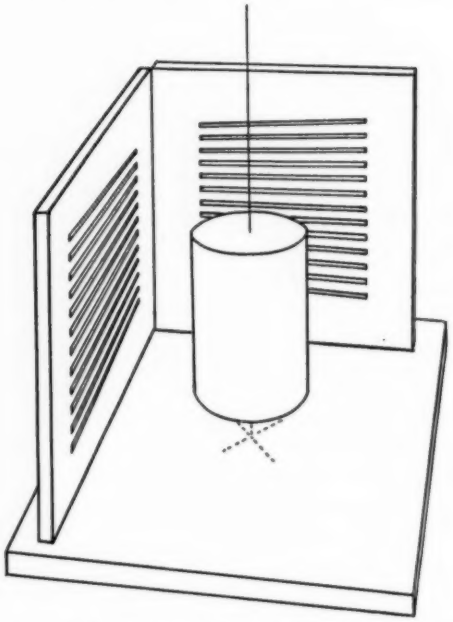

Fig. 3. Cylindrical scatterer in position relative to incidence and emergence grids for measurement of double scattering.

Theory

The primary scattering at 90° is due solely to the E_n component of the incident rays and has, to a first approximation, the Thomsonian intensity $E_n^2M^2\rho V/r_3^2$, where V is the volume of the scatterer. This requires correction for absorption which is roughly achieved by multiplication by $e^{-\mu L}$, and correction for energy lost to recoil electrons, accomplished by application of the factor $J+1/[J+(1+\alpha)^3]$ where J is the ratio of unmodified to modified scattered intensity for the adopted wave-length, scattering material and angle of scattering.

Since the absorption and recoil corrections vary oppositely with variation of incident wave-length their product is not very sensitive to such variation and so neither monochromatization nor precise knowledge of wave-lengths employed is necessary. The wave-length 0.3A has been assumed and the linear absorption coefficient in paraffin taken to be 0.19 per cm.

The radiation observed without the grids contains also a doubly scattered ingredient which may be calculated from Eq. (7) by putting $r=L$, $P=1$, and $h/L=3.17$. Correction factors for absorption and recoil losses are obtained by squaring those applied in the single scattering case. This is equivalent to assuming that the effective path in the scatterer is $2L$ and that 90° is a proper effective scattering angle to represent both primary and secondary scattering for the purposes of this correction.

The radiation observed with the grids is calculated as explained in Section III for the case of double scattering by co-axial disks. For each primarily irradiated section as many as six emergence slots pass appreciable doubly scattered radiation. All such calculated contributions, corrected as in the preceding paragraph, are combined to give the total measurable radiation. Traces of higher order scattering will be present in the observed radiation both with and without the grids but no calculation of such intensities has been made.

Results

The calculated ratio of observable intensities without and with the grids, carried through as outlined above, is 47. The ratio as observed was 44 at an x-ray tube potential of 40 kv, 46 to 50 kv, and 44 at 60 kv, the agreement being somewhat closer than might reasonably have been expected.

The methods of calculation outlined in this paper will subsequently be utilized for the correction of conclusions now in print concerning the polarization of primary x-rays, and for the interpretation of experiments in progress. The author is greatly indebted to Mr. Keith Harworth for assistance in the experimental part of this investigation.

DECEMBER 15, 1937 PHYSICAL REVIEW VOLUME 52

Preliminary Analysis of the First Spark Spectrum of Cerium—Ce II

WALTER E. ALBERTSON AND GEORGE R. HARRISON
George Eastman Laboratory of Physics, Massachusetts Institute of Technology, Cambridge, Massachusetts

(Received November 5, 1937)

By applying the spectral interval sorter and a newly designed interval recorder to new data obtained with the automatic recording spectrum comparator on the M.I.T.-W.P.A. wavelength program, a preliminary term array for Ce II has been set up in which 584 lines have been accounted for as transitions between 31 lower and 51 upper states. The term diagram is found to be the most complex yet observed for a three-electron spectrum. Both configurations $4f5d6s$ and $4f5d^2$ appear to be low in Ce II, contrary to the analysis of Haspas. Most of the differences between observed wave numbers and those computed from the term array are less than 0.02 cm^{-1}, and 60 percent of the lines are found to be consistent to within 0.002A. Several of the term assignments have been checked with partially resolved Zeeman patterns recorded by King and Albertson, and the absolute J values have been determined by this means. An inclusive description of the spectra of the cerium atom is being undertaken in the range 10,000 to 1000A.

THAT the spectra emitted by rare earth atoms would be unusually difficult to analyze has been expected by spectroscopists for some time, but fortunately a number of these atoms whose spectra are so complex emit outstanding groups of lines. By attacking such lines the beginnings of term arrays have been constructed in a number of cases.[1] Cerium (58), the first element of the rare earth group, which is of unusual interest spectroscopically because of its position in the periodic table, presents no such suggestive features for attack. When we made

[1] Sm I, Sm II, W. E. Albertson, Phys. Rev. **47**, 370 (1934); Astrophys. J. **84**, 26 (1936). Eu I, Eu II, H. N. Russell and A. S. King, Phys. Rev. **46**, 1023 (1934); W. E. Albertson, Phys. Rev. **45**, 499 (1934). Gd I, W. E. Albertson, Phys. Rev. **47**, 370 (1934). Yb I, Yb II, W. F. Meggers and H. N. Russell (see C. E. Moore, *Term Designations for Excitation Potentials* (Princeton, N. J., 1934)). Lu I, Lu II, Lu III, W. F. Meggers and B. G. Scribner, Nat. Bur. Stand. J. Research **5**, 73 (1930).

preliminary attempts to analyze Ce I and Ce II several years ago[2] we came to the conclusion that more precise wave-length values, or more highly resolved Zeeman patterns, or both, would be required before the term arrays of these spectra could successfully be unravelled.

A comprehensive resurvey of the cerium spectrum was then undertaken, and with the improved wave-length values so obtained we have developed a quadratic array for Ce II which in its present status accounts for 584 lines, including a majority of the stronger lines, as transitions between 31 lower and 51 upper states. This array is of special interest because it shows a new order of complexity in three-electron spectra. For example, about 700 lines due to Ti II are known, whereas more than 3000 lines have already been ascribed to Ce II on the basis of studies not yet complete. The difficulty of starting a term array is now explained, since we find more than two dozen low energy levels within 6000 cm^{-1} of the lowest, while Fe I, for example, shows only five levels in the same range.

Haspas[3] has published a term array for Ce II with which we can find no point of agreement. He assigns 430 lines to 137 states, and the deviation between his observed and calculated wave numbers (O−C) is sometimes as great as 0.70 cm^{-1}, which he justifies on the basis that the wave-lengths used, as measured by different observers, disagreed among themselves by as much as 0.3A. Haspas' average value of (O−C) for his lines is over 0.2 cm^{-1}, while our average is something under one-tenth this, as discussed below.

We calculate the probability of finding by accident a solid array of even four columns and 10 rows with the tolerance which we have used as being less than one in a million, starting with any random interval and the actual density of Ce II lines. If the tolerance were doubled the probability would increase to 1 in 10. With the use of Haspas' tolerance, ten times ours, such chance arrays become very numerous in a spectrum so complex.

The present note illustrates the application of the spectral interval sorter[4] and the spectral interval recorder[5] to the analysis of a complex term array, where the combination principle has little power for analysis unless precise wave-lengths are available. Our results also show the internal consistency to be expected of wave-length values obtained by means of the automatic recording comparator[6] in the program undertaken in this laboratory, with the assistance of the Works Progress Administration, on a systematic resurvey of atomic spectra.

Procedure

A revised master-list of all known Ce II lines in the range 5500–2850A was prepared, using the M.I.T.-W.P.A. wave-length values. The wave numbers of all lines on this list were then punched on a tape for the interval recorder, using a scale of 7.5 mm per cm^{-1}. A similar tape was then prepared for the interval sorter, containing only the 337 strongest lines, to cut down the probability of accidental coincidences.[4] No quadratic arrays grew from the intervals which were shown by the machine to occur most frequently, so the 700 strongest lines were punched on the tape. From this tape were recorded all intervals in the range 57 to 1000 cm^{-1}, in four settings covering 300 cm^{-1} each. The most probable number of chance occurrences of any specified interval within a tolerance of ± 0.10 cm^{-1} was calculated to be about 10, but many intervals were found occurring on the developed chart from 14 to 20 times. The interval recorder was then set for each of these highly recurrent intervals in turn, and with it all pairs of lines in the master list which gave these intervals to within ± 0.10 cm^{-1} were automatically recorded. With the intervals thus determined a quadratic array was set up which was soon demonstrated to be valid by the ease and precision with which other intervals found from the record fitted into it.

Once a quadratic array has been started, both its validity and the mutual consistency of the wave-length values used can be tested by calculation of the differences (O−C) mentioned

[2] G. R. Harrison and W. E. Albertson, Phys. Rev. **45**, 289 (1934).
[3] K. Haspas, Zeits. f. Physik **96**, 410 (1935).
[4] G. R. Harrison, Rev. Sci. Inst. **3**, 753 (1932); Rev. Sci. Inst. **4**, 581 (1933).
[5] To be described elsewhere shortly.
[6] G. R. Harrison, J. Opt. Soc. Am. **25**, 169 (1935).

TABLE I. *Difference between observed and computed wave numbers for lines measured on M.I.T.–W.P.A. program.*

(O−C) ± cm^{-1}	PERCENT IN RANGE	TOTAL PERCENT
0.00	20.7	20.7
.01	28.8	49.5
.02	23.3	73.0
.03	11.9	84.9
.04	6.6	91.5
.05	4.1	95.6
.06	2.5	98.1
.07	.9	99.0
.08	.6	99.6

above. From Table I it will be seen that our average value of (O−C) is somewhat under 0.02 cm^{-1}, and the agreement is such as to indicate that over 60 percent of the wave-length values used are mutually consistent to within 0.002A.

Our wave-length data were supplemented by King's temperature classification of the 337 strongest lines.[7] Partially resolved Zeeman patterns for both the *n* and *p* components in the range 3750–2900A were also made available to us through the kindness of Drs. A. S. and R. B. King. In addition, *n* components for the range 4700–3850A were photographed by A. S. King and one of us (W. A.), who desires to record here his thanks to the National Research Council for the award of a fellowship which made this work possible. These cerium Zeeman effect plates were taken in the physical laboratory of the Mt. Wilson Observatory in Pasadena, using a 15 ft. concave grating and a large Weiss electromagnet.

While the Zeeman patterns were not sufficiently resolved to enable this powerful means of starting a term analysis to be used, our application of the combination principle, together with the selection principle for inner quantum numbers, served to determine the relative *J* values of the terms. Several of the patterns were sufficiently resolved to rule out certain *J* values, and by this means the absolute scale for *J* was determined. The partially resolved pattern types served also to check our assignments in a number of cases, with very satisfactory agreement.

TERM ANALYSIS OF CE II

Various considerations indicate that the electron configurations $4f5d6s$ and $4f5d^2$ both give rise to low lying terms in Ce II, with the former probably the lower. If $4f5d6s$ is lower the ground

[7] A. S. King, Astrophys. J. **68**, 194 (1928).

TABLE II. *Energy levels of Ce II.*

LEVEL	TERM VALUE WAVE NUMBERS	*J* VALUE	NO. OF COMBINATIONS	LEVEL	TERM VALUE WAVE NUMBERS	*J* VALUE	NO. OF COMBINATIONS	LEVEL	TERM VALUE WAVE NUMBERS	*J* VALUE	NO. OF COMBINATIONS
1	0.00	3½	19	29	6,638.25	4½	12	125	29,984.08	1½	7
2	1,410.30	4½	20	30	7,259.08	3½	16	126	30,065.19	3½	15
3	1,873.95	3½	23	31	8,280.96	3½	13	127	30,166.08	1½	5
4	2,382.26	4½	22	101	24,663.05	4½	9	128	30,245.89	4½	14
5	2,563.26	5½	11	102	25,359.69	2½	7	129	30,425.37	2½	10
6	2,581.27	4½	27	103	25,681.50	1½	4	130?	30,576.84	4½	7
7	2,595.65	1½	12	104	25,945.40	3½	13	131	30,637.17	4½	12
8	2,634.68	2½	21	105	26,841.40	4½	13	132	30,702.64	4½	16
9	2,641.57	3½	29	106	26,900.37	3½	13	133	30,829.13	3½	15
10	2,879.71	5½	14	107	27,187.06	3½	15	134	31,075.60	5½	8
11	3,363.44	2½	21	108	27,249.69	2½	13	135	31,207.96	4½	14
12	3,593.89	4½	25	109	27,379.95	5½	9	136	31,558.64	3½	13
13	3,703.61	3½	23	110	27,514.68	3½	11	137	31,738.50	5½	8
14	3,995.48	3½	30	111	27,811.52	4½	13	138	31,851.42	2½	9
15	4,266.41	3½	29	112	27,812.41	2½	12	139	32,138.73	2½	12
16	4,322.70	3½	21	113	27,835.23	1½	4	140	32,318.21	3½	14
17	4,459.89	3½	24	114	27,934.66	4½	19	141	32,862.80	3½	16
18	4,511.26	2½	20	115	28,297.49	3½	14	142	33,552.59	2½	11
19	4,523.01	4½	25	116	28,334.77	4½	11	143	33,808.31	2½	12
20	4,844.63	1½	8	117	28,337.82	2½	16	144	33,977.16	3½	16
21	4,910.98	5½	10	118	28,634.51	5½	11	145	34,155.33	3½	19
22	5,010.88	2½	15	119	28,725.16	4½	14	146	34,333.12	2½	11
23	5,118.81	2½	18	120	29,166.61	4½	16	147	34,426.07	2½	11
24	5,437.46	3½	25	121	29,281.37	2½	10	148	34,920.78	3½	11
25	5,716.22	3½	20	122	29,438.83	5½	9	149	34,934.46	2½	10
26	5,819.12	4½	25	123	29,807.09	4½	11	150	35,346.30	3½	14
27	5,942.79	3½	19	124	29,908.92	4½	18	151	35,558.70	3½	12
28	6,389.93	4½	10								

TABLE III. *List of classified Ce II lines.*

WAVE-LENGTH	INT.	WAVE NUMBER	COMB.	WAVE-LENGTH	INT.	WAVE NUMBER	COMB.	WAVE-LENGTH	INT.	WAVE NUMBER	COMB.
4984.42	1	20,056.94	31–117	4390.59	1	22,769.61	17–108	4197.511	3	23,816.95	14–112
4914.938	8 V	20,340.47	16–101	4384.44	1	22,801.54	22–112	4196.335	75 V	23,823.63	11–107
4865.12	1	20,548.76	29–107	4381.779	4	22,815.39	26–118	4195.819	3	23,826.56	18–117
4795.22	2	20,848.29	18–102	4380.057	3	22,824.36	22–113	4193.875	5	23,837.60	17–115
4755.51	2	21,022.38	26–105	4375.932	60 V	22,845.88	14–105	4192.757	2	23,843.96	24–121
4744.91	3	21,069.34	12–101	4373.820	50 V	22,856.91	19–109	4189.176	2	23,864.34	27–123
4742.22	1	21,081.29	26–106	4373.220	3	22,860.04	24–115	4187.324	6	23,874.90	17–116
4739.49	25 V	21,093.44	15–102	4372.401	4	22,864.33	16–107	4185.334	5	23,886.25	11–108
4722.31	2	21,170.17	18–103	4365.520	2	22,900.36	24–117	4179.291	2	23,920.79	12–110
4705.85	1	21,244.22	27–107	4364.659	125 IV	22,904.88	14–106	4176.081	3	23,939.17	14–114
4692.02	2	21,306.84	27–108	4364.502	?	22,905.71	26–119	4174.386	2	23,948.89	30–135
4678.61	1	21,367.91	26–107	4361.661	6	22,920.63	15–107	4172.152	1	23,961.71	10–105
4670.76	2	21,403.82	24–105	4360.444	3	22,927.02	16–108	4171.384	2	23,966.13	27–124
4666.70	1	21,422.44	19–104				31–135	4169.878	30 V	23,974.78	16–115
4664.11	1	21,434.34	18–104	4352.733	75 IV	22,967.64	20–112	4162.89	1	24,015.04	16–117
4657.85	1	21,463.14	24–106	4349.790	100 IV	22,983.18	15–108	4160.107	2	24,031.09	15–115
4657.22	1	21,466.05	30–119	4348.190	3	22,991.63	19–110	4159.033	50 IV	24,037.30	31–140
4644.22	2	21,526.13	31–123	4345.963	5	23,003.42	18–110	4153.130	4	24,071.46	3–104
4636.72	1	21,560.95	26–109	4344.920	1	23,008.94	25–119				15–117
4623.47	1	21,622.74	16–104	4342.137	3	23,023.68	21–114	4149.936	50 V	24,089.99	26–124
4589.37	1	21,783.40	10–101	4337.777	125 IV	23,046.83	8–103		60 V		25–123
4571.47	1	21,868.69	27–111	4330.444	30 IV	23,085.85	7–103	4146.235	75 IV	24,111.49	19–118
4567.12	1	21,889.52	22–106	4320.723	60 IV	23,137.78	13–105	4137.475	4	24,162.54	23–121
4563.35	1	21,907.60	28–115	4315.404	3	23,166.31	30–129	4132.633	3	24,190.85	29–133
			30–120	4314.939	2	23,168.80	29–128	4131.099	100 V	24,199.82	9–105
4554.54	1	21,949.98	14–104	4313.100	2	23,178.68	23–115	4130.705	100 V	24,202.14	19–119
4545.878	2	21,991.80	27–114	4310.700	5	23,191.59	14–107	4128.067	4	24,217.60	12–111
4544.961	5	21,996.25	11–102	4309.740	50 IV	23,196.75	13–106	4125.776	2	24,231.05	13–114
			29–118	4305.609	2	23,219.11	23–117	4123.230	5	24,246.01	26–126
4539.755	200 IV	22,021.46	9–101	4304.723	4	23,223.79	27–120	4121.595	1	24,255.63	21–120
4527.354	200 V	22,081.78	6–101	4300.331	60 IV	23,247.51	12–105	4120.829	150 V	24,260.14	6–105
4524.590	1	22,095.27	25–107	4299.362	60 IV	23,252.75	2–101	4119.886	5	24,265.70	8–106
4520.410	0	22,115.71	26–114	4299.092	3	23,254.21	14–108	4114.141	2	24,299.58	30–136
4508.084	4	22,176.17	22–107	4296.069	6	23,270.57	29–124	4113.722	4	24,302.05	14–115
4499.52	1 u	22,218.38	25–114	4294.756	3	23,277.68	31–136				27–128
4495.389	4	22,238.80	22–108	4292.905	1	23,287.72	24–119	4111.923	2	24,312.69	28–132
4494.226	4	22,244.55	28–118	4292.767	4	23,288.47	19–111	4110.840	3	24,319.09	6–106
4486.909	150 V	22,280.83	4–101	4290.435	2	23,301.13	18–112	4107.426	200 V	24,339.31	14–116
4483.900	100 V	22,295.78	31–130	4289.937	300 IV	23,303.84	9–104	4106.881	5 d	24,342.54	14–117
4479.35	30 V	22,318.39	11–103	4289.453	5	23,306.46	12–106	4092.715	4	24,426.79	26–128
	50 V		19–105	4288.671	1	23,310.71	8–104	4090.942	4	24,437.37	29–134
4472.716	6	22,351.53	12–104	4283.550	2	23,338.58	27–121	4089.006	3	24,448.94	11–112
4472.11	1	22,354.56	27–115	4281.914	1	23,347.49	26–120	4087.371	4 d	24,458.72	15–119
4468.023	2 u	22,375.01	24–112	4281.156	3	23,351.63	17–111	4087.297	4	24,459.17	4–105
4467.537	5	22,377.44	19–106	4280.998	3	23,352.49	17–112	4085.232	100 V	24,471.53	24–124
4463.87	1 u	22,395.82	23–110	4278.865	5	23,364.12	6–104	4080.435	5	24,500.30	10–109
4462.03	1	22,405.06	20–108	4270.189	60 IV	23,411.60	19–114	4077.470	75 V	24,518.11	4–106
4454.984	3	22,440.49	17–106	4264.372	3	23,443.54	30–132	4075.853	125 IV	24,527.84	21–122
4449.337	200 V	22,468.97	21–109	4258.699	1	23,474.77	17–114	4074.646	2	24,535.11	2–104
4443.752	4	22,497.21	24–114	4257.120	4	23,483.47	13–107	4066.910	1	24,581.78	31–141
4442.43	1	22,503.90	22–110	4256.156	5	23,488.79	16–111	4065.164	3	24,592.33	30–138
4440.13	1	22,515.56	26–116	4255.992	4	23,489.70	16–112	4064.904	3	24,593.91	13–115
4439.50	1	22,518.76	16–105	4255.359	3	23,493.19	20–117	4062.941	3	24,605.79	6–107
4437.612	4	22,528.34	29–120	4250.651	1	23,519.21	14–110	4061.421	2	24,615.00	8–108
4433.708	2	22,548.18	31–133	4245.976	6	23,545.10	15–111	4059.314	1	24,627.77	24–126
4428 437	5	22,575.01	15–105	4242.726	7	23,563.14	4–104	4058.76	4	24,631.13	13–116
4427.917	6	22,577.66	16–106	4241.403	2	23,570.49	31–138	4058.245	4	24,634.26	13–117
4427.070	5	22,581.98	11–104	4234.726	2	23,607.65	29–128	4054.944	50 IV	24,654.01	7–108
4419.89	1	22,618.67	25–116	4233.949	2	23,611.99	16–114	4053.508	100 IV	24,663.05	1–101
4419.298	3	22,621.70	25–117	4232.569	4	23,619.68	26–122	4049.80	1	24,685.63	28–134
4416.904	4	22,633.96	15–106	4223.882	4	23,668.26	15–114	4048.367	1	24,694.37	27–131
4413.805	2	22,649.85	30–124	4214.041	50 IV	23,723.53	21–118	4046.341	100 V	24,706.73	17–120
4400.872	3	22,716.41	23–113	4213.035	3 u	23,729.20	24–120	4045.976	?	24,708.96	25–129
4400.545	3	22,718.09	9–102	4202.944	150 IV	23,786.17	12–109	4042.584	200 IV	24,729.69	14–119
4399.204	60 IV	22,725.02	8–102				18–115	4040.758	300 IV	24,740.87	12–116
4398.790	5	22,727.16	17–107	4198.431	4	23,811.74	19–116	4037.664	5	24,759.83	27–132
4396.585	3	22,738.56	18–108	4197.998	5	23,814.19	21–119	4031.339	150 IV	24,798.67	6–109
4391.663	250 IV	22,764.04	7–102	4197.668	4	23,816.06	14–111	4030.343	4	24,804.80	4–107

TABLE III.—*Continued.*

WAVE-LENGTH	INT.	WAVE NUMBER	COMB.	WAVE-LENGTH	INT.	WAVE NUMBER	COMB.	WAVE-LENGTH	INT.	WAVE NUMBER	COMB.
4029.75	1	24,808.45	24–128	3898.949	?	25,640.70	3–110	3769.046	5	26,524.41	2–114
4028.413	150 IV	24,816.68	5–109	3898.674	1	25,642.51	15–124	3766.514	4 u	26,542.23	13–128
4028.198	2	24,818.01	26–131	3896.804	100 IV	25,654.81	18–127	3765.044	4	26,552.60	19–134
			28–135	3896.637	1	25,655.91	9–115	3764.117	150 IV	26,559.14	10–122
4027.633	2	24,821.49	17–121	3895.114	125 IV	25,665.93	21–130	3763.612	3	26,562.70	15–133
4020.542	2	24,865.27	23–125	3890.986	6	25,693.17	9–116	3760.404	2	26,585.36	6–120
4019.274	2	24,873.11	9–110	3890.519	2	25,696.26	9–117	3757.858	4	26,603.37	5–120
4018.213	1	24,879.68	30–139				31–144	3755.425	75 IV	26,620.61	11–125
4017.596	2	24,883.54	26–132	3889.478	3	25,703.13	8–117	3752.453	2	26,641.69	14–131
4014.899	125 V	24,900.22	15–120	3888.388	4 u	25,710.34	23–133	3751.002	1	26,652.00	12–128
4012.389	300 IV	24,915.79	19–122	3886.495	3	25,722.86	19–128	3746.373	2 d	26,684.93	19–135
4011.559	2	24,920.95	25–131	3883.983	1	25,739.50	26–136	3746.260	2	26,685.73	7–121
4003.168	1	24,973.18	22–125	3883.583	4	25,742.15	7–117	3744.05	1	26,701.48	11–126
4002.975	4	24,974.38	11–117	3881 874	4	25,753 48	6–116				24–139
4001.049	4	24,986.41	25–132	3881.675	5	25,754.80	10–118	3741.721	3	26,718.10	30–144
3999.242	500 IV	24,997.69	4–109	3879.313	3	25,770.48	24–135	3739.691	2	26,732.61	23–138
3996.481	4	25,014.97	15–121	3878.372	150 IV	25,776.73	2–107	3737.540	3	26,747.99	17–135
3995.429	2	25,021.55	13–119	3876.975	6	25,786.02	17–128	3729.918	4	26,802.65	11–127
3992.385	125 IV	25,040.63	12–118	3876.129	4	25,791.65	21–132	3726.462	3	26,827.50	21–137
3991.317	3	25,047.33	23–127	3875.036	6 d	25,798.91	15–126	3724.639	5	26,840.63	22–138
3990.105	5	25,054.94	10–114	3873.117	1	25,811.71	14–123	3722.291	4	26,857.56	6–122
3989.444	30 V	25,059.09	30–140	3872.137	1	25,818.24	22–133	3719.797	3	26,875.57	5–122
3982.901	60 V	25,100.25	29–137	3868.516	2	25,842.41	25–136	3719.091	1	26,880.67	24–140
3980.895	100 V	25,112.90	25–133	3868.138	4	25,844.93	12–122	3718.190	150 IV	26,887.19	2–115
3977.807	4	25,132.40	4–110	3863.741	4	25,874.34	31–145	3716.938	4	26,896.24	30–145
3976.67	1	25,139.58	20–125	3857.928	2 u	25,913.33	14–124	3716.365	600 IV	26,900.39	1–106
			24–130	3857.813	2	25,914.10	18–129	3713.648	2	26,920.07	27–141
3974.201	2	25,155.20	22–127	3857.644	5	25,915.24	4–115	3711.783	3	26,933.59	13–131
3972.071	6	25,168.69	28–136	3857.240	4	25,917.95	11–121	3710.684	2	26,941.57	15–135
3971.873	3	25,169.95	9–111	3857.032	5	25,919.35	26–137	3704.979	4	26,983.06	12–130
3971.684	100 V	25,171.14	14–120	3854.322	100 IV	25,937.57	3–111	3702.785	5	26,999.05	13–132
3970.646	5	25,177.72	8–112	3854.187	100 IV	25,938.48	3–112	3701.730	1	27,006.74	20–138
3967.185	4	25,199.68	24–131	3853.158	125 IV	25,945.41	1–104	3699.920	50 V	27,019.95	23–139
3967.048	100 IV	25,200.55	8–113	3852.103	2	25,952.51	4–116	3698.650	5	27,029.23	5–124
3964.503	6	25,216.73	7–112	3849.562	2	25,969.65	2–109	3696.673	2	27,043.68	26–141
3960.914	125 IV	25,239.58	7–113	3848.105	3	25,979.48	15–128	3694.911	60 V	27,056.58	4–122
3958.266	6	25,256.47	26–134	3837.210	3	26,053.24	6–118	3693.720	3	27,065.30	31–150
3956.901	4	25,265.12	24–132	3836.110	6	26,060.69	3–114	3689.165	3	27,098.72	17–136
			27–135	3834.785	3	26,069.71	14–126	3687.802	30 V	27,108.73	12–132
3953.957	4 u	25,283.99	19–123	3834.556	100 IV	26,071.27	5–118	3685.516	2 u	27,125.55	13–133
3953.660	5	25,285.89	14–121	3832.745	4	26,083.59	9–119	3682.660	2	27,146.59	25–141
3952.573	125 V	25,292.84	9–114	3829.946	2	26,102.65	16–129	3680.084	4	27,165.59	9–123
	125 IV			3829.694	4	26,104.37	2–110	3679.92	1	27,166.80	30–147
3950.436	5	25,306.52	23–129	3827.227	3	26,121.19	24–136	3677.176	2	27,187.07	1–107
3949.412	5	25,313.11	3–107	3823.903	50 IV	26,143.90	6–119	3673.739	2	27,212.50	14–135
3944.101	3 u	25,347.11	17–123	3821.702	6	26,158.96	15–129	3672.166	5 d	27,224.16	2–118
3943.888	100 IV	25,348.54	28–137	3821.270	5	26,161.91	5–119	3671.941	4	27,225.83	6–123
3943.141	5	25,353.34	6–114	3820.871	5	26,164.64	21–134	3670.669	2	27,235.26	12–133
3942.151	125 IV	25,359.71	1–102	3819.024	5	26,177.30	17–131	3668.727	4	27,249.68	1–108
3940.338	100 IV	25,371.38	5–114	3818.688	5	26,179.60	19–132	3666.346	2	27,267.38	9–124
3939.662	3	25,375.73	3–108	3814–942	2	26,205.31	13–124	3664.944	1	27,277.81	31–151
3938.086	7	25,385.89	19–124	3808.384	3	26,250.43	14–128	3663.005	2	27,292.25	15–136
3937.643	2	25,388.74	26–135	3808.124	300 IV	26,252.22	4–118	3659.972	6	27,314.86	2–119
3931.369	100 IV	25,429.26	4–111	3803.097	200 IV	26,286.88	10–120	3658.258	3	27,327.66	6–124
3931.088	125 IV	25,431.08	2–105	3800.324	1	26,306.11	19–133	3656.756	3	27,338.88	29–144
3928.312	4	25,449.05	17–124	3799.097	3	26,314.56	16–131	3655.851	500 IV	27,345.65	5–124
3927.383	4	25,455.07	10–116	3799.035	2	26,315.03	12–124	3655.349	2	27,349.40	8–125
3926.163	2	25,462.98	13–120	3792.326	50 IV	26,361.58	13–126	3653.108	125 V	27,366.18	10–128
3924.644	60 IV	25,472.83	18–125	3790.342	3	26,375.38	27–140	3650.134	3	27,388.48	7–125
3921.731	100 V	25,491.75	25–135	3786.632	150 IV	26,401.22	2–111	3649.730	1	27,391.51	17–138
3913.995	2	25,542.14	19–126	3783.569	5	26,422.59	25–139	3645.455	4	27,423.63	9–126
3912.424	300 IV	25,552.39	4–114	3782.524	75 IV	26,429.89	14–129	3645.226	5 u	27,425.36	24–131
3912.191	5	25,553.91	18–126	3781.620	150 IV	26,436.21	15–132	3644.539	1	27,430.53	8–126
3909.313	6	25,572.73	12–120	3781.102	3	26,439.83	23–136	3639.868	1	27,465.73	11–133
3908.543	100 IV	25,577.76	13–121	3777.668	2	26,463.87	3–117	3637.459	2	27,483.98	6–126
3908.094	3	25,580.70	20–129	3776.611	5	26,471.28	12–126	3633.391	3	27,514.68	1–110
3904.582	2	25,603.71	30–141	3772.650	4	26,499.07	26–140	3631.194	125 V	27,531.33	8–127
3904.340	5	25,605.30	17–126	3771.602	6	26,506.43	16–133	3627.001	2	27,563.16	14–136

TABLE III.—*Continued.*

WAVE-LENGTH	INT.	WAVE NUMBER	COMB.	WAVE-LENGTH	INT.	WAVE NUMBER	COMB.	WAVE-LENGTH	INT.	WAVE NUMBER	COMB.
3623.837	200 V	27,587.22	28–144	3471.546	1	28,797.39	22–143	3286.020	5 d	30,423.22	18–149
3618.576	2	27,627.33	18–139	3467.776	4	28,828.70	3–132	3285.224	125 V	30,430.59	14–147
3613.701	150 V	27,664.60	6–128	3466.952	4	28,835.55	2–128	3284.221	4	30,439.88	23–151
3611.331	3	27,682.75	4–126	3464.160	6	28,858.79	10–137	3283.680	4	30,444.90	11–143
	2		5–128	3463.138	1	28,867.31	14–141	3280.485	4	30,474.55	17–149
3603.355	3	27,744.03	23–141	3457.177	4	28,917.08	9–136	3279.842	125 V	30,480.52	4–141
3600.583	60 V	27,765.39	28–145	3456.772	3	28,920.47	29–151	3271.151	4	30,561.50	12–145
3598.196	50 V	27,783.81	9–129	3456.340	1 u	28,924.08	8–136	3267.245	2	30,598.08	16–148
3596.725	2	27,795.17	19–140	3452.623	3	28,955.22	3–133	3263.884	5	30,629.54	13–146
3594.61	3	27,811.52	1–111	3451.617	3	28,963.66	20–143	3263.071	2	30,637.17	1–131
3594.496	1	27,812.41	1–112	3449.910	1	28,977.99	27–148	3261.242	1	30,654.36	15–148
3593.134	2	27,822.95	10–132	3448.290	3	28,991.60	27–149	3259.784	3	30,668.07	15–149
3589.390	1	27,851.96	22–141	3442.955	3	29,036.53	23–145	3254.013	5	30,722.45	13–147
3587.639	4	27,865.56	27–143	3442.380	75 V	29,041.38	18–142	3246.678	60 V	30,791.86	11–145
3586.753	2	27,872.45	15–139	3436.304	4	29,092.73	17–142	3243.370	200 V	30,823.27	19–150
3578.738	1	27,934.87	1–114	3428.697	3	29,157.27	6–137	3242.135	2	30,835.01	18–150
3574.906	1	27,964.81	12–136	3427.605	2 u	29,166.56	1–120	3236.735	150 V	30,886.45	17–150
3570.983	3	27,995.53	6–130	3426.583	4	29,175.26	2–130	3234.165	300 V	30,910.98	9–142
			9–131	3421.556	2	29,218.12	5–137	3233.441	3	30,917.91	8–142
			16–140				25–149	3231.236	200 V	30,939.01	14–149
3566.77	1	28,028.60	2–122	3420.534	2	29,226.85	2–131	3229.363	4	30,956.95	7–142
3563.823	3	28,051.77	15–140	3420.176	5	29,229.91	16–142	3228.024	1	30,969.79	11–146
3559.328	2	28,087.20	30–150	3414.168	2	29,281.34	1–121	3226.036	2	30,988.88	3–141
3558.706	3	28,092.11	25–143	3412.334	4	29,297.08	18–143	3221.171	250 V	31,135.68	19–151
3555.788	2	28,115.16	24–142	3409.405	2	29,322.25	22–146	3218.380	5	31,062.59	11–147
3554.993	150 V	28,121.45	6–132	3406.364	2	29,348.43	17–143	3207.624	3	31,166.75	9–143
3552.727	5	28,139.39	5–132	3394.138	2	29,454.14	19–144	3206.921	2	31,173.58	8–143
3552.067	2	28,144.60	12–137	3392.784	2	29,465.89	18–144	3202.906	2	31,212.66	7–143
3551.664	4	28,147.80	13–138	3390.515	5	29,485.61	16–143	3190.341	3	31,335.58	9–144
3546.651	2	28,187.59	9–133	3389.212	1	29,496.95	9–139	3189.638	4	31,342.49	8–144
3546.190	150 V	28,191.25	3–126				24–149	3188.787	6	31,350.85	14–150
3545.781	2	28,194.51	4–130	3388.407	2	29,503.95	8–139	3184.212	4	31,395.84	6–144
			8–133	3383.925	1	29,543.03	7–139	3178.485	3	31,452.46	2–141
3545.603	3	28,195.92	10–134	3373.729	125 V	29,632.31	19–145	3172.299	4	31,513.79	9–145
3543.520	4	28,212.49	27–145	3368.690	5	29,676.64	9–140	3171.615	200 V	31,520.60	8–145
3539.086	300 V	28,247.84	6–133	3366.554	150 V	29,695.46	17–145	3167.918	3	31,557.37	11–148
3537.43	?	28,261.06	25–144	3364.821	4	29,710.76	15–144	3167.324	3	31,563.29	14–151
3532.878	3	28,297.48	1–115	3361.853	3	29,736.99	6–140	3166.243	5	31,574.06	6–145
3532.609	3	28,299.63	30–151	3361.555	3	29,739.63	26–151	3164.154	200 V	31,594.91	4–144
3530.022	5	28,320.37	4–132	3355.011	7	29,797.63	2–135	3155.793	5	31,678.61	3–142
3529.043	2	28,328.23	10–135	3354.520	2	29,802.09	23–148	3154.506	5	31,691.54	9–146
3528.052	2	28,336.18	26–145	3352.986	3	29,815.62	23–149	3149.937	2	31,737.50	7–146
3527.850	4	28,337.80	1–117	3352.283	4 d	29,821.88	18–146	3148.458	4	31,752.42	12–150
3527.607	2	28,339.76	19–141	3351.077	2	29,832.61	16–145	3146.407	200 V	31,773.11	4–145
3520.522	150 V	28,396.79	2–123	3349.967	5	29,842.49	25–151	3145.282	150 V	31,784.48	9–147
3515.776	5	28,435.12	13–139	3346.517	4	29,873.26	17–146	3144.596	5	31,791.41	8–147
3509.254	3	28,487.97	11–138	3344.761	300 V	29,888.94	15–145	3138.296	3 u	31,855.23	13–151
3508.470	4	28,494.33	6–134	3342.531	2	29,908.88	1–124	3127.529	80 V	31,964.89	12–151
3507.945	125 V	28,498.60	2–124				24–150	3125.762	1	31,982.96	11–150
3506.256	5	28,512.32	5–134	3341.868	100 V	29,914.82	18–147	3114.055	1 u	32,103.19	3–144
3503.978	3	28,530.86	28–148	3340.886	4	29,923.61	22–149	3097.079	2	32,279.15	9–148
3502.888	3	28,539.74	24–144	3339.505	4	29,935.98	4–140	3096.876	3 d	32,281.27	3–145
3502.650	3	28,541.68	22–142	3334.896	1	29,977.35	3–138	3095.098	2	32,299.77	8–149
3501.453	60 V	28,551.44	3–129	3331.224	3	30,010.40	16–146	3093.348	3	32,318.09	1–140
3495.941	4	28,596.45	15–141	3324.985	3	30,066.70	15–146	3091.292	3 d	32,339.57	6–148
3493.728	5	28,614.56	13–140	3320.940	2	30,103.32	16–147	3079.906	1	32,459.12	3–146
3492.249	3	28,626.68	6–135	3320.781	2	30,104.77	13–143	3072.391	1	32,538.52	4–148
3482.355	6	28,708.01	20–142	3318.964	5	30,121.25	24–151	3071.109	4	32,552.10	3–147
			29–150				14–141	3056.775	200 V	32,704.74	9–150
3482.139	5	28,709.79	25–147	3314.731	100 V	30,159.71	15–147	3051.163	2	32,764.89	6–150
3481.155	3	28,717.91	24–145	3311.497	5 d	30,189.16	11–142	3037.049	2	32,917.15	9–151
3480.382	4	28,724.29	12–140	3307.233	5	30,228.09	8–141	3032.727	3	32,964.06	4–150
3480.279	3	28,725.14	1–119	3303.225	3	30,264.76	3–139	3025.124	1	33,046.90	3–148
3475.670	5	28,763.22	3–131	3295.289	80 V	30,337.65	14–146	2986.669	2	33,472.39	3–150
3474.216	6	28,775.26	11–139	3290.341	4	30,383.27	12–144	2862.787	3	34,920.77	1–148

state should be $^4H_{3\frac{1}{2}}$, whereas if $4f5d^2$ is lower it should be $^4I_{4\frac{1}{2}}$. The J value of the lowest state which we have thus far found is $3\frac{1}{2}$, this possibly being $^4H_{3\frac{1}{2}}$. In any case the spectrum is not like that of La I, which Haspas' analysis purported to show.

Experimental g values have been determined for several of the levels. While these are not very precise they do show large departures from the theoretical g values, evidence of large interactions between the various levels. This perturbation is to be expected, since our term diagram, though far from complete, shows the greatest density of low levels yet observed. The fact that 13 low levels having J values of $3\frac{1}{2}$ have already been found means that at least 13 multiple terms lie within 8300 cm^{-1} of the lowest state. The large number of times this value of J is found shows also that some of the low levels belong to $4f5d^2$, since $4f5d6s$ can account for only eight at the most. The two configurations probably interact so strongly that exact electron configuration assignments will have little meaning.

The energy levels found are presented in Table II. The low levels are numbered from 1 up in order of energy, and the middle levels are numbered from 101 up.

Table III contains a list of the lines which have thus far been classified. Those wave-lengths given to hundredths of an angstrom only are taken from Exner and Haschek;[8] the remainder are M.I.T.-W.P.A. measurements. The second column contains the estimated intensity of the line as given by Klein[9] or by Exner and Haschek,[8] and, where known, King's temperature classification.

We record with gratitude assistance from a grant by the Rumford Committee of the American Academy of Arts and Sciences. We are particularly happy to acknowledge our debt to Colonel R. C. Eddy and the staff members of the W.P.A. project for their conscientious work on the wave-length determinations.

[8] F. Exner and E. Haschek, *Die Spektren der Elemente bei normalen Druck* (Franz Deuticke, Leipzig, 1911).
[9] Ph. Klein, Zeits. f. wiss. Phot. **18**, 45 (1918).

DECEMBER 15, 1937 PHYSICAL REVIEW VOLUME 52

Pressure Effects of Homogeneous K Vapor in Absorption

D. S. HUGHES* AND P. E. LLOYD
California Institute of Technology, Pasadena, California

(Received September 7, 1937)

By use of the newly developed corrosion-resistant MgO windows, the K resonance lines in absorption of a homogeneous vapor, were obtained for pressures ranging from 0.001 to 20 mm Hg. The "dispersion" equation was generally adequate to describe the observed contours. The corresponding half-breadths were linear in the density, equal as between components, but of magnitude several times that predicted by the theory of the resonance interaction. The slight asymmetry which appeared at the highest pressure was attributed to van der Waals forces. But it is pointed out that, in contradistinction to the circumstance for Hg, a quantitative verification of the inverse sixth power law is probably not possible. The infrared bands of the K_2 molecule were also observed.

THE strong asymmetries and shifts, characteristic of spectral lines arising from absorption by a metallic vapor in the presence of a foreign gas, have recently been the subject of extended investigation. The pressure effects in a homogeneous absorbing vapor,[1] with the typical marked symmetrical broadenings, are, however, not only less well understood, but their experimental study has been comparatively neglected. It is the purpose of this paper to describe an experimental investigation of the contours of the K resonance lines (λλ7664.9, 7699.0) for the latter case.

In what follows, it will be supposed that foreign gases are present in negligible quantity, so that the interactions among like particles only,

* National Research Fellow, 1931–1933. Now with Shell Petroleum Corporation, Houston, Texas.
[1] For a recent review article dealing with the general subject of pressure effects, see H. Margenau and W. W. Watson, Rev. Mod. Phys. **8**, 22 (1936).

need be considered. Furthermore, the discussion will, for the most part, be pertinent only to the lowest (resonance) transitions of the atom, in absorption.

Theory

The contour of a line otherwise determined by radiation damping, will be strongly modified in consequence of the presence of atoms in the vicinity of the absorbing one. The perturbations here involved arise by virtue of the existence of both resonance and van der Waals forces. For the resonance forces, the net change in the energy of the absorbing atom in the field of a single perturbing atom at distance R, is given by

$$\Delta\epsilon = \pm h(e^2f/8\pi^2 m\nu_0)(1/R^3), \qquad (1)$$

approximately,[2] where f is the oscillator strength of the transition of natural frequency ν_0. For the van der Waals forces, the corresponding equation is,[3] for not too small R,

$$\Delta\epsilon = -h(C/R^6), \qquad (2)$$

where C is a constant of the transition, in general positive. Exact numerical evaluation of C has not been made. When more than one perturbing atom is involved, the $\Delta\epsilon$'s of (2) are additive. This is not true in the case of (1), and the precise nature of the relation is not known.

We shall not here concern ourselves with the effects that result from very close approaches[4] except to note that there is the possibility of the formation of molecular states as a consequence of the existence of a minimum in the potential energy of a configuration.

A rigorous application of the foregoing considerations to the determination of the absorption coefficient has not been made. But the approximate solutions are instructive. It will be convenient to discuss first the "statistical" distribution of frequencies, ignoring for the moment the contribution of the "velocity" effect.

The frequency actually absorbed is then related to the perturbation energy by $\nu - \nu_0 = \Delta\epsilon/h$, simply. The intensity at a given $\nu - \nu_0$ depends, of course, upon the statistical probability of the existence of a configuration capable of producing the corresponding $\Delta\epsilon$. Thus, the center of the line (small $|\nu - \nu_0|$) arises from the perturbations of many distant particles, and is of high intensity relative to the wings. But for larger $|\nu - \nu_0|$, the single encounter is determinative, because of the smaller probability of sufficiently close multiple approaches. Then, for moderately large $|\nu - \nu_0|$, the resonance perturbation prevails, because of the slower decay with distance of (1) in comparison to (2). But, as concerns the far part of one wing, the van der Waals force contributes strongly, and the line takes on the asymmetrical character of foreign gas broadening.[5] We turn now to quantitative considerations.

Margenau and Watson,[1] for the statistical distribution on the basis of resonance forces, obtained the familiar "dispersion" equation,[6]

$$\alpha x = \frac{A\Delta\nu_{\frac{1}{2}}/2\pi}{(\nu_0 - \nu)^2 + (\Delta\nu_{\frac{1}{2}}/2)^2}, \qquad (3)$$

or, more properly, for $|\nu_0 - \nu| \gg \Delta\nu_{\frac{1}{2}}$,

$$\alpha x = (A\Delta\nu_{\frac{1}{2}}/2\pi)/(\nu_0 - \nu)^2, \qquad (4)$$

for, as the authors have pointed out, (3) cannot hold at the line center[7] in view of the non-additivity of the resonance interaction. The quantity A is the integrated absorption, and numerically equal to $(\pi e^2/mc)Nfx$ sec.$^{-1}$, where N is the number of atoms per cc, and x is the length of the absorbing column. They found, for the half-breadth,

$$\Delta\nu_{\frac{1}{2}} = (e^2f/6m\nu_0)N \text{ sec.}^{-1}. \qquad (5)$$

As indicated above, the van der Waals forces will, at sufficiently high pressures, result in a measurable intensity at the distant part of one wing (long wave-length for positive C). Kuhn[8]

[2] See, for example, reference 1, p. 33.

[3] F. London, Zeits. f. Physik **63**, 245 (1930); Zeits. f. physik. Chemie **B11**, 222 (1930).

[4] For recent investigations in this connection, see H. Kuhn, Proc. Roy. Soc. **158**, 212 and 230 (1937); W. M. Preston, Phys. Rev. **51**, 298 (1937).

[5] Of course, in order to have a measurable intensity at these larger $|\nu - \nu_0|$, high density of the absorbing vapor is required.

[6] The absorption coefficient αx, is connected with the (observable) transmission I/I_0 by $I/I_0 = \exp[-\alpha x]$.

[7] This need not concern the experimenter, for because of the general practically complete absorption that occurs at the center of the line, the half-breadth is not directly measurable, but only the product $A\Delta\nu_{\frac{1}{2}}$ of (4). The circumstance is different for the case of a nonhomogeneous gas, since an additional parameter enters, *viz.*, the density of the foreign gas.

[8] H. Kuhn, Phil. Mag. **18**, 987 (1934). See also H. Margenau, Phys. Rev. **48**, 755 (1935).

has given

$$\alpha x = (2\pi A N C^{\frac{1}{3}}/3)/(\nu_0-\nu)^{\frac{1}{3}}. \quad (6)$$

It is apparent that, because of its slower decline with increasing $\nu_0-\nu$, (6) may overshadow (4).

Unfortunately, the above distributions are confused as a result of the velocity effect. In fact, at the center of the line, this latter is probably determinative. But as Kuhn and London[9] have shown in connection with the van der Waals forces, in the wings of the line the velocity effect contributes merely a "diffuseness;" one that is proportional to the square root of the velocity, approximately, and that decreases with increasing $\nu_0-\nu$. Thus (6) may, within the limits of its validity, be supposed to be satisfied the better the smaller the velocity and the larger the $\nu_0-\nu$. The same considerations can be extended to apply to the resonance case as given by (4), but certainly, the "diffuseness" decreases less rapidly with increasing $|\nu_0-\nu|$. This last may be seen as well, in connection with the Lorentz collision theory. This theory, as modified by Weisskopf,[10] also leads to (3), but (for the here more important case of resonance forces) the half-breadth is defined by

$$\Delta\nu_{\frac{1}{2}} = (e^2 f/4\pi m v_0)N \text{ sec.}^{-1}. \quad (7)$$

This distribution, which may be considered as the limiting case of the velocity effect, falls off no more quickly with increasing $|\nu_0-\nu|$ than does (4). But the interpretation of Weisskopf's result is somewhat uncertain in view of the failure of the velocity to enter explicitly.

Recently, Furssow and Wlassow[11] have critically analyzed the foundations of the theory of resonance broadening discussed above. It suffices here only to point out that their method of attacking the problem again yields the dispersion Eq. (3), where now

$$\Delta\nu_{\frac{1}{2}} = (2e^2 f/3\pi m v_0)N \text{ sec.}^{-1}. \quad (8)$$

It is to be noted that (5), (7) and (8) differ from one another only by a numerical factor.

To recapitulate, theory predicts for moderate pressures the distribution (4) for the wings of the line. The velocity effect will contribute strongly, but the dependence of αx upon frequency may remain approximately unchanged. The half-breadth given by (5) must then be considered only as the limiting value. At higher pressures, the line will exhibit an asymmetrical extension. This distant wing may be describable very nearly by (6), since the velocity effect is of less moment.

The foregoing discussion, although containing nothing new, seems appropriate here, in view of the absence of any recent consolidation of existing theoretical knowledge. It may well be interpreted in conjunction with the material of reference 4.

Experiment

Many investigators have confirmed the predictions of the radiation damping theory.[12] They noted deviation from constant half-breadth at pressures ranging from 0.001 to 0.01 mm Hg. This last fact permits estimation of the Lorentz collision diameter ρ,[13] found variously to be between 100 and 200A for the Na D lines.[14] These considerations are rather indirect.

By actually obtaining the absorption contours for higher pressures, the correctness of (3) was verified by Harrison and Slater[15] for the Na principal series, and again by Trumpy[16] and for Hg 2537 as well, and by Waibel[17] for the Cs principal series ($\rho \leqq 100$A). But each found the half-breadths proportional to $N^{\frac{1}{2}}$. In these investigations, the pressure variation was, for the most part, small. Furthermore, some of the results may be questioned in view of the use of what is now known to be faulty technique, i.e.,

[9] H. Kuhn and F. London, Phil. Mag. **18**, 983 (1934); H. Kuhn, Proc. Roy. Soc. **158**, 212 (1937). See also H. Margenau, reference 8.

[10] V. Weisskopf, Zeits. f. Physik **75**, 287 (1932). Kuhn (reference 8) has shown from considerations of a geometrical nature in connection with the mean free path of the collision process, that the half-breadth should increase somewhat more rapidly with N than indicated by (7).

[11] W. Furssow and A. Wlassow, Physik. Zeits. Sowjetunion **10**, 378 (1936).

[12] R. Minkowski, Zeits. f. Physik **36**, 839 (1926); W. Schütz, ibid, **45**, 30 (1927); M. Weingeroff, ibid, **67**, 679 (1931); S. A. Korff, Astrophys. J. **76**, 124 (1932).

[13] This is a convenient measure of the magnitude of the pressure effect. As is well known, the Lorentz collision theory leads to (3), with $\Delta\nu_{\frac{1}{2}} = N\rho^2\bar{v}$ sec.$^{-1}$, where $\bar{v}$ is the mean relative velocity of the colliding pairs.

[14] The value $\rho \leqq 50$A is yielded for Hg from the data on the quenching of resonance radiation of W. Orthmann and P. Pringsheim, Zeits. f. Physik **46**, 160 (1927).

[15] G. R. Harrison, Phys. Rev. **25**, 768 (1925); G. R. Harrison and J. C. Slater, Phys. Rev. **26**, 176 (1925).

[16] B. Trumpy, Zeits. f. Physik **34**, 715 (1925); **40**, 594 (1927).

[17] F. Waibel, Zeits. f. Physik **53**, 459 (1929).

the employment of a foreign gas in the absorption cell, to retard diffusion of the vapor to the (cold) windows. It appears that a systematic study of the pressure effects in a homogeneous atomic absorbing vapor has not been made. In particular, the dependence of the half-breadth upon density has not been resolved experimentally to accord with theory.

This is excepting a recent investigation by Kuhn[18] of Hg 2537 for pressures yielding van der Waals forces. He confirmed (6) for the long wave-length wing, and determined the constant C. Interesting conclusions were drawn as to the nature of the potential energy curves.

Experimenters have invariably been hampered by the inability of the conventional windows (quartz or glass) of the absorption cell to chemically withstand the hot vapors, particularly as to the alkali metals. This difficulty was eliminated in the present instance by the use of the newly developed corrosion-resistant MgO windows.[19] They showed no sign of attack throughout the experiment (K vapor up to 500°C).

Procedure

The source used was a high intensity tungsten incandescent lamp with replaceable filament. The absorption cell consisted of a copper cylinder of internal and external diameters of approximately 1.5 cm and 2.5 cm, respectively. Two lengths were used, 0.2 cm and 15 cm. The cell fitted snugly into a cylindrical resistance-heating-element of 31 cm length, both being enclosed in a vacuum-tight water-cooled steel cylinder having glass end-windows. MgO windows, of diameters of about 2 cm, could be pressed, one at either end, against the absorption cell, and this under vacuum, by virtue of a head, threaded, and containing a sylphon, forming one end of the outermost cylinder. A seal at the windows resulted from the collapse of the thin ring turned at either end of the soft copper cell.

A thermocouple yielded the temperature. It was calibrated *in situ* from the melting points of strips of appropriate metals placed within the cell.

Prior to use, the cell, and the potassium, were independently heated under vacuum to release foreign gases. For each tube-length, and at increasing cell temperature settings, a series of spectrograms was obtained with an astigmatic grating (2.64A/mm dispersion in first order). Eastman type I–R plates were used, with exposure times of the order of a few hours.

Each plate was calibrated from the image of a pair of step-weakeners placed just before it, one on either side of the absorption doublet. The transmission of the step-weakeners was previously determined photographically, *in situ*, using a constant intensity source in conjunction with a high speed rotating sector of variable aperture placed before the slit. A trace of the plates was obtained on a Krüss microphotometer having magnification ratios up to 40 : 1.

All contours were tested graphically for fit to (4). At lower pressures, some deviation is to be expected because of the Doppler effect, and because of the finite resolving power of the spectrograph. And at higher pressures, uncertainty resulted from incipient overlapping of the members of the doublet. This then, was a sufficient reason for using a long tube and a short tube, respectively, for the two cases. At the highest pressure (20 mm), the lines were completely overlapped, and accordingly were treated as a single line of strength equal to the sum of the components, a reasonably valid procedure for large $|\nu_0-\nu|$. In addition, the outer wings for the higher pressures were tested for fit to the equation

$$\alpha x = \text{const}\ (N^2 f x)(\nu_0-\nu)^{-a}, \qquad (9)$$

where a, a positive constant, is to be determined.

Vapor pressure data for potassium are rather incomplete. Fiock and Rodebush,[20] for a lower limit of 680°K, found

$$\log_{10} p = -4433/T + 7.183, \qquad (10)$$

where p is the vapor pressure in mm Hg, and T is the absolute temperature. This formula, when extrapolated to lower temperatures, yields pressures only in approximate agreement with those given by other observers; but the latter show considerable disagreement among themselves. For the sake of definiteness, (10) was used here throughout.[21] The density then follows from

[18] H. Kuhn, Proc. Roy. Soc. **158**, 230 (1937).
[19] J. Strong and R. T. Brice, J. O. S. A. **25**, 207 (1935).
[20] Fiock and Rodebush, J. Am. Chem. Soc. **48**, 2522 (1926).
[21] A. R. Gordon, J. Chem. Phys. **4**, 100 (1936), has determined the molecular concentration. At 800°K there is only a 2 percent formation of molecules.

$N=9.70\times10^{18}p/T$. It is probable that (10) yields too small a pressure. Hence, although the relative values of the half-breadths here determined cannot be seriously in error, the absolute values may be a little high.

In evaluating the constant A of (4) for each line, the density N was determined as in the foregoing paragraph, the tube-length x was measured directly, and the oscillator strengths were assumed to have the values $f_s=\frac{2}{3}$, $f_l=\frac{1}{3}$, where s and l refer to the short and long wave-length component, respectively.

Discussion

With the exception of the higher pressures, the dispersion formula (4) was adequate to describe the observed contours, thus confirming the theory of the resonance interaction. The half-breadths were determined for each line from the measured value of $A\Delta\nu_{\frac{1}{2}}$, in conjunction with the known value of A. In Table I is given $(\Delta\nu_{\frac{1}{2}})_s/N$ and $(\Delta\nu_{\frac{1}{2}})_l/N$ (cm³/sec.) for each pressure. No differentiation is there made explicitly as to wing, or as to tube-length. The value given parenthetically for $p=20$ mm, is the average for each wing of the completely overlapped line.

The ratios of the half-breadths, as between the components, are shown in the last column.[22] They are scattered uniformly over the whole pressure range about a mean of 1.05. The theory of the resonance interaction has not been refined sufficiently to deal with fine structure. Hence it is not possible to compare theory and experiment in this connection.*

Table I. *Observed half-breadths.*

T	p	N	$(\Delta\nu_{\frac{1}{2}})_s/N\times10^7$	$(\Delta\nu_{\frac{1}{2}})_l/N\times10^7$	$(\Delta\nu_{\frac{1}{2}})_s/(\Delta\nu_{\frac{1}{2}})_l$
444	1.58×10^{-3}	3.45×10^{13}	2.0	2.3	0.9
461	3.67	7.73	2.0	2.2	0.9
463	4.05	8.47	6.4	6.4	1.0
481	9.18	1.85×10^{14}	3.2	2.8	1.1
498	1.90×10^{-2}	3.71	2.9	2.8	1.0
516	3.89	7.31	2.7	2.7	1.0
518	4.20	7.87	3.1	2.6	1.2
545	1.11×10^{-1}	1.98×10^{15}	4.5	4.1	1.1
555	1.56	2.73	2.2	2.2	1.0
584	3.89	6.47	4.3	4.2	1.0
593	5.09	8.32	3.2	2.4	1.3
633	1.51×10^{0}	2.31×10^{16}	2.4	2.8	0.9
664	3.21	4.69	3.6	3.7	1.0
696	6.47	9.03	3.1	2.4	1.3
755	2.00×10^{1}	2.62×10^{17}	(2.5)		

[22] The difference in the wave-lengths of the components may be disregarded.

The linear dependence of the half-breadths upon N, though evident from the table, is best seen graphically.[23] A plot of $\log_{10}(\Delta\nu_{\frac{1}{2}})$ (without regard to component) against $\log_{10}N$ is given in Fig. 1. The points fit a line of unit slope reasonably well over the entire range.[24] The dashed line represents the theoretical value of $\log_{10}\Delta\nu_{\frac{1}{2}}$ for radiation damping, which should be the limiting value of the half-breadths with decreasing pressures. Observations in this region were not obtained. But agreement with other observers as to the pressure at which "deviation" from natural breadth occurs (see above), is not precluded (here at 0.001 mm, about).

The average value of $\Delta\nu_{\frac{1}{2}}/N$ (both components) is 3.2×10^{-7} cm³/sec., which is about $3/f$, $6/f$, and $2/f$ times that value given by (5), (7), and (8), respectively. Since, in any case, $f\leq1$, a considerable discrepancy exists, one which can hardly be attributable to experimental error. The mean value of the Lorentz collision diameter[13] is $\rho=2.0\times10^{-6}$ cm, in approximate agreement with the results of other observers for Na.

The interpretation of the observed contours at higher pressures is difficult, because of overlapping of the lines, as noted, because of the nonlinear characteristics of the plate, and because of overlapping of the wings of the lines upon the step-weakener images.

The application of (9) yielded a value of the exponent a, usually somewhat greater than 2. Accordingly, for pressures above about a mm, the half-breadths determined by the use of (4) (listed in Table I) are only approximately correct. The completely overlapped contour for $p=20$ mm yielded, from (9), $a_s=2.5$ and $a_l=2.0$, about. This result for the long wave-length wing is hardly a confirmation of (6). But its smaller value, as compared to that for the short wave-

* *Note added in proof.* Dr. W. V. Houston has recently extended the theory to include fine structure. He shows that the component half-breadths should indeed be equal. See abstract of paper presented at the 217th meeting of the American Physical Society (to appear shortly in this publication).

[23] A dependence upon velocity is hardly to be observed unless the temperature be variable independently of N.

[24] Some prior (unpublished) results showed deviations at the lower end. But this may presumably be explained away, as arising from a faulty manner of thermocouple calibration then used.

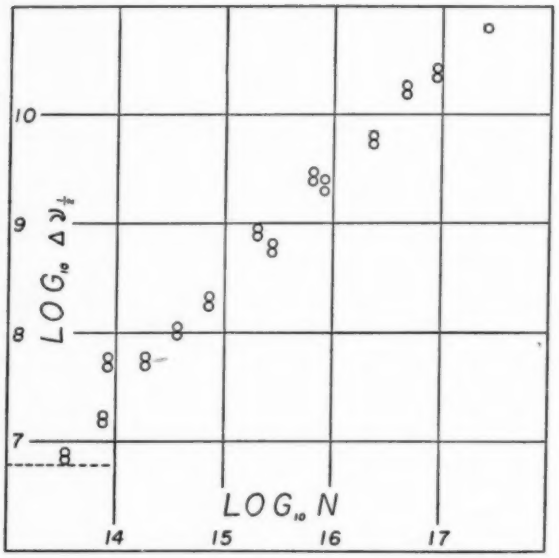

FIG. 1. Showing the linearity of $\Delta\nu_{\frac{1}{2}}$ in N.

length wing, may be attributable to the influence of the van der Waals interaction.

Superimposed upon the long wave-length wing of the much broadened line there appeared a discrete structure, clearly visible only for the plate corresponding to $p=20$ mm. This spectrum was identified as being the infrared bands of K_2,[25] the molecules arising from a weak chemical bond.[26]

A comparison of our K contour at $p=20$ mm, to the microphotometer trace of Kuhn[18] for Hg at $p=7.7$ mm, indicates that the latter exhibits a greater long wave-length asymmetry despite only about $\frac{2}{3}$ the density, but that the broadening (with allowance for a factor N^2fx, and for the difference in wave-length), is considerably less. This result is not surprising, for the resonance forces are expected, theoretically, to be of great importance for K.[27] Kuhn obtained $C=5.4\times10^{-32}$. Then, for Hg, the perturbation energy of (2) is equal to that of (1) ($f\cong1/35$) for $R=9$A, about. But, for K, if we assume the same value of C, and use $f=\frac{1}{3}$, the corresponding distance is only about 3A. This result cannot be correct. But it shows that the neglect of the resonance forces for R values even only slightly greater than that corresponding to the potential minimum, is probably unjustified. Furthermore, in order to separate the effects, higher pressures are required for K, as compared to Hg. Using the above value of C, and $R=4$A, (2) yields $\nu_0-\nu=400$ cm^{-1} (240A). This is within the range of out contour for $p=20$ mm. Now (2) is not likely to be valid for much smaller R values, but if the true value of C for K is appreciably greater than that for Hg, the effect of the van der Waals forces may possibly be separable from that of the resonance forces, and for values of $\nu_0-\nu$ greater than those at which occurs a measurable absorption in the present experiment. But in any case, the statistical contour (6) is less readily observable for K, because of the greater masking of the velocity distribution in view of relatively greater speeds of the atoms. It is to be conceded that these last conclusions may be straining the available experimental data. But it seems likely that accurate quantitative determination of the constant C of the van der Waals interaction for K, is hardly to be expected by this method. The circumstance for Cs, however, is more favorable.

The authors wish to express their considerable indebtedness to Drs. I. S. Bowen and W. V. Houston for their many helpful suggestions, to Dr. R. T. Brice for his having kindly supplied the MgO windows, and to Mr. K. Watanabe for valuable assistance.

[25] For their analysis, see W. O. Crane and A. Christy, Phys. Rev. **36**, 421 (1930).

[26] The existence of van der Waals type molecules for the alkalis has been demonstrated by H. Kuhn, Zeits. f. Physik **76**, 782 (1932), in connection with the higher members of the principal series. Their presence was not here in evidence.

[27] Confirmation of this is forthcoming from comparison of our value of ρ to that given in reference 14 for Hg. For, assuming $N_K=N_{Hg}$, $(\Delta\nu_{\frac{1}{2}})_K/(\Delta\nu_{\frac{1}{2}})_{Hg}\cong(\rho_K)^2/(\rho_{Hg})^2=(200/50)^2=16$.

Collision of Proton and Deuteron

K. OCHIAI*
Physical Institute, Imperial University, Tokyo, Japan
(Received September 7, 1937)

The present calculation is similar to that of Schiff on neutron-deuteron collisions, and is based on the suggestion of Morse that the function $\sin(kr+\delta)-e^{-\alpha r}\sin\delta\cos kr$ will be a good approximation to the actual wave function if the parameters are properly adjusted. By joining this function smoothly with the Coulombian field wave function, we obtain the scattering formula for proton-deuteron collisions, while, by extending this function to infinity, we get the neutron-deuteron scattering. The coordinate system, in which the Hamiltonian is separable, was used, and this is the main difference from Schiff's calculation. The cross section for neutron-deuteron scattering was found to be 3.2×10^{-24} cm² at vanishing neutron energy, in good agreement with experiments. For proton-deuteron scattering, no good agreement was obtained. In the range of angle of scattering less than about 70°, the calculation gives still a tolerable result, but, for larger angles, the experimental scattering increases very rapidly. Such a rapid increase does not seem to be explained without some other important improvement of the theory.

THE wave equation for a system of a deuteron and a proton,[1] in the rest coordinate system, is

$$\left[-\frac{\hbar^2}{2\mu}\Delta_r-\frac{\hbar^2}{M}\Delta_{r_{23}}+V_{12}+V_{13}+V_{23}+\frac{e^2}{r_{12}}-W_D-W\right]\Psi=\left[-\frac{\hbar^2}{2\mu}\Delta_{r'}-\frac{\hbar^2}{M}\Delta_{r_{13}}+V_{12}+V_{13}+V_{23}+\frac{e^2}{r_{12}}-W_D-W\right]\Psi=0, \quad (1)$$

where

μ = reduced mass $=\frac{2}{3}M$,
W_D = binding energy of deuteron,
W = collision energy in the rest system $=\frac{2}{3}W_0$,
W_0 = collision energy in the laboratory system (deuteron initially at rest),
$\mathbf{r}_1$, $\mathbf{r}_2$ = space coordinates of protons 1 and 2,
$\mathbf{r}_3$ = space coordinates of neutron 3,

$$\mathbf{r}=\mathbf{r}_1-\frac{\mathbf{r}_2+\mathbf{r}_3}{2}, \qquad \mathbf{r}'=\mathbf{r}_2-\frac{\mathbf{r}_1+\mathbf{r}_3}{2}=P(\mathbf{r}_1\mathbf{r}_2)\mathbf{r},$$

$$\mathbf{r}_{23}=\mathbf{r}_2-\mathbf{r}_3, \qquad \mathbf{r}_{13}=\mathbf{r}_1-\mathbf{r}_3$$

and P is the interchange operator. We assume a solution of the form

$$\Psi=\psi_D(23)\psi(r,\theta)S(1,2,3)+\psi_D(13)\psi'(r',\theta')S'(1,2,3), \quad (2)$$

$$S'(1,2,3)=S(2,1,3),$$

where S is the spin function,[2] and $\psi_D(ij)$ is the deuteron wave function, satisfying

$$[-(\hbar^2/M)\Delta_{r_{ij}}+V_{ij}-W_D]\psi_D(ij)=0.$$

θ and θ' are the angles between the direction of the initial current and the vectors $\mathbf{r}$ and $\mathbf{r}'$, respectively.

Putting (2) into (1), we have

$$[-(\hbar^2/2\mu)\psi_D(23)\Delta_r\psi+V\psi_D(23)\psi-W\psi_D(23)\psi]S+[-(\hbar^2/2\mu)\psi_D(13)\Delta_{r'}\psi'+V'\psi_D(13)\psi'-W\psi_D(13)\psi']S'=0 \quad (3)$$

with

$$V=V_{12}+V_{23}+(e^2/r_{12}), \quad V'=V_{12}+V_{23}+(e^2/r_{12}).$$

Considering the nature of nuclear forces, these potential energies may be replaced by

$$V=\begin{cases}V_{12}+V_{13}, & r<r_0\\ (e^2/r) & r>r_0\end{cases}, \qquad V'=\begin{cases}V_{12}+V_{23}, & r'<r_0\\ (e^2/r'), & r'>r_0\end{cases} \quad (4)$$

where r_0 is a certain distance of the order of nuclear radius, at which nuclear forces practically vanish.

We will try to solve the Eq. (3) by the method of pertubation.[3] For this purpose, it is convenient to introduce a new potential U instead of V, which can be interpreted as the average potential of a proton in the field of a deuteron.

* At present a guest at the Massachusetts Institute of Technology.

[1] Schiff, Phys. Rev. **52**, 149 (1937).

[2] For spin functions, see Schiff, reference 1. We will write S and S' for $S(1,2,3)$ and $S'(1,2,3)$, respectively.

[3] This may be allowed for a qualitative discussion of lightest nuclei, where statistical treatment is impossible, although the method is in general inapplicable to heavier nuclear collisions (Bethe, Rev. Mod. Phys. **9**, 71 (1937)).

$$U(r)=\begin{cases}\bar{V}_{12}+\bar{V}_{13}, & r<r_0\\ (e^2/r), & r>r_0\end{cases}$$
$$U(r')=\begin{cases}\bar{V}_{12}+\bar{V}_{23}, & r'<r_0\\ (e^2/r'), & r'>r_0\end{cases} \quad (5)$$

Here $\bar{V}$ is some suitable average of V over the deuteron coordinates, the position of the unbound proton being fixed. If a good choice of this U were obtained, we may consider

$$V-U(r)\ll V, \quad V'-U(r')\ll V'.$$

Now we assume that, proton 2 is initially bound to neutron 3. Then the main term in (2) is that which contains $\psi(r,\theta)$. Dividing $\psi(r,\theta)$ into two parts $\psi(r,\theta)=\psi_0(r,\theta)+\psi_1(r,\theta)$, where ψ_0 satisfies

$$[-(\hbar^2/2\mu)\Delta_r+U(r)-W]\psi_0(r,\theta)=0. \quad (6)$$

we may consider solution (2) as consisting of three parts: ψ_0 (first approximation), ψ_1 and ψ' (second approximation).

Multiplying (3) by $S\psi_D^*(23)$ and integrating (spin summation also included), we get

$$[-(\hbar^2/2\mu)\Delta_r+U(r)-W]\psi_1 = -\int S\psi_D^*(23)(V-U)\psi_D(23)\psi_0 Sd\tau_{23}. \quad (7)$$

Similarly

$$[-(\hbar^2/2\mu)\Delta_{r'}+U(r')-W]\psi' = -\int S'\psi_D^*(13)(V-U)\psi_D(23)\psi_0 Sd\tau_{13}. \quad (8)$$

The problem is now: (i) to find U, (ii) to solve (6), (7), (8). It will be found later that

$$U(r)=\begin{cases}1-De^{-\beta r^2}, & r<r_0\\ (e^2/r), & r>r_0\end{cases} \quad (9)$$

is a good approximation for U, where the constant D must be chosen differently for the two different spin states, quartet and doublet.

For $r>r_0$, where $U(r)$ is Coulombian, the Eq. (6) (if expanded into spherical harmonics) has two linearly independent solutions $F_l(\rho)$ and $G_l(\rho)$, which behave asymptotically like[4]

$$F_l(\rho)\sim\sin(\rho-(l\pi/2)-\eta\log 2\rho+\sigma_l),$$
$$G_l(\rho)\sim\cos(\rho-(l\pi/2)-\eta\log 2\rho+\sigma_l).$$

Hence

$$\psi_0=\sum_{l=0}^{\infty}i^l(2l+1)P_l(\cos\theta)e^{i(\sigma_l+K_l)} \times\{A_lF_l(\rho)+B_lG_l(\rho)\}/\rho, \quad r>r_0 \quad (10)$$
$$\rho=kr, \quad k=(2\mu W)^{\frac{1}{2}}/\hbar=\mu v/\hbar, \quad \eta=e^2/(\hbar v),$$
$$\sigma_l=\arg\Gamma(l+1+i\eta),$$

v=initial relative velocity, $\tan K_l=B_l/A_l$. This becomes asymptotically

$$\psi_0\sim\left[1-\frac{\eta^2}{2ikr\sin^2\theta/2}\right]e^{ikr\cos\theta+i\eta\log 2kr+i\eta\log\sin^2(\theta/2)}-\frac{e^{ikr-i\eta\log 2kr-i\eta\log\sin^2(\theta/2)+2i\sigma_0}}{r} \times\left[\frac{\eta}{2k\sin^2\theta/2}+\frac{i}{2k}\sum_{l=0}^{\infty}(2l+1)(e^{2iK_l}-1)P_l(\cos\theta)e^{i\eta\log\sin^2(\theta/2)+2i(\sigma_l-\sigma_0)}\right].$$

The important quantity K_l (or the ratio B_l/A_l) for the calculation of the cross section can be deetrmined by requiring that the solution of (6) for $r<r_0$, should join smoothly with (10) at $r=r_0$. Namely, if we put for $r<r_0$, instead of (10),

$$\psi_0=\sum_{l=0}^{\infty}i^l(2l+1)P_l(\cos\theta)e^{i(\sigma_l+K_l)}R_l(\rho)/\rho \quad (r<r_0), \quad (11)$$

then the conditions

$$\left.\begin{aligned}R_l(\rho)&=A_lF_l(\rho)+B_lG_l(\rho)\\ \frac{dR_l(\rho)}{d\rho}&=A_l\frac{dF_l(\rho)}{d\rho}+B_l\frac{dG_l(\rho)}{d\rho}\end{aligned}\right\}\text{at } r=r_0 \ (\text{or } \rho=kr_0=\rho_0)$$

determine $\tan K_l=B_l/A_l$. Assuming that only the partial wave $l=0$ is appreciably affected by the internuclear forces, while all other partial waves $l\geqq 1$ remain practically the same as in the

[4] Breit, Condon and Present, Phys. Rev. **50**, 825 (1936); Yost, Wheeler and Breit, Phys. Rev. **49**, 174 (1936).

case of purely Coulombian field (i.e., $K_l=0$ for $l\geqq 1$), we need only to calculate K_0 by

$$\frac{\rho}{R_0(\rho)}\cdot\frac{dR_0(\rho)}{d\rho}=\frac{\Phi_0^*(\rho)}{\Phi_0(\rho)} - \frac{1}{\Phi_0(\rho)\Theta_0(\rho)+C_0^2\rho\Phi_0^2(\rho)\cot K_0} \quad \text{at } \rho=\rho_0$$

Φ_0, Φ_0^*, Θ_0 and C_0 being defined in the papers mentioned above. Following the procedure of Morse,[5] we set

$$R_0=A[\sin(kr+\delta)-e^{-\epsilon r}\sin\delta\cos kr], \quad (12)$$

where A takes care of the possible change of amplitude due to the Coulombian field, and ϵ is obviously of the order of magnitude of the constant $(\beta)^{\frac{1}{2}}$ in the potential function (9). We put simply $\epsilon/(\beta)^{\frac{1}{2}}=2$, since this choice of the ratio seems to provide a good correspondence of the potential $e^{-\beta r^2}$ to that of Morse type $-2e^{\epsilon r}+e^{-2\epsilon r}$. The parameter δ will be determined later for each specified value of k.

We will now proceed to solve the equations of second approximation (7) and (8). These equations differ from the equation of first approximation (6) only by the existence of their right-hand side integrals, and these integrals vanish as r or r' becomes greater than r_0, the Coulombian parts in U and V canceling each other out. So that, for r or $r'>r_0$, the solutions ψ_1 and ψ' are again expressible by the Coulombian field wave functions F_l and G_l. Further we want such a solution which asymptotically represents only a divergent spherical wave. Such a solution is obtainable, when the solution of the homogeneous equation is already known. The method is given by Mott and Massey,[6] which applies also to our case with a slight modification due to the existence of Coulombian potential.

Retaining only the partial wave $l=0$, we get

$$\psi_1\sim\frac{e^{i(kr-\eta\log 2kr+2\sigma_0+2K_0)}}{r}g,$$

$$\Psi'\sim\frac{e^{i(kr'-\eta\log 2kr'+2\sigma_0+2K_0)}}{r'}g',$$

$$g=-\frac{1}{4\pi}\cdot\frac{2\mu}{h^2}\int S\frac{R_0(kr)}{kr}\psi_D^*(23)(V-U)\times\psi_D(23)\frac{R_0(kr)}{kr}Sd\mathbf{r}_{23}d\mathbf{r}, \quad (13)$$

$$g'=-\frac{1}{4\pi}\cdot\frac{2\mu}{h^2}\int S'\frac{R_0(kr')}{kr}\psi_D^*(13)(V-U)\times\psi_D(23)\frac{R_0(kr)}{kr}Sd\mathbf{r}_{13}d\mathbf{r}'. \quad (14)$$

After antisymmetrizing the final wave function with respect to the two protons 1 and 2, the cross section will be given by the square of the absolute value of the coefficient of e^{ikr}/r in the asymptotic expression of $\psi_0(r,\theta)+\psi_1(r,\theta)-\psi'(r,\theta)$: namely by

$$\left|-\frac{\eta}{2k\sin^2(\theta/2)}+\frac{e^{iK_0}\sin K_0}{k}e^{i\eta\log\sin^2(\theta/2)} +(g-g')e^{2iK_0+i\eta\log\sin^2(\theta/2)}\right|^2. \quad (15)$$

Results

As a first step to approximation, we have calculated $U(r)$ by

$$U(r)=\int\psi_D^*(23)S(V_{12}+V_{13})\psi_D(23)Sd\mathbf{r}_{23}$$

with

$$V_{ij}=-e^{-\alpha r_{ij}^2}[C_M P(\mathbf{r}_i\mathbf{r}_j)+C_H P(\mathbf{r}_i\mathbf{r}_j)P(\boldsymbol{\sigma}_i\boldsymbol{\sigma}_j)]$$

$$\psi_D(ij)=(N_D)^{\frac{1}{2}}e^{-(\nu_D/2)r_{ij}^2}.$$

The values of the constants are[7]

$$C_M+C_H=60,\ C_H=12.7,\ \alpha=11.5,\ \nu_D/\alpha=0.89$$

in nuclear units (length $h/c(nM)^{\frac{1}{2}}$, energy mc^2).

The integration is to be performed under fixed r, and the space exchange operator was omitted for the moment, keeping only the spin exchange operator. It was found that $U(r)$ is of the form (9), with the constants: $D=D_q=82.6$ for quartet, $D=D_d=56.4$ for doublet, and $\beta=9.0$ (always in nuclear units unless otherwise stated). Thus the

[5] Morse, Phys. Rev. **51**, 1003 (1937); Morse, Fisk and Schiff, Phys. Rev. **51**, 706 (1937).

[6] Mott and Massey, *The Theory of Atomic Collisions*, p. 101.

[7] These values are roughly in agreement with those of Morse and Schiff, if appropriate correspondence is established between both types of potential.

TABLE I. *Values of* δ.

$W_0(mc^2)$	QUARTET	DOUBLET
0	$\pi(\Delta_q=-0.462)$	$\pi(\Delta_d=-0.500)$
1	$\pi-24°.3$	$\pi-26°.2$
2	$\pi-33°.7$	$\pi-36°.1$

constant ϵ in the function R_0 was fixed: $\epsilon=2(\beta)^{\frac{1}{2}}=6.0$. Another constant δ for the case $k=0$, or the constant Δ defined by $\Delta=-\lim_{k\to 0}(\sin\delta/k)$ is found to be $\Delta_q=-0.412$ for quartet and $\Delta_d=-0.451$ for doublet.

These values must be corrected so as to include to some extent the exchange operator $P(\mathbf{r}_i\mathbf{r}_j)$ in V_{ij}. For this we will require that the function R_0 should represent the true wave function as nearly as possible apart from the exchange integral g', or in other words, g should be zero. This was done only for vanishing energy $k\to 0$. Namely we have adjusted D and Δ in such a way that $g\to 0$ as $k\to 0$. In carrying out the integration g, we must deal with the integral of the form

$$\int\frac{R_0(kr)}{kr}\exp\left[-ar^2-b\rho^2-c(\mathbf{r}\cdot\boldsymbol{\rho})\right]\frac{R_0(kr')}{kr'}d\mathbf{r}d\boldsymbol{\rho},$$

$$r'=\text{const.}\,[(\mathbf{r}-\boldsymbol{\rho})^2]^{\frac{1}{2}}$$

and $R_0(kr)/kr$ is of the form const$\cdot[1+(\Delta/r)\times(1-e^{-\epsilon r})]$ for $k\to 0$. The expansion[8]

$$\frac{e^{-\lambda[(r^2+\rho^2-2r\rho\cos\varphi)]^{\frac{1}{2}}}}{[(r^2+\rho^2-2r\rho\cos\varphi)]^{\frac{1}{2}}}=\sum_{n=0}^{\infty}(2n+1)\times\frac{K_{n+\frac{1}{2}}(\lambda\rho)}{(\rho)^{\frac{1}{2}}}\frac{I_{n+\frac{1}{2}}(\lambda r)}{(r)^{\frac{1}{2}}}P_n(\cos\varphi)\quad(\rho>r)$$

and similar ones for $e^{\lambda\cos\varphi}$ and

$$1/[(r^2+\rho^2-2r\rho\cos\varphi)]^{\frac{1}{2}}$$

were used. However, these are already very complicated. We have, therefore, averaged the integrand with respect to $\cos(\widehat{\mathbf{r}\boldsymbol{\rho}})$ before integration, i.e., we have taken only the first terms of the expansions into account. Then the integration over $\boldsymbol{\rho}$ produces terms expressed in error functions. The last step was done numerically.

The corrected values are

$$D_q=53,\quad \Delta_q=-0.462,\quad D_d=44,\quad \Delta_d=-0.500,$$

for which $g=0$ for both cases. We adopted these values for $U(r)$, and calculated δ for each assigned value[9] of k (Table I).

The exchange integral g' can be carried out in the same manner as g. This was calculated only for vanishing k, and the values obtained are: $g_q'=+0.151A^2$, $g_d'=-0.047A^2$ for quartet and doublet, respectively.

Before entering into the calculation of K_0, we will briefly discuss neutron-deuteron collisions. If we omit all the terms arising from the Coulombian interaction and extend the function R_0 to infinity, therefore, if we put $\eta=\sigma_0=0$, $A=1$, $K_0=\delta$ in (15), it becomes the cross section formula for neutron-deuteron scattering. For the values given above, the mean cross section is 3.23×10^{-24} cm^2 at vanishing neutron energy. If the exchange integral g' is omitted it is only 2.28×10^{-24} cm^2. This is about one-half of Schiff's result, and the agreement with experiments is satisfactory. The cross section decreases to 1.82×10^{-24} cm^2 at the neutron energy of 1 Mev (without exchange; exchange effect would probably be small). We believe that this improvement of agreement (although the calculation is still a qualitative one) is due to the different use of the coordinate system from that used by Schiff, rather than the different forms of the potential functions. The exchange integral makes the quartet-scattering larger than the doublet-scattering by a factor about 2 (omitting different statistical weights). This effect is much more remarkable in Schiff's result (factor 6 instead of 2). We have now to join the function R_0 with the Coulombian field wave function at some suitable distance $r=r_0$. For this r_0, we have taken (i) the distance at which the combined potential Coulombian plus $-De^{-\beta r^2}$ attains its maximum, (ii) the distance at which these potentials just cancel each other. The results are only slightly different in both

TABLE II. *Values of* K_0.

$W_0(mc^2)$	QUARTET	DOUBLET
1	$\pi-14°.2$	$\pi-15°.6$
2	$\pi-24°.1$	$\pi-26°.1$

[8] Watson, *Theory of Bessel Functions* (1922), p. 366.

[9] Professor Morse has kindly provided me with the table of integrals of the form $\int_0^\infty e^{-\frac{1}{4}r^2-ar}\frac{\sin}{\cos}\beta r dr$ necessary for this calculation.

cases. We give here only the result based on the latter choice. The values of K_0 are given in Table II. The amplitude A in (12) was found to be increasing slightly with increasing energy. It is about 0.90 at $W_0=1$ mc², and is about 0.94 at $W_0=2\ mc^2$.

The cross sections for quartet and doublet states were calculated by (15) and, by adding them in the ratio 2 : 1, the mean cross section was obtained.

The ratio of actual cross section to that of Rutherford is given in Table III. Here Θ is the scattering angle in the laboratory coordinate system. In the fourth column, we have attempted to estimate the effect of exchange. It was assumed that the exchange integral is decreasing with increasing energy, and at $W_0=1\ mc^2$ it is about one-half of its value at vanishing energy. At $W_0=2\ mc^2$, the exchange effect would probably be unimportant.

According to the experiment of Tuve, Heydenburg and Hafstad[10] at the energy of 0.83 Mev, this ratio of cross sections does not show a smooth increase with increasing scattering angle. In the range $60°<\Theta<75°$, the experimental points are found between about 10 to 20. It increases suddenly at about $\Theta=80°$, reaching a value more than 120 at 90°, and increasing still more rapidly with increasing Θ. It is impossible to get such a high value by taking only K_0 into account. We also tried to see whether it is possible to check the experimental curve by choosing K_0 and K_1 suitably. But no appreciable improvement in the agreement was obtained. The assumption[11] that many more K_l values are playing an important

TABLE III. *Ratio of cross sections actual/Rutherford.*

θ	Θ	$W_0=1\ mc^2$ WITHOUT EXCHANGE	$W_0=1\ mc^2$ WITH EXCHANGE	$W_0=2\ mc^2$ WITHOUT EXCHANGE
20°	13°.4	1.076	1.082	1.21
40°	26°.9	1.47	1.53	2.30
60°	40°.9	2.30	2.49	5.0
80°	55°.6	3.6	4.0	9.7
100°	71°.7	5.3	6.1	16.4
120°	90°	7.2	8.4	24
140°	112°.5	9.0	10.5	32
160°	142°.1	10.3	12.1	38
180°	180°	10.7	12.6	40

rôle in the scattering formula, does not seem to be probable in the case of short range interaction.

Finally, the effect of polarization of the deuteron due to the Coulombian interaction with the incoming proton was estimated as follows. We have assumed, as the wave function of the polarized deuteron,

$$\psi_D=\frac{1}{[1+f^2(r)/3]^{\frac{1}{2}}}\phi_0(23)[1+f(r)\cos\varphi],$$

where r has the same meaning as before, ϕ_0 is the unpolarized deuteron wave function, and φ is the angle between the vectors $\mathbf{r}$ and $\mathbf{r}_{23}$.

$f(r)$ was determined by the method of variation, so as to minimize the energy of the polarized deuteron, for each assigned value of r. It was found that $|f(r)|<0.04$, and the effect seems to be quite small.

Therefore, it does not seem likely that such a large backward scattering as is found in the experiments of Tuve, Heydenburg and Hafstad can be explained satisfactorily by calculations of the sort discussed here.

In conclusion, the writer wishes to express his cordial thanks to Professor Philip M. Morse and Dr. L. I. Schiff for much helpful advice.

[10] Tuve, Heydenburg and Hafstad, Phys. Rev. **50**, 806 (1936).

[11] *Note added in proof:* It is possible that a resonance effect, such as is discussed by Primakoff, Phys. Rev. **52**, 1000 (1937), will account for part of the discrepancy with experiment, though not with all of it.

Indication of a Genetic Relation Between Indium and Tin

E. D. EASTMAN
Department of Chemistry, University of California, Berkeley, California
(Received November 1, 1937)

Existing data reveal a widespread association of indium with tin in ores of the latter element. This is taken as an indication of a genetic relation, ascribed to a "forbidden" transition of Sn^{115} to In^{115}.

ISOBARS of adjacent elements of the periodic system (nuclei of equal mass number and unit difference in atomic number) are mutually transformable, in the direction of increasing atomic number by the emission of an electron and a neutrino, and in the reverse direction by the emission of a positron or absorption of an electron, again with emission of a neutrino. The existence of couples of this type in which there is no detectable activity raises at once the question as to whether such species are energetically stable with respect to each other, or whether one member is unstable but of long life. According to the theory of Yukawa and Sakata[1] true stability is possible within a range of mass difference of the atoms of the pair equal to twice the mass of the neutrino. Only if the mass of the neutrino is zero is stability impossible for both members of the pair. But if the neutrino mass, though finite, is very small in comparison with the electronic mass, as the slope near the end point of β-ray distribution curves indicates, occurrence of stable pairs should be very infrequent. The occurrence of apparently stable pairs actually is relatively infrequent,[2] but more common than would be probable on the above basis.

Failure of direct detection of radioactivity in these cases may most probably be ascribed therefore to low rates of transformation. These might result from very small mass differences, from unfavorable spin relationships, or from unfavorable mass differences as far as the K electrons (which have the highest probability of reaction) are concerned in cases where the only process possible is the absorption of an extra-nuclear electron by one member of the pair. In the attempt to prove the occurrence of a transformation, resort must then be made to indirect evidence, such as the universal association, or lack of it, of the two members of the pair in minerals of sufficient geological age.

One of the best established examples of the couples in question is found in In^{115} and Sn^{115}. A rough calculation outlined in the earlier paper[2] indicates the instability of the tin isotope. In the hope of obtaining evidence concerning the transformation, a review of existing data on the mineralogical association of indium with tin has been made, with results outlined below.

Indium occurs associated in small amounts with many other elements, among which tin is often included. Interest centers in the present connection, however, in minerals in which tin is present in large proportion. The earliest data bearing upon this point are found in the work of Hartley and Ramage,[3] who investigated spectroscopically many samples of various ores and minerals. Among these were included five ores of tin, two cassiterites (SnO_2) and one tinstone (SnO_2) from Cornwall, one tinstone from Saxony and one stannite ($FeCu_2SnS_4$) of unknown origin. Each of these showed the presence of indium.

The next observations of interest are those of Garrett[4] and Green[5] concerning the presence of indium in metallic tin. Garrett found the element to be present in spectroscopically detectable quantity in all available samples of tin metal, including highly refined samples. Green also investigated a number of samples of the metal, in only four of which indium was not detected. Two of these were highly purified samples, and two less pure of unknown source. These obser-

[1] Yukawa and Sakata, Proc. Phys. Math. Soc. Japan **17**, 467 (1935).

[2] This fact, in connection with the assumption that both members of isobaric pairs cannot be stable, was used in an earlier paper (Phys. Rev. **46**, 1 (1934), cf. pp. 5, 15) in support of the idea that electron capture is a process of considerable probability in energetically favored cases.

[3] Hartley and Ramage, J. Chem. Soc. **71**, 533 (1897).

[4] Garrett, Proc. Roy. Soc. **114A**, 289 (1927).

[5] Green, Nature **119**, 893 (1927).

vations indicate a widespread occurrence of indium in the ores of tin.

Brewer and Baker,[6] interested in the discovery of richer sources of indium through a study of its association with other elements in minerals, and actuated by the observations of Garrett, carried out a systematic investigation of tin ores. They examined a total of thirteen oxide ores and four sulfide ores. The oxides comprised ten samples of cassiterite, of which seven were from Cornwall and one each from Malay, Bolivia and Tasmania, one sample of Cornish stream tin, noted to be geologically distinct from the tinstones, and two samples, one pegmatite and one alluvial, from Nigeria. The sulfides were cylindrite ($Pb_6Sb_2Sn_6S_{21}$), franckeite ($Pb_5Sb_2Sn_2S_{12}$) and teallite ($PbSnS_2$), all from Bolivia, together with a Cornish stannite. Several of the Cornish cassiterites proved to be of very high purity, and afforded the only examples in which no indication of indium was found. Six of these samples, including the three in which indium was not detected, were obtained from one mining company. The more perfectly crystallized material, presumably occurred therefore together with less pure material which did contain indium. The crystallization process in these cases had evidently taken place under conditions resulting in very complete exclusion of impurities. If the crystallization occurred in relatively recent time, the failure to find indium by the technique employed (which was not intended to be of maximum sensitivity,[7] does not necessarily offset in the present argument the otherwise uniformly established association.

The chemistry of indium and tin is not sufficiently similar to result in frequent association of the type often found with elements of the same periodic group. Tin in its ores is usually tetravalent and indium trivalent. The crystal radii in these valences are about 0.73 and 0.86A, respectively. These differences in valence and radius of the ions make any significant isomorphism of their compounds unlikely. The latter phenomenon however may well be responsible for the relative enrichment of indium in the complex sulfide ores containing antimony, which is trivalent and no doubt of about the same ionic radius as indium. On the whole, it appears improbable that a chemical segregation of indium with tin is responsible for its presence in the minerals discussed above.

Before complete acceptance of evidence of the kind presented here, further experimental studies designed to discover any relation which may exist between the proportion of indium and tin and the age and history of the ore, and also the proportion[8] of the isotopes of indium in the element obtained from tin ores are desirable. As far as the present evidence goes, however, it indicates a genetic relation of indium to tin, of which the transformation discussed above is the most obvious explanation.

The spin of In^{115} is given by Jackson[9] as 9/2. That of Sn^{115} is unknown but the species Sn^{117} and Sn^{119} are assigned by Tolansky[10] a value of $\frac{1}{2}$. The transition between Sn^{115} and In^{115} would seem therefore to be of a strongly "forbidden" type, accounting for its slowness, if it occurs.

[6] Brewer and Baker, J. Chem. Soc., 1286 (1936).

[7] The percentages of indium when reported as definitely present were usually of the order of 0.001 to 0.01, except in the samples of cylindrite and franckeite, where they were 0.1 to 1.0.

[8] In^{115} comprises 95.5 percent of the element and In^{113} 4.5 percent. There are eleven known isotopes of tin, Sn^{115} comprising 0.44 percent.

[9] Jackson, Zeits. f. Physik **80**, 59 (1933).

[10] Tolansky, Proc. Roy. Soc. **A144**, 574 (1934).

The Neutron Absorption Limit in Cadmium

J. G. HOFFMAN AND M. STANLEY LIVINGSTON
Cornell University, Ithaca, New York

(Received November 1, 1937)

In order to find the high energy absorption limit in Cd the absorption in boron of the transmitted neutrons was measured. The slow neutron absorption coefficient in boron is found to be 38 cm²/g in agreement with Amaldi and Fermi. The Cd penetrating neutrons are inhomogeneous in energy and therefore are not absorbed exponentially but according to the law $(1-e^{-x})/x$, where $x=\kappa\delta$, κ is the absorption coefficient for neutrons just penetrating Cd and δ is the thickness of boron traversed. κ is found to be 9.5 cm²/g B. A sheet of Cd 0.5 mm thick reduces the neutron counts to 8.4 percent of the total; 5.7 percent are absorbable in heavy layers of boron. Assuming the $1/v$ law for the absorption of neutrons in boron the absorption limit in Cd is found to be 0.41 ev. With the aid of data from the wheel experiment of Rasetti and collaborators the resonance energy and the half-width are calculated and are $E_r=0.18$ ev and $\Gamma=0.15$ ev, respectively. An estimate is made of the neutron width which turns out to be $\Gamma_n=1.3\times10^{-3}$ ev.

INTRODUCTION

THE Wigner-Breit formula for the absorption cross section, σ, for neutrons in a given element,

$$\sigma=\frac{1}{E^{\frac{1}{2}}[(E-E_r)^2+\Gamma_i^2]} \qquad (1)$$

indicates that the absorption of neutrons should take place as $1/E^{\frac{1}{2}}$, or $1/v$, in an energy interval far removed from the region of the resonance energy, E_r. Experimental results obtained from the mechanical velocity selector of Rasetti and collaborators[1] indicate that the absorption of slow neutrons in Cd does not follow the $1/v$ law but remains constant in an interval of neutron energies of approximately 20 percent about $\frac{3}{2}kT$. On the other hand, Moon and Tillman[2] and Powers and collaborators[3] have shown that neutrons cooled down to 95°K have a greater absorption coefficient in Cd than neutrons in thermal equilibrium at 300°K, the difference amounting to 7 percent. Thus, if it is assumed that neutrons are in thermal equilibrium with the paraffin at these temperatures, it appears that the absorption of slow neutrons in Cd is governed by no simple law. The Wigner-Breit formula suggests a resonance level lying in or just above the region of thermal energies.

The method for determining the high energy limit has been described by Bethe.[4] The absorption coefficient for neutrons transmitted by Cd was measured in boron, it being assumed that the absorption in boron follows the $1/v$ law.

EXPERIMENTAL PROCEDURE

The Rn-Be source of neutrons was placed inside a lead sphere of 3.65 cm radius around which was fastened a paraffin shell 7.1 cm thick as shown in Fig. 1. The distance from the center of the Rn-Be source to the outer surface of the paraffin shell was 10.75 cm. The outer wall of the BF_3 gas chamber for the detection of the neutrons was placed 6.4 cm from the paraffin surface. This chamber had a shielding jacket of B_4C of thickness equivalent to 0.391 g B/cm² the end of which lapped over the end of the chamber in order to define accurately the aperture, 2.6 cm diameter, over which the absorbers were placed. A shield of 20 mil Cd equivalent to 0.582 g Cd/cm² covered the boron shield. The chamber was operated at 500 volts. The pulses due to the disintegration of B were fed directly to the first tube of a linear amplifier of the type described by Dunning,[5] and recorded by a scale-of-eight counter.[6] The sphere was suspended by a $\frac{1}{8}''$ brass rod from the ceiling into the center of the room so that the nearest scattering surface was 150 cm away. Similarly, in order to reduce scattering effects, the chamber was mounted on

[1] Rasetti, Segrè, Fink, Dunning and Pegram, Phys. Rev. **49**, 104 (1936).
[2] Moon and Tillman, Nature **136**, 66 (1935).
[3] Powers, Fink, and Pegram, Phys. Rev. **49**, 650 (1936).
[4] H. Bethe, Rev. Mod. Phys. **9**, 148 (1937).
[5] J. R. Dunning, R. S. I. **5**, 387 (1934).
[6] Wynn-Williams, Proc. Roy. Soc. **A136**, 312 (1932).

an iron pipe framework. It was found that with no absorber before the aperture a Rn-Be source of 462 mC gave 700 counts per minute. The number of counts produced by neutrons penetrating 20 mil thick layer of Cd was 8.4 percent of the total; 5.7 percent are absorbable in thick layers of boron. The remaining 2.7 percent of counts is probably due to fast neutrons disintegrating B or F, gas atoms recoiling from fast neutrons, or stray neutrons entering the chamber through the shields.

Experimental Results and Discussion

Boron absorption curves were taken with and without a 20 mil Cd filter. Pyrex plates gave thin boron layers, there being 0.0294 g B/cm² in a $\frac{1}{8}$″ plate. Fig. 2 shows the trend of the absorption. Since neutrons enter the chamber from a spherical surface, an obliquity correction is necessary. This was calculated assuming that the distribution of neutrons emerging from the surface is given by the Fermi law, $\cos\theta+\sqrt{3}\cos^2\theta$, where θ is the angle from the normal to the surface. It must also be taken into account that the neutrons entering along the axis of the chamber traverse more BF_3 than those entering obliquely and therefore have a greater probability of being counted. Mainly for this reason, the obliquity correction turns out to be very small, *viz.* about 10 percent. With this correction applied the absorption coefficient of the neutrons emerging from the sphere is 36 cm²/g B. This figure was obtained in an absorber which reduced the intensity of thermal neutrons by a factor $e^{-1.16}$; according to reference 4, Fig. 15, this

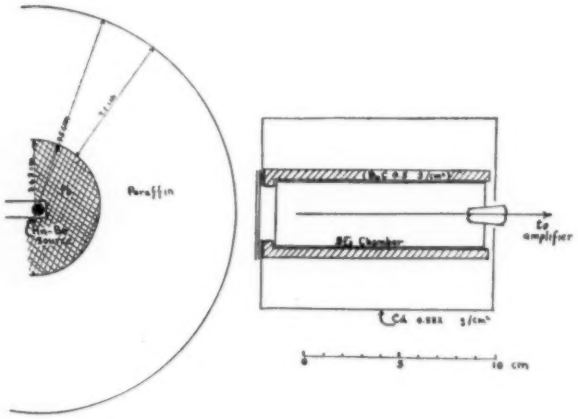

Fig. 1. Arrangement of source and ionization chamber.

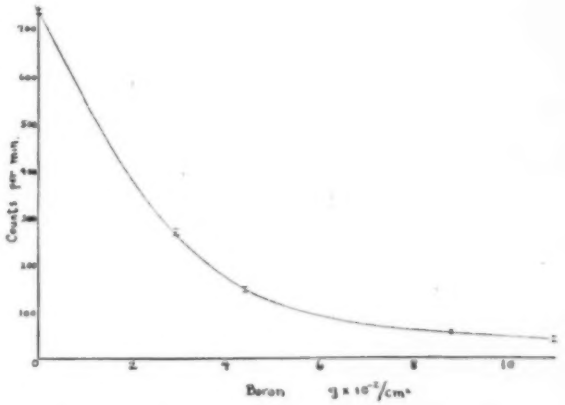

Fig. 2. Absorption of neutrons in Pyrex plates.

corresponds to neutrons having an average energy of 1.12 kT. Therefore, the boron absorption coefficient determined from the $1/v$ law for an energy kT would be $36(1.12)^{\frac{1}{2}}\approx 38$ cm²/g B. This is in exact agreement with the result of Amaldi and Fermi[7] who give 38 cm²/g B for the "C" group (exact energy not stated). Goldsmith and Rasetti[8] give 28 cm²/g B for neutron energies $E=kT$.

The absorption curve for neutrons in Cd is given in Fig. 3; its essential feature is that the 20 mil Cd filter (0.582 g Cd/cm²) reduces the counts per minute to 8.4 percent of the initial rate. The ratio of the number of transmitted neutrons to the number with no Cd present was determined by taking 10,024 counts over a period of 60 minutes with no Cd and 841 counts in 60 minutes with the 20 mil Cd. The ratio was found to be 0.084 ± 0.002.

Absorption curves in thick layers of boron were taken with neutrons filtered through 20 mil Cd, Fig. 4. These layers were made of B_4C of various thicknesses up to 2.44 g B_4C/cm². It can be shown that this absorption curve is given by the expression:

$$I/I_0=1-e^{-x}/x, \qquad (2)$$

where $x=\kappa\delta$, κ is the absorption coefficient of neutrons just penetrating Cd, and δ is the thickness of the absorbing layer of boron. This expression follows from the Fermi distribution law according to which the number of neutrons per cm² and second in the energy interval dE is

[7] Amaldi and Fermi, Phys. Rev. **50**, 899 (1936).
[8] Goldsmith and Rasetti, Phys. Rev. **50**, 328 (1936).

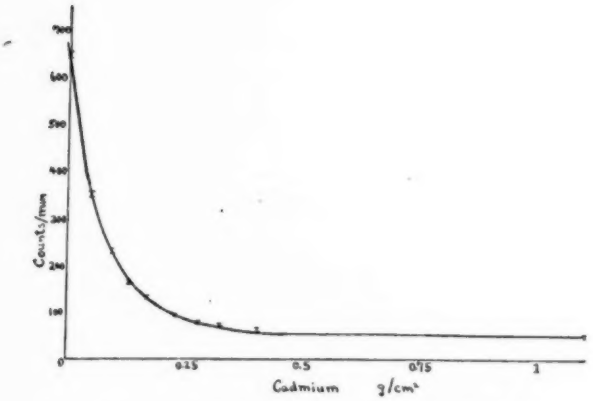

FIG. 3. Absorption of neutrons in cadmium.

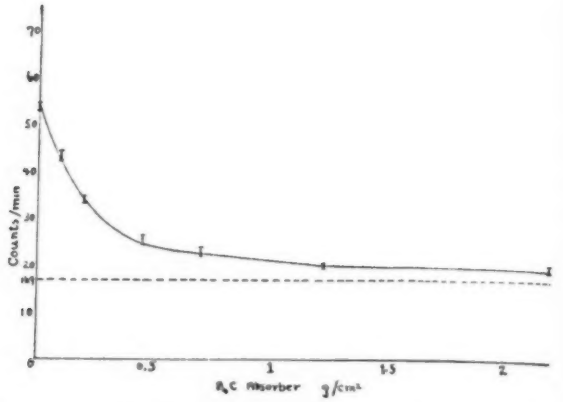

FIG. 4. Absorption of neutrons in B_4C filtered through 0.582 g/cm² Cd.

$N(E)\sim dE/E$. The BF_3 chamber sensitivity is a function of neutron energy given by $1/E^{\frac{1}{2}}$. The boron layer absorbs as $\exp[-\kappa\delta(E_L/E)^{\frac{1}{2}}]$ according to the $1/E^{\frac{1}{2}}$ law of absorption, where E_L is the upper energy limit for neutrons absorbed in Cd. Thus the total number of neutrons detected will be:

$$C\int_{E_L}^{\infty}(1/E^{\frac{1}{2}})\exp[-\kappa\delta(E_L/E)^{\frac{1}{2}}]dE/E$$
$$=2C(E_L)^{-\frac{1}{2}}(1-e^{-\kappa\delta})/\kappa\delta.$$

The proportionality constant, C, is determined by the condition $I=I_0$ for $\delta=0$ which immediately gives the expression (2). The dotted line in Fig. 4 is a background line determined by calculating the number of neutrons which would penetrate the 20 mil Cd and an infinitely thick layer of boron. With this background taken into account the value of κ is 9.5 cm²/g B.

Since the absorption of neutrons in boron is taken as proportional to $1/E^{\frac{1}{2}}$, the energy of the upper absorption limit in Cd may be calculated from $E_L=E_{\text{th}}(\mu/\kappa)^2$ where $\mu=38$g/cm and $E=kT=0.026$ v. The result is[9] that $E_L=0.026\ (38/9.5)^2=0.41$ ev from which it appears that Cd absorbs neutrons having energies considerably higher than the thermal. Frisch and Plazcek[10] found in a preliminary measurement that $E_L\leq 1$ ev.

The absorption limit, E_L, in Cd combined with the results of the wheel experiment by Rasetti *et al.* permits a calculation of the resonance energy, E_r, and the half-width of the resonance band, Γ. The calculation which is given in detail by Bethe (reference 4, p. 149) gives:

$$E_r=\frac{E_L^2+2\lambda kT-(kT)^2}{2(E_L+\lambda-kT)}, \tag{3}$$

$$\epsilon=\frac{(E_r-kT)^2+(\Gamma/2)^2}{2(E_r-kT)}, \tag{4}$$

where
$$\lambda=\epsilon(p_{\text{th}}-p_L)/p_L. \tag{5}$$

Here p_{th} and p_L are the capture probabilities in Cd for thermal neutrons and neutrons just penetrating 20 mils Cd, respectively, the capture probability being defined by $p=\kappa E^{\frac{1}{2}}$. The absorption coefficient for thermal neutrons in Cd was taken as 15 cm²/g according to Amaldi and Fermi and to our own experiments, Fig. 3. The absorption coefficient, κ_{th}, of neutrons penetrating 20 mils (0.582 g/cm²) of Cd was assumed to be about $1/0.58\approx 2$ cm²/g. Therefore:

$$p_{\text{th}}/p_L=15/2\ (kT/E_L)^{\frac{1}{2}}$$
$$=15/2\ (0.026/0.37)^{\frac{1}{2}}=1.99. \tag{6}$$

The quantity ϵ in (3) and (5) is obtained from Rasetti's wheel experiment. If $\Delta p/p$ is the relative change in the absorption coefficient in that experiment, then

$$\epsilon=2muv_a(p/\Delta p)\sin\theta, \tag{7}$$

where u is the velocity of rotation of the edge of the wheel and $v_a=(2kT/M)^{\frac{1}{2}}$ is the average Maxwell velocity of thermal neutrons. In

[9] This result is independent of the obliquity correction of 10 percent because this correction applies equally to the absorption coefficients for thermal and Cd penetrating neutrons.

[10] Frisch and Placzek, Nature **137**, 357 (1936).

Rasetti's experiment, $v_n = 2200$ meters/sec., $u = 140$ m/sec., and $\Delta p/p = 6.3$ percent. From (7):

$$\epsilon = 0.09_5 \text{ ev.} \tag{8}$$

Inserting (6) and (8) in (3), (4), we obtain:

$$E_r = 0.18 \text{ ev}, \quad \Gamma = 0.15 \text{ ev}. \tag{9}$$

This result is, unfortunately, very sensitive to small errors in $\Delta p/p$ as can be seen from an inspection of (7). If ϵ is changed to 0.11 ev, the result is that $E_r = 0.17$ ev and $\Gamma = 0.19$ ev. With the present measurements it seems that E_r and Γ are of the same order of magnitude and are both about 0.15 ev. Bethe and Placzek[11] have made calculations using Amaldi and Fermi's data[7] on the absorption of "D" neutrons in Cd and find $E_r = 0.14$ ev and $\Gamma = 0.20$ ev. According to Eq. (9) the experimental ratio $\Gamma/E_r = 0.80$, which would correspond to the case of a fairly pronounced resonance hump in the curve of cross section plotted against E/E_r as given by Bethe and Placzek. The figures calculated by Bethe and Placzek give $\Gamma/E_r = 1.42$ approximating the case $\Gamma/E_r = \sqrt{2}$ which has a less pronounced resonance hump and a region of almost constant cross section as the energy varies from 0.05 to 0.12 ev.

From the values given in (9) an estimate may be made of the neutron width according to the calculations of Bethe and Placzek[11]

$$\Gamma_N = \frac{E_r \kappa_r \Gamma_{\text{eff}}}{1.23 \times 10^3}, \tag{10}$$

where κ_r is the absorption coefficient at resonance and Γ_{eff} is the effective cross section which may be replaced by $\pi\Gamma$ if the natural width, Γ, is large compared with the Doppler width. κ_r is about 1.3 times the absorption coefficient at thermal energies. Thus $\Gamma_N = (1.3 E_r \kappa_r \pi \Gamma)/1.23 \times 10^3$ and $\Gamma_N = 1.3 \times 10^{-3}$ ev.

The authors are indebted to Professor H. A. Bethe for major assistance in the calculations and interpretations of the experimental data, and to the Committee on Radiation of the National Research Council for financial support.

[11] Bethe and Placzek, Phys. Rev. **51**, 450 (1937).

DECEMBER 15, 1937 PHYSICAL REVIEW VOLUME 52

Production, Characteristics, and Reliability of Geiger-Müller Counters*

O. S. DUFFENDACK, H. LIFSCHUTZ AND M. M. SLAWSKY
University of Michigan, Ann Arbor, Michigan

(Received September 16, 1937)

A technique for the production of reliable Geiger-Müller counters is described. By the use of pure hydrogen gas and by cleaning the electrodes by sputtering in a glow discharge in hydrogen previous to filling the tubes with hydrogen gas, tubes with plateaus of 400 volts are produced. Copper, nickel, and tungsten have been found suitable for cathode cylinders while aluminum was not. Tubes filled with pure argon, pure oxygen, or air were found to give many spurious counts. An extensive series of reliability tests is described which shows that carefully made counter tubes used in properly designed circuits give completely reliable quantitative data.

THE use of Geiger counters for quantitative measurements on natural and artificial radioactivity has been practically abandoned because they have been found to be unreliable. However, their many advantages made it seem desirable to investigate the characteristics of the tubes and the circuits in an effort to develop reliable counting apparatus. Consequently, a systematic study has been made of the electric discharges in the tubes and of the characteristics of the electric circuits. The variations in the constants and the characteristics of the discharges produced by changing the electrode materials and the gas were investigated. Observations were made on the effects of impurities on the surface of the cathode and in the gas. After a

* Reported at the Washington Meeting of the American Physical Society. Phys. Rev. **51**, 1027, 1937.

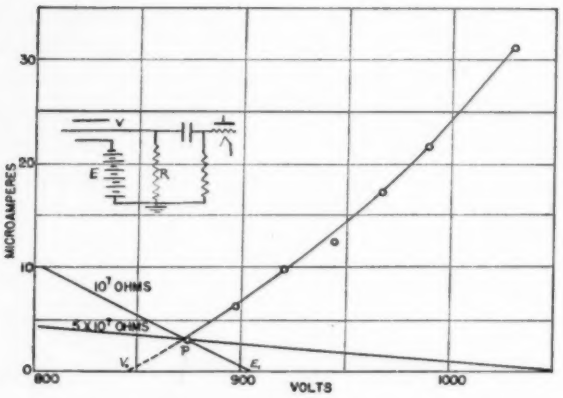

FIG. 1. The corona characteristic of a Geiger-Müller counter tube and diagram of a conventional circuit.

technique for making tubes of the desired characteristics had been developed and properly designed circuits had been built, a series of reliability tests was made. These tests show that properly made counters used in properly designed circuits give reproducible and reliable data.

First, the type of discharge produced in a Geiger counter tube was identified as the corona. Some of the experiments of Werner[1] were repeated and these confirmed his conclusion that the essential characteristic of the discharge which makes it adaptable for counting is that, with weak ionizing radiation, the discharge is not self-maintaining when the current falls below a minimum value characteristic of the tube. The value of the current and the voltage at the minimum point determine for a given circuit the range of voltage over which counting is possible; the larger the minimum current, the longer the counting range, as was pointed out by Werner. A consideration of Fig. 1 will make this clear and will likewise emphasize inherent weaknesses in the conventional circuit that has been widely used with Geiger-Müller counter tubes.

The conventional circuit employed is sketched as an insert in Fig. 1 and consists of a battery, or other source of d.c. e.m.f., with a tube and high resistance in series. The tube has concentric cylindrical electrodes. The anode is a fine tungsten wire and is connected to the grid of a vacuum tube by resistance-capacity coupling. We shall be concerned only with the series circuit containing the tube, quenching resistance, and source of e.m.f. Except when ionization is produced in the tube following the passage of a β-particle or γ-ray, the current through the tube is substantially zero, and the difference of potential between the electrodes is equal to the e.m.f. of the circuit. When a current is maintained, two equations must be satisfied simultaneously:

$$V=f(i), \tag{1}$$

$$V=E-Ri, \tag{2}$$

where V is the voltage across the tube, E the e.m.f. of the circuit, R the resistance, and i the current in the circuit.

Equation (1) is the corona characteristic and is plotted for a hydrogen filled, tungsten cathode Geiger-Müller counter tube in Fig. 1. V_0 is the minimum corona voltage. P is the minimum point for the corona under the influence of the weak radiation irradiating the tube; its coordinates represent the minimum voltage and current for a sustained discharge. Eq. (2) is represented by the straight line in the figure, and it will be noted that the slope of this line is determined by the resistance of the circuit which is practically equal to the high quenching resistance, R. Two lines representing Eq. (2) are drawn through the, minimum point for a self-maintained discharge and so the voltage intercepts represent the minimum e.m.f.'s that will maintain a discharge in the tube with the amount of quenching resistance shown on each line. For a given resistance, lines for larger values of the e.m.f. would be parallel to the one shown and would intercept the corona characteristic at points above the minimum point and thus would maintain a discharge in the tube. On the other hand, lines for smaller e.m.f.'s would intersect the characteristic below the minimum point and therefore would not maintain a discharge. The e.m.f. in the circuit under these conditions is the "operating voltage" of the tube, as the tube voltage has this value except for the brief intervals during which there is a discharge.

The voltage at which counting begins is not much above V_0 and the maximum voltage at the counting range is the value, E_1, of the voltage intercept of Eq. (2) for the line which passes

[1] S. Werner, Zeits. f. Physik **90**, 384 and **92**, 705 (1934). See also Evans and Mugele, Rev. Sci. Inst. **7**, 441 (1936). Henning and Schade, Zeits. f. Physik **90**, 605 (1934); von Hippel, Zeits. f. Physik **97**, 455 (1935); Schulze, Zeits. f. Physik **78**, 92 (1932) and references given therein.

through P, for at higher voltages a continuous discharge is maintained. Suppose the operating voltage is less than E_1. When an electron is set free in the electric field of the tube a sequence of events is started, including ionization of gas molecules and the liberation of electrons from the cathode, which results in an avalanche of electrons coursing toward the anode. The collection of these electrons causes a reduction in the anode potential while they escape slowly through the quenching resistance. Positive ions are simultaneously drawn toward the cathode, but they move more slowly than the electrons. The result of the collection of these charged particles is a current through the resistance R and a change in the condition of the circuit toward the equilibrium condition for a sustained discharge represented by the intersection of the two curves representing Eqs. (1) and (2). As this is below the minimum point, the discharge breaks, but the potential of the center wire has been reduced momentarily from E to some value near V_0, and so a voltage pulse is produced which causes a reaction in the amplifying circuit coupled with the counter tube and the recording of a count. For a given circuit, the amplitude of voltage pulse necessary to produce a count must exceed a certain minimum, and so the operating voltage must exceed V_0 by this small amount before counting begins. Counting is thus observed to begin after the operating voltage has been raised above V_0 a few volts and will continue until the operating voltage is increased to E_1, but the so-called plateau will consist of only a portion of this counting range for reasons to be given later.

It will be obvious from the reasoning given above and from a consideration of Fig. 1 that the extent of the counting range may be increased by increasing the quenching resistance R. The counting range has the value of approximately $i_{\min} R$. As shown by the curves, the counting range of the counter illustrated is increased from about 50 to 250 volts by increasing the resistance from 10^7 to 5.10^7 ohms.

But an increase in the quenching resistance increases the relaxation time of the circuit containing the tube in direct proportion, as this time is given by the product of the resistance and the capacitance of the circuit. When large resistances are necessary, the relaxation time becomes so large that an excessive loss of counts results, and the apparatus becomes useless for quantitative measurements. This cause alone is a sufficient reason why Geiger-Müller counters used in the conventional circuits are not suitable for collecting quantitative data in nuclear physics and came to be mistrusted by many research workers.

The counting range is also proportional to the minimum current of a sustained discharge, as a glance at Fig. 1 reveals. Therefore it is important to make tubes having large values of $i_{\min}$. Measurements on a number of small air-filled tubes showed that $i_{\min}$ often had a value of less than one microampere. In order to have an adequate counting range, the quenching resistance used with these tubes had to be of the order of 10^9 ohms and the relaxation time of the tube circuit under these conditions was of the order of one hundredth second, much too large for accurate counting. Hydrogen-filled tubes of the same size with well-cleaned electrodes of copper, nickel, or tungsten were found to have minimum maintaining currents of 3 to 5 microamperes, and so could be operated with correspondingly smaller quenching resistances.

The proper solution of the difficulty arising from a long relaxation time, and the one adopted by the writers and being rapidly adopted by others, is to replace the quenching resistance by a properly designed vacuum tube circuit. Several circuits have been successfully used. We have adopted the Neher-Harper[2] circuit and found it completely dependable. It requires a resistance of only from 10^6 to 10^7 ohms through which the collected electrons flow, and so the relaxation time is greatly reduced, having now the value of 10^{-4} to 10^{-5} seconds. The limitation of the speed of counting is now mainly in the thyratron operated recorder circuit. Good Geiger-Müller tubes used in a Neher-Harper circuit coupled to a scale of eight circuit built up with vacuum tubes instead of thyratrons have been found to show no losses when counting at the rate of 2000 counts per minute. Such a circuit has recently been developed in this laboratory by one of us (H. L.) and Mr. J. L. Lawson and will be described in a subsequent publication. The limitation to about 2000 counts per minute is, in fact, imposed by the

[2] Neher and Harper, Phys. Rev. **49**, 940 (1936).

Cenco recorder used. A higher scale counter will increase the rate of counting without loss. The circuit constants would permit 30,000 counts per minute or more.

It is desirable for the Geiger-Müller tube to have a relatively high minimum maintaining current, 3 to 5 microamperes, and it is essential to reliable counting for the tube to have a definite minimum point. Observations on a number of tubes indicate that this is not always the case and that impurities in the gas and unclean electrodes are the principal causes for lack of definiteness of this point. Consequently we developed a technique for making tubes that has produced uniformly good tubes with very sharp and definite minimum points.

The tubes are made in pairs, and after two of them have been sealed onto a vacuum system, they are exhausted while being heated with a soft flame until a good vacuum is obtained. The electrodes should be thoroughly outgassed by using an induction furnace or otherwise. Then hydrogen is admitted to a pressure of 2 to 7 mm and an a.c. glow discharge is produced between the cathode cylinders of the two tubes by means of a small neon sign transformer. The tubes are made in pairs because the fine center wire might be melted if it were used as one of the electrodes of the glow discharge. As the gas becomes contaminated, it is pumped out and replaced by fresh hydrogen. Care must be taken to disconnect the transformer during the exhaustion when tubes with thin windows are being made as these may be punctured by the discharge at low pressures. This process is repeated until the electrodes are sputtered clean and bright and the gas is spectroscopically pure. During the later stages, the center wires are connected to the cathode cylinders so that any sharp points on them are sputtered off and they will be clean. Liquid air is put onto the trap, too, during this time to collect the mercury vapor. The tubes are then filled with hydrogen to the desired pressure. At first, we admitted the hydrogen through a palladium regulator so as to improve its purity, but later we found out that ordinary tank hydrogen serves very well. For small tubes, with cathode cylinders not over 15 mm diameter, 100 mm pressure of hydrogen has been found to be satisfactory. The whole process usually requires from four to twelve hours depending on the condition of the cathodes at the beginning.

Before the tubes are sealed off, their static characteristics are taken and the minimum point determined. If the minimum point is not sharp and definite and the minimum maintaining current not at least 3 microamperes, the gas is pumped out and the sputtering is resumed. In no case has a tube been found to behave unsatisfactorily in a counter circuit if it meets these requirements as to its minimum point. With these precautions the yield of good tubes is 100 percent.

Various combinations of cathode materials and gases were tried. The anode center wires were all of tungsten of 3 mil diameter. Al, Cu, Ni and W cathodes were tried with air, oxygen, argon, and hydrogen gases. The tubes were all made according to the same procedure. When air or oxygen was used, the electrodes never became bright but were coated with oxide. Of the electrode materials, all proved satisfactory except aluminum. Tubes with Al cathodes had too low an end-point and in many cases could produce no counts at all. When they did produce counts, many of these were spurious and so made such tubes unreliable. Our experience with aluminum seems to be in accord with that of a number of workers with whom we have discussed the matter, but others apparently are able to make satisfactory counters with aluminum cathodes.

We never succeeded in making a reliable counter with pure argon. None of them had any plateau and all produced many spurious counts. When the pulses were examined with a cathode-ray oscillograph at the input to the thyratron operating the Cenco recorder, trains of pulses of varying amplitude were frequently observed instead of sharp, clean, single pulses, such as indicate reliable counting. Oxygen and air were better than argon, and tubes filled with these gases sometimes had fairly definite plateaus. However, trains of pulses could often be observed with a cathode-ray oscillograph when these tubes were used, and the number of spurious counts was too high to be ignored in quantitative work. The minimum point of the static characteristic was often not very definite with air-filled counters. The discharge current would sometimes vary in an irregular manner at a voltage of 10 to 15 volts

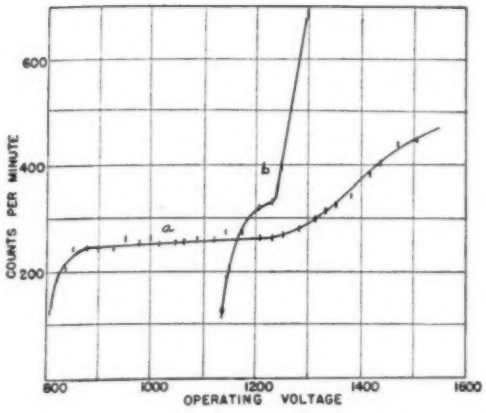

FIG. 2. Plateau curves for (*a*) hydrogen-filled and (*b*) air-filled counters. Copper cylinders, tungsten wire anodes.

above the minimum, though the discharge would not break. Tubes which exhibited these characteristics were invariably erratic in counting.

Hydrogen-filled tubes were far more reliable and regular in their behavior than any of the others that we tried. When the electrodes had been well cleaned by sputtering and the gas was pure, these tubes had very definite end points, the discharge breaking suddenly and sharply when the voltage was reduced to $V_{min.}$ The pulses observed with a cathode-ray oscillograph were clean, single pulses and remarkably uniform in amplitude. Few spurious counts could be detected before the end of the plateau. Furthermore, the counting range always began at V_0 with hydrogen-filled tubes while the beginning of the counting range was sometimes considerably higher than V_0 for tubes filled with air or other gases. The hydrogen-filled tubes had much wider and more definite plateaus than any of the others, as has previously been reported by Cosyns and de Bruyn.[3] Fig. 2 shows plateau curves for two similar counter tubes, one filled with hydrogen and the other with air. As may be seen from the figure, the hydrogen tube has a plateau of about 400 volts. The vertical lines drawn through the observation points indicate the standard deviations for the number of counts taken to determine each point. Because of the obvious superiority of hydrogen-filled tubes we have come to use them exclusively, and the reliability tests described below were made with a hydrogen-filled tube.

The behavior of tubes filled with different gases has led us to postulate that one of the chief sources of spurious counts and erratic behavior in Geiger-Müller counter tubes and one cause for the ending of the plateau before the counting range, is in the action of metastable atoms. The reason for the failure to make successful tubes with pure argon is probably because argon has very prominent metastable states. Other gases with prominent metastable states as Ne, N_2, etc. have been shown to give narrow plateaus.[3] On the other hand, the reliability of hydrogen-filled tubes we ascribe mainly to hydrogen's lack of metastable states. Furthermore, it is the common practice of many workers with Geiger-Müller counters to add an admixture of oxygen or some other gas to argon if this gas is used as the filling gas. The improvement in the behavior may then be ascribed to the destruction of the metastable argon atoms by impacts of the second kind with the molecules of the admixed gas.

If the discharge mechanism described above is correct, one would expect spurious counts when a gas whose molecules have metastable states is used. Since metastable atoms are not propelled by an electric field, they will remain in the gas until destroyed by some impact of the second kind or by collision with an electrode or the tube wall. They may remain for a considerable time in a pure gas at high pressure. Any one of a number of different processes involving metastable atoms may result in the extraction of an electron from the cathode or in the ionization of a molecule of an impurity in the gas. An electron thus produced would have the same chance of starting a discharge and causing a count as an electron produced by the ionizing radiation being studied, and so spurious counts may occur at any time during the interval metastable atoms are present.

By an impact of the second kind, a metastable atom may ionize a gas molecule whose ionization potential is less than the potential of the metastable state. Or the metastable atom may excite the molecule with which it collides or be itself shifted to a radiating state. Light quanta thus produced may fall upon the cathode and cause the emission of a photoelectron and produce a count. If a metastable atom strikes the cathode,

[3] Cosyns and de Bruyn: Académie royale de Belgique, Bulletin de la Classe des Sciences [5] **20**, 371 (1934).

it may extract an electron therefrom and so cause a count. Consequently it seems best to use for Geiger-Müller counter tubes a gas like hydrogen which has no metastable states. We advocate doing this rather than putting in an admixture of some gas in sufficient amount to destroy metastable atoms so quickly that a short relaxation time is attained. The amount of the admixed gas necessary is enough so that its own excitation, direct and by second kind impacts, cannot be neglected in comparison with that of the main gas, and, if its molecules should have metastable states, they would not be quickly destroyed as their potentials would generally be lower and not in resonance with the excited states of the argon.

A rather extensive series of reliability tests was made on a Geiger-Müller counter apparatus consisting of a hydrogen-filled counter tube coupled to a thyratron single scale recorder by means of a Neher-Harper circuit. The tube had a 400 volt plateau, 850–1250 volts, and the operating voltage was set at about 100 volts above the threshold counting voltage. The tube was mounted on a paraffin block and surrounded by a brass frame into which small sources of radioactive material could be inserted in fixed positions. The tube and the sources could not easily be displaced with respect to each other. The sources were made by carefully dropping a drop of radium dial paint into a hole drilled into the end of a brass rod. A number of these sources were made in this way and numbered so that they could be identified. They were then inserted into numbered holes in the brass frame surrounding the counter tube and used singly or in combination. When a source was not in its place in the frame, a similar brass rod without any radioactive material was inserted in its stead so that there was always the same distribution of metal around the tube no matter how many of the sources were in use. Thus the scattering was always the same and an accurate multiple addition test could be carried out by calibrating the sources singly and using them in combination. Also other methods of calibrating the counters and circuits were devised and will be described in another paper.

TABLE I.

COUNTS	COUNTS PER MIN.	STAND. DEVIATIONS
9255	48.97	0.52
9595	49.97	.51
10935	49.48	.48
21757	50.13	.34
51542	49.75	.22
9616	54.02	.54
9832	53.15	.53
10210	52.63	.52
14599	52.89	.44
9688	53.82	.53
12984	54.10	.46
10665	52.28	.51
29222	52.00	.31
16664	52.08	.41
123480	52.79	.15
10181	58.85	.58
29857	58.09	.34
14956	56.23	.48
7140	59.01	.69
21784	59.68	.40
20329	58.92	.41
16830	57.03	.45
121077	58.24	.17
95096	130.45	.42
13708	131.81	1.11
21983	129.31	.89
9835	131.13	1.32
140622	130.45	.35

The apparatus designed for making addition tests was used for the reliability tests. A sufficient number of sources were inserted in the frame to give the desired average rate of counting, and then a considerable number of counts, from 7000 to 30,000, were taken and the average rate of counting was determined. This was repeated several times until the total number of counts at a given average rate reached 50,000 to 140,000. Tests were made at four different average rates of counting and the data are given in Table I and in Fig. 3. The tests extended over a period of three weeks during which time the apparatus was started and stopped many times. The zero or background count was taken at different times during this period and was found to be remarkably constant as is shown by the data in Table II. Six different observers participated in taking the data.

In Fig. 3, the horizontal lines for a given test are separated by twice the amount of the standard deviation for the total number of counts taken at one rate. The vertical lines through the points representing the individual

observations are drawn of lengths indicating the standard deviations for the number of counts taken for that observation. It will be noted that more than half of these lines intersect with the horizontal lines and that the maximum deviation of an individual observation from the mean rate of counting is less than 2 counts per minute. Thus the deviations are within the expected limits for a random phenomenon like the one observed, and we conclude that the counting apparatus gave completely reliable quantitative data.

Counter tubes made according to the technique described above are photoelectrically sensitive to daylight and also to light from incandescent tungsten lamps. In using them it is best to shield them from such light, as the zero count is thus reduced and accidental variations in the intensity of the light are avoided. The tubes were shielded from light during the reliability tests but were not shielded from secondary cosmic radiation. When the tube was surrounded by two inches of lead, the zero count dropped from 12 to about 2 counts per minute. The remaining counts were probably due to primary cosmic rays. The cylindrical cathode for this counter was a copper gauze cylinder 7 mm in diameter and 40 mm long.

TABLE II. *Background due to primary and secondary cosmic rays.*

DATE	COUNTS	COUNTS PER MIN.
Mar. 23	6143	12.80
" 24	4094	12.41
" 25	4857	12.78
" 25	3958	12.81
" 31	6628	12.25
Apr. 1	3894	11.84
" 16	17840	12.52
Total	47414	12.50

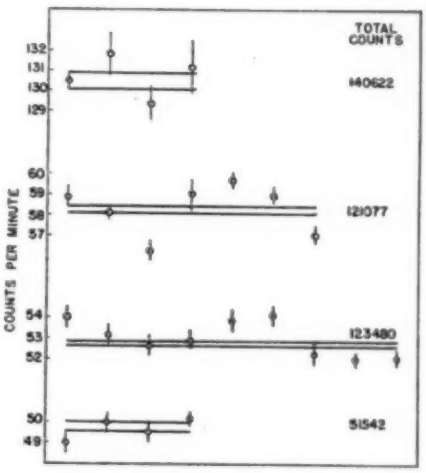

FIG. 3. Reliability tests on a single scale Geiger-Müller counter apparatus.

There is nothing in the tests described to indicate what might be the absolute efficiency of the counter. Such tests are important and are often made by research workers on cosmic rays by inserting an additional tube in a bank of coincidence counters and observing the decrease in the counting rate which follows. It might be pointed out in this connection that one may make a mistake in trying to make counter tubes with considerable volume and a low zero count. Unless the tube is well shielded with lead, secondary cosmic rays are invariably present and a too low zero count then indicates that the counter tube is insensitive and has a low absolute efficiency.

We wish to acknowledge with thanks financial aid from the Horace H. Rackham Foundation which made it possible to undertake this research.

Large Angle Scattering and Energy Loss of Potassium Ions Scattered by Heavy Monatomic Gases

ARTHUR G. ROUSE
*University of Iowa, Iowa City, Iowa**

(Received October 29, 1937)

A beam of potassium ions with energies in the range between 90 and 360 volts was scattered by collision with the heavy monatomic gases argon, krypton, xenon, and mercury vapor and the angular distribution was observed. For slower particles the scattering per unit solid angle relative to the center of mass of the colliding particles decreases with angle. At higher voltages the scattering increases at larger angles with a minimum about 60. The scattering at the larger angles increases with voltage. The results are not compatible with a rigid sphere model of the atom. The large deviations may be associated with exciting or ionizing collisions.

INTRODUCTION

WHEN an ionic beam is sent into a gas at low pressure the ions are scattered by collision. For collisions between rigid spheres the classical kinetic theory predicts equal scattering in all directions (if the angles are measured relative to the center of mass of the colliding particles rather than to the apparatus). Wave mechanics give substantially the same result for rigid spheres excepting for a great increase in very small angle scattering. For models with less abrupt force fields the large angle scattering should decrease more or less with angle; the Rutherford scattering in a Coulomb field is an extreme case. For rigid spheres the scattering should be independent of the speed of the ions; for other laws of force one should expect, so long as ionization and excitation play no role, the scattering to decrease with increasing energy of the beam.

It is not easy to obtain unambiguous experimental results in this field. Along with the scattered primary ions there may be electrons produced by ionization or ejected from the walls of the apparatus. There may be, at least at smaller deviations, ions of the scattering gas. The deviated particle may suffer multiple collisions or may lose its charge. To a certain extent these effects may be controlled by proper experimental conditions. Nevertheless the phenomena in the tube remain complicated. In an exploratory investigation in the field probably the best evidence that the data are reliable is to measure the energies of the scattered particles and show that energy and momentum are conserved in the impact.

The small angle scattering of low velocity neutral atoms has been studied by Zabel,[1] Broadway,[2] and others. It was found that the results were in accord with the scattering expected by wave mechanics applied to a rigid sphere. Frische[3] has reported that alkali ions are scattered from mercury vapor through large angles (in the neighborhood of 180°) and that these ions loose approximately the amount of energy expected in a single elastic collision. This paper is a report on an investigation of the angular distribution of potassium ions (in the range from 90–360 volts) scattered through large angles by heavy monatomic gases.

DESCRIPTION OF THE APPARATUS

In this experiment a beam of ions of known velocity was sent into a gas and the scattered ions were collected in a collector which could be set at various angles with the incident beam. The current to this collector was then measured with an electrometer.

A cross-sectional view of the apparatus is shown in Fig. 1. The apparatus is divided into two chambers by a plate which holds in place the collimator for the incident beam. Above the collimator is the potassium ion source, a flat tungsten filament coated with Kunsman catalyst. The filament was adjusted to its position above the collimator by means of a sylphon arrangement not shown in the figure. Below the dividing

* Now at St. Louis University.

[1] Roland Zabel, Phys. Rev. **96**, 411 (1934).
[2] L. F. Broadway, Proc. Roy. Soc. **A141**, 634 (1933).
[3] Carl A. Frische, Phys. Rev. **43**, 160 (1933).

plate is the scattering chamber which contains the collector. By means of a ground glass joint the collector could be rotated through an angle of 135° with the beam. This angle was read by a pointer attached to the ground glass joint.

The scattering gases were admitted to the scattering chamber through the inlet shown. Argon was pumped through and out the system, its pressure being controlled by a needle leak valve. Mercury vapor pressure was controlled by a mercury well at a fixed temperature, the remainder of the apparatus being maintained at a higher temperature. The technique for krypton and xenon was somewhat different. Small quantities of spectroscopically pure gas were admitted to the system and used until slightly contaminated as shown by a change in pressure. The gas was kept in circulation while in use, thus maintaining a low pressure in the upper chamber and the desired pressure in the scattering chamber. The pressure was measured with a McLeod gauge connected directly to the scattering chamber.

Figure 2 is a more detailed picture of the collector and collimator both drawn to scale. The collector proper was a plate enclosed in a metal shielding box with a double top. The collecting plate was connected to the electrometer by a lead which passed through a shielding metal tube and out through the ground joint. Slits in the double top 4×0.5 mm and 3 mm apart provided resolution for the scattered beam.

The axis of rotation of the collector was adjusted to intersect the incident beam just below the collimator. Under these conditions the scattered beam was symmetrical. When the axis of rotation was raised about 2 mm above the end of the collimator it was observed that no ions reached the collector at large angles. If the collector was pointed to one side of the beam no ions reached the collector. This indicated that the collector admitted ions only from the direction defined by its slits.

The shape of the incident beam as defined by the collimator is indicated in Fig. 3. The graph shows the logarithm of the current to the collector for ions with 360 volts energy in a vacuum. From the dimensions of the collimator and collector slits, the geometrical edge (i.e., shadow) of the beam should be at about 15° and the graph shows that at this angle the intensity has dropped to one thousandth of its maximum value. Thus most of the ions of the incident beam move practically parallel with the axis of the collimator. A small spurious background at 90° (in a vacuum) was negligible in comparison with the scattered current from the heavier gases. However, for argon which scattered practically nothing through 90°, this background was important.

In measuring scattering the gas pressure in the scattering chamber was kept low to avoid the possibility that the scattered current observed could be due to multiple collisions. The pressure of the scattering gas was maintained at 0.01 mm of Hg or less and the observed scattering, at a particular angle, was actually found to be proportional to the pressure within experimental error. Further, Frische,[3] and Durbin[4] have shown that positives have as a rule longer mean free paths, for appreciable angle deflections, than neutral atoms. Mean free paths of neutrals at the

[4] F. M. Durbin, Phys. Rev. 30, 844 (1927).

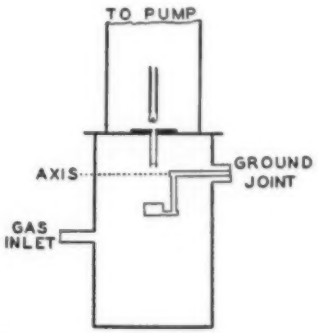

FIG. 1. Arrangement of ion source and collector.

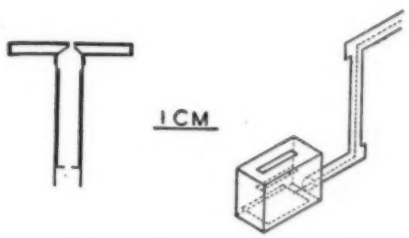

FIG. 2. Detail of ion source and collector.

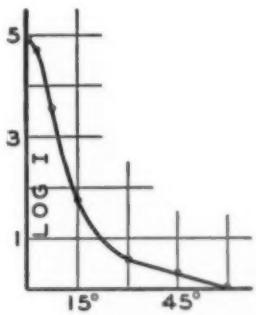

FIG. 3. Distribution of current in incident beam.

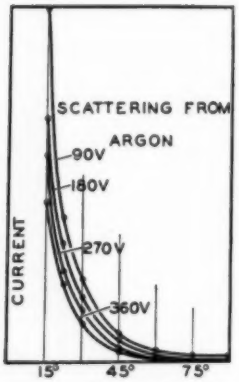

FIG. 4. Scattering of potassium ions in argon.

pressure mentioned are somewhat greater than the dimensions of the apparatus.

Energy momentum considerations show that in a single collision potassium ions cannot be deviated more than 30° by neon nor more than 90° by argon in the laboratory system of reference. This agrees with the experimental results. Also the measured energies of the scattered particles agree with the values expected for single elastic collisions.

The possibility of double collisions is very greatly reduced by the collimating effect of the collector slits. The double slits insured that only ions moving in a particular direction could enter. Hence only two collisions which both occurred within a very small volume just below the collimator could produce ions which could reach the collector. The collector allowed some control over charges which entered it by means of a potential applied between the collecting plate and its shielding container. This potential was made to repel electrons and attract positives. The space outside the collector was not affected by this potential so that the scattering took place in a field free region.

ANGULAR DISTRIBUTION

To obtain the angular distribution of the scattered ions the current to the collector was measured at various angles both with and without a scattering gas, the difference of the two currents being taken as the scattering due to the gas. The filament current controlled the intensity of the beam and a voltage applied between the filament and the collimator gave the incident ions their initial energy. A potential of from 22 to 67 volts was applied between the collecting plate and its shielding container so that positives which entered the slits reached the collector and the negatives were repelled. This potential was found particularly necessary at the higher voltages which produced ionization.

The scattering volume from which ions can enter the collector is approximately the volume cut out by two intersecting cylinders, one along the incident beam and the other along the scattered beam. This volume evidently varies with the angle between the axes of these two cylinders.

The data, reduced to a standard scattering gas pressure and incident beam intensity and corrected for scattering volume, were plotted in arbitrary units against the scattering angle in Figs. 4, 5, 6, and 7. The scattering angle plotted was measured with respect to the apparatus. This sort of a graph gives an idea of the actual space distribution of the scattered ions.

The classical theory for rigid spheres predicts equal scattering in all unit solid angles when measured in a system of coordinates at rest with respect to the center of mass of the two colliding particles (the so-called relative system of coordinates). For the case of particles of equal mass, this uniform scattering becomes a cosine curve when observed in a system of coordinates fixed in the apparatus. Argon and potassium have masses of 40 and 39 respectively and so almost satisfy the condition of equal masses. The scattering curve for argon does become zero at 90° as it must from energy momentum considerations but otherwise does not resemble the cosine curve. Neglecting the part of the scattering curve above 75° where the scattering is too small to draw definite conclusions, one must say that the curve falls off more rapidly than the cosine curve and therefore more rapidly than predicted classically for rigid spheres. Fig. 4 also shows that the scattering at any angle decreases with voltage.

Figures 5, 6, and 7 show the scattering from gases heavier than argon and therefore heavy enough to scatter the potassium ions through more than 90°. At lower voltages the curves more or less resemble those of argon, decreasing with angle. Confining attention to some particular angle, the scattering may increase or decrease with voltage, although always at the large angles the scattering is greatest at 360 volts.

For purposes of comparison it is better to have

the scattering function plotted against the relative scattering angle. A simple transformation will accomplish this. Two changes are brought about in transforming the scattering curve from fixed coordinates to relative coordinates; first the angle of scattering is changed, thereby altering the abscissa, second the scattering per unit solid angle is changed, thereby altering the ordinate. The changes are less important for target atoms much heavier than the incident ions but in every case the scattering at large angles is increased.

Figure 8 shows the transformed data for the three heavier gases. Curves *A*, *B*, *C*, and *D* are the voltages 90, 180, 270, and 360, respectively. The remarkable things about these scattering curves for the heavier gases are the maxima have now disappeared, at sufficiently high voltages there is an increase in scattering with angle, and at large angles there is an increase in scattering at the higher voltages. No simple theory predicts these phenomena. The curves would suggest that a new interaction is occurring at higher voltages which increases the probability of collision especially for large angle deflections. This new interaction may be some sort of an inelastic collision or a resonance or interference phenomenon. But in any case the scattering curves are unusual and unexpected and for that reason very interesting.

Energy Loss

In order to establish the validity of these results and to show that the ions scattered to the collector were indeed, as was assumed, those scattered by single collisions, the residual energy of the ions was measured by applying a retarding potential between the collector and its shielding container. Fig. 9 shows two curves obtained in this manner. Curve *A* is for 90 volt ions scattered through 30° by krypton and curve *B* is for 180 volt ions scattered through 45° by krypton. The ion current is reduced to zero by retarding potentials of 74 and 140 volts respectively in the two cases; that is, the fastest ions had lost $90-74=16$ volts and $180-140=40$ volts in the collision. The curves cut the axis at 16 and 40 volts, respectively. The kinetic energy lost by the ion in an elastic collision can of course be computed from simple energy momentum considerations and for these particular cases, it is 12 and 45 volts, respectively. The agreement is within the experimental error.

It would be supposed that the scattered ions (at a given angle) would all have the same velocity; under ideal conditions the drop in these curves should occur suddenly at the theoretical voltage. Actually it does not do so; the curves for these voltages are always of the general type shown. However this is not to be interpreted as casting doubt upon the hypothesis of single elastic collisions. When similar retarding potential curves are taken on the incident beam (with no gas in the chamber) the same shape of the curves results. Fig. 10 is such a curve for a beam of 90 volt ions. The absence of a sharp break may be inherent in this method of measuring the

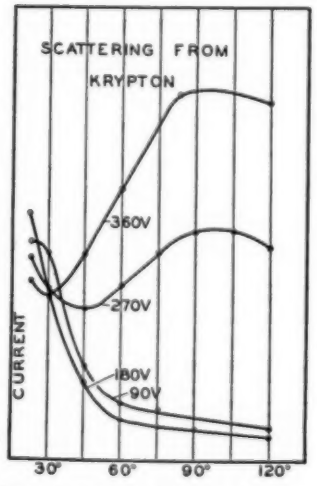

FIG. 5. Scattering of potassium ions in krypton.

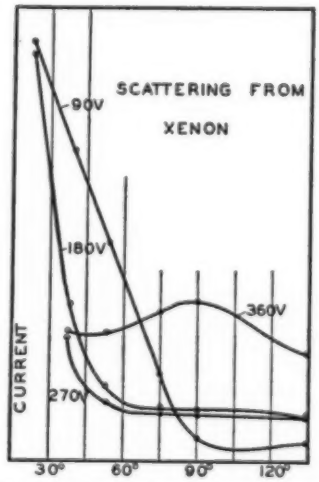

FIG. 6. Scattering of potassium ions in xenon.

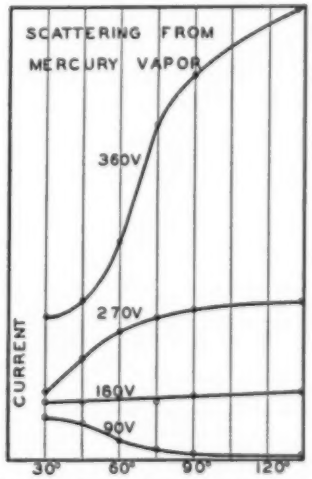

FIG. 7. Scattering of potassium ions in mercury vapor.

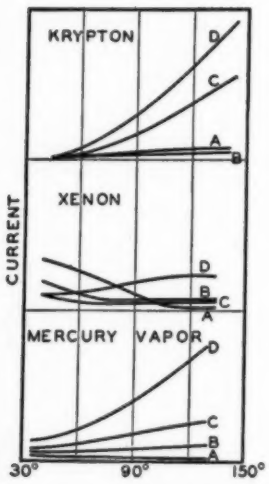

FIG. 8. Scattering of potassium ions in krypton, xenon, and mercury vapor. The angles are in the system moving with the center of mass of the colliding particles. Curves *A*, *B*, *C*, and *D* are for 90, 180, 270, and 360 volt ions, respectively.

energy of positive ions or it may be due to a spread in the energy of the primary beam. Since the curve for the incident beam becomes zero at zero potential there is this justification for taking the intersection of the curve with the axis as a measure of the energy lost.

A summary of several retarding curves is presented in Table I. The angle of scattering and the initial energy of the ion are given in the column at the left while the target atom is indicated above. In each case two numbers are given, the first is the calculated energy loss for a single elastic collision and the second is the observed loss. The last three lines (for higher voltage ions and larger angles) are data not obtained on this apparatus and will be explained later.

IONIZATION

In the retarding curves just presented the ion current dropped to zero and remained zero even at very large retarding potentials. However, above 180 volts, there was considerable ionization in the tube and the retarding curve, as shown in Fig. 11, became negative; more electrons than positives reached the collector. This naturally made it impossible to make a reliable determination of the potential at which the positives ceased to reach the collector. The curve also indicates that an attracting potential of approximately 45 volts was necessary for saturation of the positives and, as was mentioned previously, this potential was used in obtaining the scattering curves in Figs. 4–7. Fig. 11 is a retarding curve for 225 volt ions scattered through 90° by krypton. The increased positive current of the collector at an attracting voltage was observed only when there was a scattering gas in the chamber which proved that the ions were scattered from the target atoms.

It seemed advisable to design another apparatus in which the negative and positive currents could be separated and the speed of either measured. Also, in view of the surprising results of the earlier scattering curves it seemed possible that the increase in total scattering at high voltages might be associated with the inset of ionization and confirmation of these scattering curves was sought in an apparatus of radically different design.

Figure 12 shows an apparatus the scattering chamber of which contains four co-axial insulated brass cylinders. The outer one serves as a collector while the inner three define the scattered beam and can be used as grids for control and observation of the scattered beam. A slot which nearly encircled the cylinder was made in each of the inner three only enough of the metal being left for support. By properly adjusting the voltages on the several grids, it is possible to separate the positive and negative scattered particles; also, of course, this apparatus collects all ions scattered through 90° and therefore from a larger solid angle than did the other apparatus which consequently allows the use of a lower scattering gas pressure.

One function of this second apparatus was to measure the energy of the electrons (products of ionization) because the obvious interpretation of Fig. 11 is that the electrons have a surprisingly large amount of energy. Fig. 13 shows the electron current to the collector as a function of the potential of the middle cylinder. The scattering gas was xenon, the incident ions had 360 volts energy, and the collector was at such a potential that no positive could reach it. The sharp break in the curve is characteristic of a retarding curve for electrons all of which have approximately the same energy. The maximum energy of the scattered electrons as shown by this curve is 1 or 2 volts.

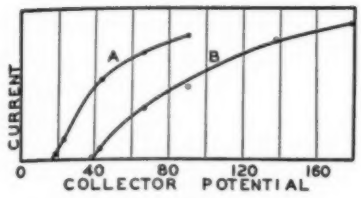

FIG. 9. Current *vs.* retarding potentials. Curve *A*, 90 volt ions scattered through 30°; curve *B*, 180 volt ions scattered through 45°, both in krypton.

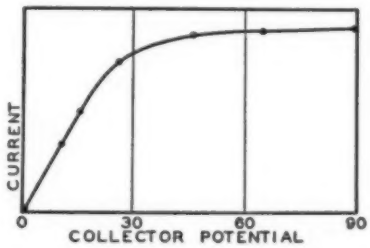

FIG. 10. Current *vs.* retarding potential for 90 volt ions in vacuum.

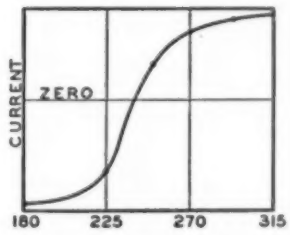

FIG. 11. Current *vs.* retarding potentials for 225 volt ions scattered through 90° in krypton.

Retarding curves for determining the energy of the positives as measured with this apparatus are shown in Fig. 14. The target atom was krypton and the incident ions had 270 volts energy for curve *C*, and 360 volts for curve *D*. At these voltages electrons were numerous enough to cause complications with the first apparatus, but with this apparatus they were eliminated by a few volts on the middle cylinder as was shown possible in Fig. 13. The calculated energy loss again agreed with that measured and the results of these retarding curves for positives are summed up in the last three lines of Table I.

It might be supposed that inelastic collisions could be observed by careful analysis of the retarding curves for the higher voltage positives. An attempt was made to do this but no definite conclusions could be drawn from the data obtained.

A final check on the data was obtained by observing with this apparatus the scattering at 90° as a function of voltage. Although differing markedly in construction from the first apparatus the results obtained were in general agreement. In Table II columns *A* and *B* give the scattering under the conditions indicated with the first and second apparatus, respectively. The scattering is given in arbitrary units, the size of the unit being adjusted so that the numbers in the two columns are somewhat the same size. It is readily seen that the increase of scattering with voltage is comparable in both cases.

Column *E* in this same table is a rather rough measure of the number of electrons which were observed at these various voltages. This number was secured by putting the collecting cylinder in the second apparatus at such a potential that no positives could reach it. Although there is no one to one correspondence between the increase of scattering at 90° and the number of electrons observed the results seem to indicate a possible relation between them.

TABLE I. *Calculated (first column) and observed (second column) energy losses.*

	ARGON		KRYPTON		XENON		MERCURY	
30° 90 V	23	20	12	16	7	5	5	8
30° 180 V	45	45	23	24	14	18	9	
45° 90 V	45	46	23	20	15	18	10	10
45° 180 V	90	95	45	40	31	30	20	
90° 180 V			120	115	83	85		
90° 270 V			180	180	110	120		
90° 360 V			240	247	165	175		

DISCUSSION OF RESULTS

Data have been presented on the energy lost by a potassium ion when it undergoes a single elastic collision with a heavy atom. This energy loss depended upon the initial energy of the impining ion, the mass of the target atom, and the angle through which the ion was deflected and was found to be in agreement with that loss calculated assuming energy and momentum were conserved.

The angular distribution of the ions scattered by the various gases presents some very interesting possibilities. The marked increase of scattering with increasing angle is entirely unexpected and cannot be explained on the basis of any simple classical theory. Since there is also an increase in the scattering at the higher voltages the data suggest the possibility of an interaction which becomes effective at these voltages and increases the probability of large angle collisions.

The electrons formed by ionizing the scattering gas have been found to have a maximum energy of 1 or 2 volts.

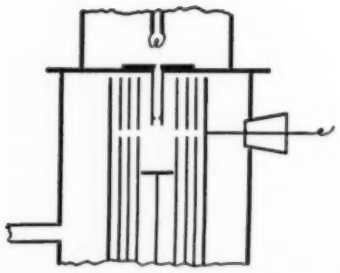

FIG. 12. Apparatus for measuring scattering at 90°.

In an attempt to correlate the increased scattering at high voltages with the phenomenon of ionization a comparison of the scattering with the ionization was made. No definite conclusion could be drawn from this comparison but a possible relationship was in evidence.

TABLE II. *Scattering at 90° in the first (column A) and the second (column B) apparatus. Column E gives the number of electrons.*

	KRYPTON			XENON			HG	
V	*A*	*B*	*E*	*A*	*B*	*E*	*A*	*E*
90	2.0	2.5	0 0	1.0	1.6	0.0	0.3	0.0
180	1.4	2.2	4.0	2.6	3.2	1.4	3.0	5.0
270	12.3	9.0	6.0	2.6	5.6	4.5	7.4	10.0
360	19.4	11.5	11.0	8.5	9.0	6.0	20.2	20.0

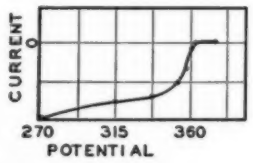

FIG. 13. Current (electron) to the outer cylinder *vs.* potential of the middle cylinder.

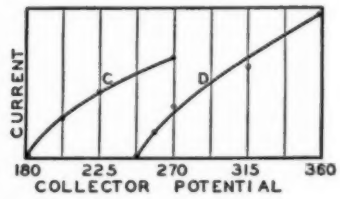

FIG. 14. Positive ion current in second apparatus *vs.* retarding potentials for 270 volt ions (curve *C*) and 360 volt ions (curve *D*) in krypton.

Further work on the scattering curves should lead ultimately to an understanding of the interaction forces between the two particles and a determination of the collision cross sections for the types of collisions which occur.

The author wishes to acknowledge his indebtedness and gratitude to Professor John A. Eldridge for his guidance in this investigation.

DECEMBER 15, 1937 PHYSICAL REVIEW VOLUME 52

Paramagnetic Measurements at Low Fields with the Rankine Balance

HAIG P. ISKENDERIAN
Stevens Institute of Technology, Hoboken, New Jersey
(Received October 18, 1937)

The Rankine magnetic balance previously reported has been adapted for making paramagnetic measurements at low fields. An analysis of the stability of the balance under these conditions is given. The volume magnetic susceptibilities of gaseous O_2 and of aqueous $NiCl_2$ solutions relative to water are reported, and from these values the relative mass susceptibilities of O_2 and $NiCl_2$ are deduced. The mass susceptibility of H_2O is assumed to be -0.7200×10^{-6}, in terms of which, that of O_2 is 104.4×10^{-6} and of $NiCl_2$ is 33.97×10^{-6}.

IN a previous paper[1] details for the construction of a Rankine balance for measuring magnetic susceptibilities were given. The results of measurements of diamagnetic susceptibilities on mixtures of heavy and light water were reported.

The adaptibility of the Rankine balance for making low field paramagnetic measurements is demonstrated herein, and the results on aqueous nickel chloride solutions and on gaseous oxygen are given.

The equilibrium condition for the Rankine balance is:[1]

$$T+T_0+\frac{\pi m^2 b\kappa \sin\theta}{2x^2}+\tau(\theta+\theta_0)=0, \qquad (1)$$

in which the symbols have the same significance as in the previous paper.[1] For small angular

[1] H. P. Iskenderian, Phys. Rev. **51**, 1092 (1937).

deflections of the beam, T is approximately constant and variations in T_0 may be rendered insignificant if appropriate precautions are taken. Let H_0 and $H_0+\Delta H$ denote respectively the vector magnetic fields of extraneous origin at the north and south poles of the magnet; then, if θ_1 denotes the angle between the increment ΔH and the direction of the beam in its fiducial position, T_0 will be given by $(bm\Delta H \sin\theta_1)$. It is seen that for small deflections of the beam variations in T_0 may in general be appreciable. For stable equilibrium, we must have, in addition to (1), the condition:

$$\left[bm\Delta H\cos\theta_1 + \frac{\pi m^2 b\kappa}{2}\left(\frac{x\cos\theta - 2b\sin^2\theta}{x^3}\right)+\tau\right]>0. \quad (2)$$

In order that the balance have a high sensitivity the magnitude of the expression in (2) should be a minimum.[1] Then, for making paramagnetic measurements over a wide range of susceptibilities, it is essential to reduce the second term in (2) to a minimum by setting the cell at an optimum orientation relative to the beam when the latter is in its fiducial position.

In the present balance, the optimum value of θ is approximately 29° corresponding to $x=1$ cm and $b=2$ cm. It was found that for volume susceptibilities of the order of magnitude of 10^{-6} the second term of (2) was small compared with the first. The improved sensitivity of the apparatus which results from such an optimum orientation of the cell could not be fully utilized in the present arrangement on account of lack of high stability of the suspension due to accidental disturbances. Electrostatic shielding of the test cell from the magnet improved the performance of the apparatus.

Volume susceptibility measurements at field strengths of about 40 oersteds and at room temperatures were made on oxygen and aqueous solutions of $NiCl_2$. The mean of nine independent measurements on oxygen at 20°C is 0.139×10^{-6} with an average deviation from the mean of 0.001×10^{-6}; the corresponding value of $\chi_M T = 0.979$ is in good agreement with the theoretical value[2] of 0.993, considering that the oxygen tested was tank oxygen, which probably contains some diamagnetic impurities. This value also agrees well with the results of other investigators:[3] 0.983 (Curie), 0.970 (Onnes and Oosterhuis), 0.975 (Soné), 1.001 (Bauer and Piccard), 1.021 (Wills and Hector), 0.979 (Lehrer), 1.002 (Woltjer, Coppoolse and Wiersma).

[1] Van Vleck, *Electric and Magnetic Susceptibilities*, p. 266.

TABLE I. *The magnetic susceptibility of aqueous solutions of $NiCl_2$.*

ρ_l	C	$-\kappa_l/\kappa_w$	$\kappa_l\times10^6$	$\chi_l\times10^6$
1.0380	0.04105	1.0161	0.7302	0.7034
1.1005	0.1014	4.287	3.081	2.800

The results of measurements on $NiCl_2$ solutions at 20°C are given in Table I.

In the first column are contained the measured densities of the solutions, in the second, the corresponding concentration by weight of $NiCl_2$ determined from data contained in the *International Critical Tables*. In the third column are listed the observed ratios of the volume susceptibilities of the solutions to that of water. The volume susceptibilities shown in the fourth column are calculated from these ratios and the assumed value for water at 20°C, $\kappa_w=-0.7186\times10^{-6}$. The last column gives the mass susceptibilities of the solutions and is calculated from the data of second and fourth columns with the formula, $\chi=\kappa/\rho$.

The mass susceptibility of $NiCl_2$ is computed from the observed mass susceptibilities of the solutions on the assumption that the constituent susceptibilities are additive. Based on the above figures the values are 33.95×10^{-6} and 33.99×10^{-6} respectively, for the solutions containing 4.105 percent and 10.14 percent $NiCl_2$. Similarly, assuming the validity of the additivity law for the Ni^{++} and 2 Cl^- ions in the $NiCl_2$ solutions, the calculated average value of the mass susceptibility of the nickel ion is 75.71×10^{-6}. The corresponding magnetic moment of the nickel ion is 16.0 Weiss magnetons, which is in good agreement with the values obtained by others.[4]

In conclusion the writer gratefully acknowledges his indebtedness to the physics department of Columbia University for the use of the apparatus.

[3] Stoner, *Magnetism and Matter*, p. 342.

[4] Reference 3, p. 327.

The Effect of Tension on the Electrical Resistance of Single Tetragonal Tin Crystals

MILDRED ALLEN
Physics Department, Mount Holyoke College, South Hadley, Massachusetts
(Received November 1, 1937)

The adiabatic tension coefficient of resistance of single tetragonal tin crystals has been determined for various orientations. Bridgman's theory, as modified by Cookson, has been extended to the tetragonal case and the experimental points found to lie within experimental error on the curves computed according to this theory. As measured directly, the tension coefficients depend both on the primary and secondary orientations of the crystal; for $\theta=90°$ they depend on the secondary orientation which is contrary to what has been found in the case of the trigonal crystals studied. The tension coefficients for specific resistance are found by allowing for the change in resistance which necessarily arises from the change in dimensions and these are found to be independent of the secondary orientation whatever the primary orientation, again contrary to what holds for trigonal crystals.

IN previous papers[1] the author has studied experimentally the effect of tension on the electrical resistance of the trigonal crystals, bismuth and antimony, and of the hexagonal crystals, zinc and cadmium. In the meantime Bridgman[2] has developed a general theory, consistent with these experimental results, which he applied specifically to the case of trigonal crystals, giving the tension coefficient of the specific resistance as a function of the primary and secondary orientations of the crystals with respect to the cylindrical axis of the casting. This theory was slightly modified by Cookson[3] who pointed out that on the basis of the necessary symmetries the matrix representing the piezoresistive coefficients was not required to be symmetrical, in that ρ_{rs} was not necessarily equal to ρ_{sr}, as Bridgman had assumed; there is, however, as yet no experimental evidence as to this. It was easy to pass from the trigonal to the hexagonal case since some of the coefficients appearing in the case of the trigonal crystals need only be put equal to zero to give the hexagonal case. Thus it came about that the tension coefficients of the hexagonal crystals were independent of the secondary orientation. It is therefore of interest to extend both the experimental and theoretical considerations to the study of a more drastically different type of crystal; and so *tetragonal tin* was chosen. The tetragonal case, however, is not completely unrelated to those previously studied, inasmuch as the hexagonal case may be considered a degenerate example of the tetragonal; for one may pass from the comparatively complicated theory of the tetragonal to the simpler hexagonal by postulating a suitable relation between its piezoresistive coefficients.

[1] Mildred Allen, Phys. Rev. **42**, 848 (1932); **43**, 569 (1933); **49**, 248 (1935).
[2] P. W. Bridgman, Phys. Rev. **42**, 858 (1932).
[3] John W. Cookson, Phys. Rev. **47**, 194 (1935).

APPLICATION OF THE BRIDGMAN THEORY TO TETRAGONAL CRYSTALS

To find the dependence of the tension coefficient on the primary and secondary orientations, the procedure is similar to that for the trigonal case.[2] As before the change in specific resistance is taken as a linear vector function of the six components of the tension tensor:

$$\begin{aligned}
\Delta r_x &= \rho_{11}X_x+\rho_{12}Y_y+\rho_{13}Z_z \\
&\quad +\rho_{14}Y_z+\rho_{15}Z_x+\rho_{16}X_y, \\
\Delta r_y &= \rho_{21}X_x+\rho_{22}Y_y+\rho_{23}Z_z \\
&\quad +\rho_{24}Y_z+\rho_{25}Z_x+\rho_{26}X_y, \\
\Delta r_3 &= \rho_{31}X_x+\rho_{32}Y_y+\rho_{33}Z_z \\
&\quad +\rho_{34}Y_z+\rho_{35}Z_x+\rho_{36}X_y, \qquad (1) \\
2\Delta r_4 &= \rho_{41}X_x+\rho_{42}Y_y+\rho_{43}Z_z \\
&\quad +\rho_{44}Y_z+\rho_{45}Z_x+\rho_{46}X_y, \\
2\Delta r_5 &= \rho_{51}X_x+\rho_{52}Y_y+\rho_{53}Z_z \\
&\quad +\rho_{54}Y_z+\rho_{55}Z_x+\rho_{56}X_y, \\
2\Delta r_6 &= \rho_{61}X_x+\rho_{62}Y_y+\rho_{63}Z_z \\
&\quad +\rho_{64}Y_z+\rho_{65}Z_x+\rho_{66}X_y.
\end{aligned}$$

The factor 2 is introduced into the last three equations to bring the notation into agreement with that of Bridgman which has been used throughout this work. Taking the Z axis in the direction of the crystallographic axis, the crystal has a tetragonal axis of symmetry in the Z direc-

tion and digonal axes of symmetry in the X and Y directions. When these conditions are applied to the general relations of Eq. (1) these take the simplified form:

$$\begin{aligned}
\Delta r_x &= \rho_{11}X_x+\rho_{12}Y_y+\rho_{13}Z_z,\\
\Delta r_y &= \rho_{12}X_x+\rho_{11}Y_y+\rho_{13}Z_z,\\
\Delta r_z &= \rho_{31}X_x+\rho_{31}Y_y+\rho_{33}Z_z,\\
\Delta r_4 &= \tfrac{1}{2}\rho_{44}Y_z,\\
\Delta r_5 &= \tfrac{1}{2}\rho_{44}Z_x,\\
\Delta r_6 &= \tfrac{1}{2}\rho_{66}X_y.
\end{aligned} \tag{2}$$

The total change in the specific resistance ΔR is then found from these values using the relation

$$\begin{aligned}
\Delta R = {} & \Delta r_x \cos^2\alpha+\Delta r_y \cos^2\beta+\Delta r_z \cos^2\gamma\\
& +2\Delta r_4 \cos\beta\cos\gamma+2\Delta r_5 \cos\alpha\cos\gamma\\
& +2\Delta r_6 \cos\alpha\cos\beta,
\end{aligned} \tag{3}$$

where α, β and γ are the angles made by the X, Y and Z axes with the axis of figure of the cylindrical casting and so are related to the primary orientation θ and the secondary orientation[1] φ in the following way:

$$\cos\alpha=\sin\theta\sin\varphi, \qquad \cos\beta=\sin\theta\cos\varphi, \qquad \cos\gamma=\cos\theta. \tag{4}$$

Carrying out these indicated substitutions, the final equation connecting the tension coefficient β (the relative change in specific resistance per unit applied tension) with the orientation angles is

$$\begin{aligned}
\beta\rho_\theta = {} & \frac{6\rho_{11}+2\rho_{12}+\rho_{66}}{8}\sin^4\theta+\rho_{33}\cos^4\theta\\
& +(\rho_{13}+\rho_{31}+\rho_{44})\sin^2\theta\cos^2\theta\\
& +\frac{2\rho_{11}-2\rho_{12}-\rho_{66}}{8}\sin^4\theta\cos 4\varphi,
\end{aligned} \tag{5}$$

where ρ_θ is the specific resistance for the primary orientation θ. Since the term in $\cos 4\varphi$ is multiplied by $\sin^4\theta$ it is immediately evident that the tension coefficient must vary with φ when θ is 90°. In this it differs markedly from the trigonal case where the coefficient of $\cos 3\varphi$ was a function of $\sin\theta\cos\theta$ and so was necessarily zero for $\theta=90°$.

To pass from the tetragonal case with its seven characteristic coefficients to the hexagonal one with six it is only necessary to substitute for ρ_{66} its value for the hexagonal case $2(\rho_{11}-\rho_{12})$. This causes the coefficient of the term in $\cos 4\varphi$ to vanish, as it must to agree with both theory and experiment according to which the tension coefficients of hexagonal crystals are entirely independent of the secondary orientation, and reduces the coefficient of $\sin^4\theta$ to its value ρ_{11} for the hexagonal case.

Experimental Procedure

The experimental procedure in the case of tin crystals was much the same as that used for zinc and cadmium.

The crystals themselves were made of Kahlbaum metal by the author in Bridgman's laboratory by slowly lowering the bent glass mold containing the tin through an electric furnace in an atmosphere of CO_2 to prevent oxidation. They had a diameter of approximately a sixteenth of an inch and a length of from one to two inches. They were also very pliable and needed to be handled with great care to prevent undesirable bending. The sensitivity of the galvanometer used, with the scale at about five meters, was 0.98×10^{-7} volts per centimeter deflection, or about twice the sensitivity of the one that had been available previously. The readings could not be made closer than to one-half a millimeter. Even under these favorable conditions, since the specific resistance of tin is small, the tension coefficients not large, and the elastic limit of tin crystals very low, it was rare to get a deflection greater than 2 cm and many of the measurements made involved deflections much smaller than this.

Results

Some two dozen tin crystals of varying orientations were measured, their temperature being kept close to 30.0°C. The reading with one crystal was discarded since it was found to be twice as large as any other and so indicated some discrepancy.

Computations were made from the observed tension coefficients of resistance in two ways. In the first the observed values of β were introduced directly into Eq. (5) and the ρ''s determined from the twenty-three measurements using the method of least squares. Logically this procedure is scarcely defensible, since the theory does apply to the change in specific resistance and not to the observed resistance which is affected by the changes in dimensions which must accompany the application of tension. However, since the change in dimensions produced by the tension

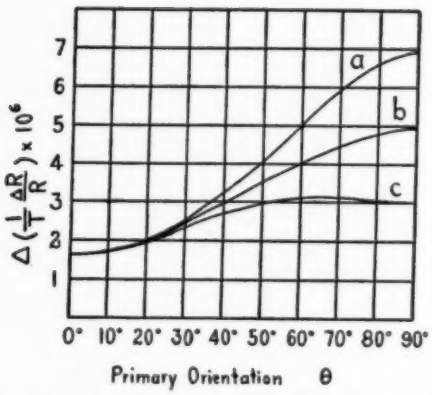

FIG. 1. Relative change of resistance per unit tension due *only* to changes in dimensions and orientation and computed from Bridgman's determination of the elastic constants of tin. *a*, $\varphi=45°$; *b*, $\varphi=22\frac{1}{2}°$; *c*, $\varphi=0°$.

has a symmetry very similar to that of the change in resistance the observed values fit Eq. (5) very well, and the ρ''s found in this way enable one to compute directly the change in resistance which will be *actually observed* by the application of a given tension to a crystal of a given orientation. The primes are used to indicate that the changes in resistance have *not* been corrected for the change in dimensions and are therefore not the piezoresistive coefficients which appear in the theory. Their values as found for tin are

$$\begin{aligned}(6\rho_{11}'+2\rho_{12}'+\rho_{66}')/8&=(0.69\pm0.44)\times10^{-11},\\ \rho_{33}'&=(11.36\pm0.76)\times10^{-11},\\ \rho_{13}'+\rho_{31}'+\rho_{44}'&=(28.5\pm2.2)\times10^{-11},\\ (2\rho_{11}'-2\rho_{12}'-\rho_{66}')/8&=(-1.88\pm0.52)\times10^{-11}.\end{aligned}\tag{6}$$

The tension is as usual expressed in kg/cm².

The second method of computation is to subtract from every observed relative change in resistance the computed relative change in resistance which would result from the change in dimensions and orientation caused by the application of the tension. That which remains then gives the relative change of specific resistance, arising perhaps from a slight rearrangement of the atoms in the crystal lattice, and is that change of resistance to which Bridgman's theory directly applies. To compute the relative change in resistance per unit applied tension which arises directly from the change in dimensions and orientation the theory sketched in the antimony paper[1] is developed for the tetragonal case and the values of the elastic constants given for tin by Bridgman[4] are used. The resulting values are presented in Fig. 1. It is to be noted that these values depend on the secondary orientation for $\theta=90°$ and that at $\theta=90°$ the maximum spread with variation of secondary orientation is 3.84×10^{-6}. From every observed tension coefficient there is then subtracted the appropriate value as interpolated from this graph, and the result is substituted in Eq. (5). Least squares are again applied and the ρ's determined which are now the real piezoresistive coefficients to which the theory sketched above applies. The numerical values found for these coefficients of specific resistance are

$$\begin{aligned}(6\rho_{11}+2\rho_{12}+\rho_{66})/8&=(-4.41\pm0.45)\times10^{-11},\\ \rho_{33}&=(8.96\pm0.77)\times10^{-11},\\ \rho_{13}+\rho_{31}+\rho_{44}&=(19.5\pm2.3)\times10^{-11},\\ (2\rho_{11}-2\rho_{12}-\rho_{66})/8&=(0.07\pm0.53)\times10^{-11}.\end{aligned}\tag{7}$$

The significance of these experimental results for the tension coefficient of resistance for tin can perhaps best be presented graphically in Fig. 2, where the curves marked *a*, *b* and *c* give the directly observed tension coefficients as a function of the primary and secondary orientations θ and φ, and the curve *d* the tension coefficients of the specific resistance. The directly observed curves are seen to depend on the secondary orientation φ at $\theta=90°$ (as did also the so-called correction curve of Fig. 1). The maximum spread with variation of φ is 3.62×10^{-6} which is within experimental error of the maximum spread of the correction curve. Hence it is to be expected that when the method of least squares is applied to the data for the tension coefficients of the specific resistance alone they will cease to be a function of the secondary orientation φ. This is shown to be true both graphically in Fig. 2(*d*) and in the numerical values of Eq. (7) where the coefficient of the term in cos 4φ is zero well within the probable error. This lack of dependence of the tension coefficients of the specific resistance on the secondary orientation for *all* values of the primary orientation is the most striking and unexpected result of this work on tin.

One or two other points deserve note. As is indicated in Fig. 2 negative values of the tension coefficients occur for certain orientations, giving further evidence that negative tension coefficients are not abnormal. These negative values were actually found for five of the crystals measured. As regards the order of magnitude of the results,

[4] P. W. Bridgman, Proc. Am. Acad. **60**, 379 (1925).

Tomlinson[5] gives for the tension coefficient of polycrystalline tin the value 5.89×10^{-6} which appears reasonable in the light of these present results. Rolnick's value[6] of 10.6×10^{-6} causes one to wonder whether his specimen was actually polycrystalline.

One test of the success of a theory lies in the agreement of the observed values with those computed according to the theory. Using the numerical values of the ρ''s (or ρ's) in Eq. (5) to compute the tension coefficients it was found that the average deviation between these computed values of the tension coefficients and the corresponding ones found experimentally is about 1.05×10^{-6}, where the actual values range from -1.33×10^{-6} to $+10.12\times10^{-6}$, the largest actual difference between the two being 3.0×10^{-6}. Various factors contribute to this somewhat large discrepancy which is consequently seen not to be exorbitant. The lower limit to which the galvanometer scale can be read introduces an uncertainty in the measured value of the tension coefficient of about 0.5×10^{-6}, the exact value depending of course on the size of the total resistance involved. The average deviation of the individual values of a single determination of the coefficient found with different tensions and with reversed current is only in three cases greater than this, so that 0.50×10^{-6} represents well the uncertainty arising from the galvanometer readings alone. A further uncertainty of about the same magnitude is caused by the difficulty of measurement of the orientations which had to be determined, as in the case of cadmium, by the reflection pattern method since tin does not cleave. The primary orientation is probably good to 3° while the secondary is uncertain to 4° or 5°. An uncertainty of a few percent in the area of cross section of the crystals is relatively not of great importance.

As noted in the paper on zinc and cadmium,[1] sufficient data are lacking, without further experimental work involving the torsion of the crystals, to allow one to disentangle the piezoresistive coefficients further. However, in the interests of collecting all the known data concerning the effect of stresses on the resistance of the tetragonal tin crystals, the pressure coefficients of specific resistance as determined by Bridgman[7] are given for reference.

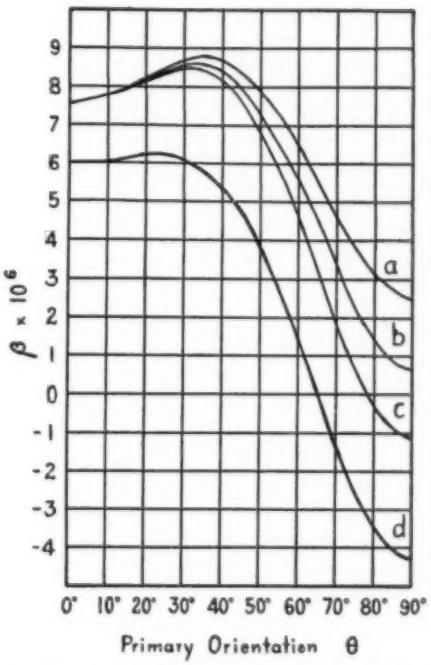

FIG. 2. Tension coefficients of tin directly observed: *a*, $\varphi=45°$; *b*, $\varphi=22\frac{1}{2}°$; *c*, $\varphi=0°$. Coefficients of *specific* resistance—curve *d*.

$$-\frac{2\rho_{13}+\rho_{33}}{\rho_{0°}}=\left(\frac{1}{p}\frac{\Delta R}{R}\right)_{\theta=0°}=-10.96\times10^{-6},$$

$$-\frac{\rho_{11}+\rho_{12}+\rho_{31}}{\rho_{90°}}=\left(\frac{1}{p}\frac{\Delta R}{R}\right)_{\theta=90°}=-10.28\times10^{-6}.$$

These pressure coefficients give two relations between the seven piezoresistive coefficients in addition to the four relations given by the application of longitudinal tensions described in this paper. The seventh necessary relation can be furnished by experiments on torsion which have not yet been carried out.

The author is much indebted to the National Research Council for a generous grant towards acquiring apparatus and supplies; in particular it made it possible to have one of the Leeds and Northrup galvanometers of high voltage sensitivity (HS No. 2285-a) as well as a large capacity 6-volt storage battery. She is also much indebted to Miss Haigouhi Haigazn, a graduate student at Mount Holyoke College in the year 1933–1934, who reassembled the apparatus after its removal from Harvard and who made the measurements on six of the crystals.

[5] Tomlinson, Phil. Trans. **174**, 1 (1883).
[6] H. Rolnick, Phys. Rev. **36**, 506 (1930).
[7] P. W. Bridgman, Proc. Am. Acad. **60**, 371 (1925).

LETTERS TO THE EDITOR

Prompt publication of brief reports of important discoveries in physics may be secured by addressing them to this department. Closing dates for this department are, for the first issue of the month, the eighteenth of the preceding month, for the second issue, the third of the month. Because of the late closing dates for the section no proof can be shown to authors. The Board of Editors does not hold itself responsible for the opinions expressed by the correspondents.

Communications should not in general exceed 600 words in length.

On the Spin of the Neutron

The intrinsic angular momenta of the proton and the deuteron imply a neutron spin (in units of $\hbar$) of either $\frac{1}{2}$ or $\frac{3}{2}$. The usual assumption of $\frac{1}{2}$ for the neutron spin is based entirely upon arguments of simplicity, since either of these two possible values is consistent with data on nuclear spins. In view of the importance of the neutron spin in nuclear theory, it would be desirable to determine this quantity by direct experiment. It has recently been shown[1] that experiments on the scattering of neutrons by ortho- and parahydrogen would enable one to obtain information about the spin dependence and the range of the neutron-proton interaction. It is the purpose of this note to point out that such experiments also permit the determination of the neutron spin.

A system composed of a proton and a neutron with S_n units of spin may have a resultant spin angular momentum of either $S_n+\frac{1}{2}$ or $S_n-\frac{1}{2}$. If the neutron spin is $\frac{3}{2}$, the excited state of the deuteron is a quintet state, as compared with a singlet excited state for $S_n=\frac{1}{2}$. In either case, the position of the excited level is determined by the requirement that σ_0, the cross section for the scattering of slow neutrons by free protons, equal the experimental value of 14×10^{-24} cm^2. For both possible values of the neutron spin, we may write

$$\sigma_0=4\pi\left(\frac{S_n+1}{2S_n+1}a^2_{S_n+\frac{1}{2}}+\frac{S_n}{2S_n+1}a^2_{S_n-\frac{1}{2}}\right), \qquad (1)$$

where the a's denote the amplitudes of the waves scattered in the states of corresponding resultant spin angular momenta. The triplet state amplitude was determined by an integral equation method from the interaction potential $-Be^{-(r/b)^2}$, with $B=36.8$ Mev and $b=2.25\times10^{-13}$ cm. The resultant value of $a_1=-5.73\times10^{-13}$ cm corresponds to a triplet scattering cross section of 4.13×10^{-24}cm^2. The values of a_0 and a_2 for the respective spins of $S_n=\frac{1}{2}$ and $S_n=\frac{3}{2}$ may then be calculated, with the results $a_0/a_1=\pm3.31$ and $a_2/a_1=\pm2.22$. For both spins, a plus sign indicates a real excited state, and a minus sign a virtual excited state.

The appropriate extension of Fermi's theorem[2] to the situation under consideration states that

$$-\frac{4\pi\hbar^2}{M}\left(\frac{S_n+1}{2S_n+1}a_{S_n+\frac{1}{2}}+\frac{S_n}{2S_n+1}a_{S_n-\frac{1}{2}}+\frac{1}{2S_n+1}(a_{S_n+\frac{1}{2}}-a_{S_n-\frac{1}{2}})\boldsymbol{\sigma}_p\cdot\mathbf{S}_n\right)\delta(\mathbf{r}_n-\mathbf{r}_p), \qquad (2)$$

where $\mathbf{S}_n$ and $\frac{1}{2}\boldsymbol{\sigma}_p$ are the spin operators of the neutron and the proton, is the effective neutron-proton interaction to be inserted in the Born approximation formula. By utilizing methods almost identical with those employed in reference 1, we may calculate the cross sections for the various transitions excited in molecular hydrogen by neutron impact. The cross sections thus obtained for *para→para*, *para→ortho*, *ortho→para*, and *ortho→ortho* transitions are, respectively, proportional to

$$\left(\frac{S_n+1}{2S_n+1}a_{S_n+\frac{1}{2}}+\frac{S_n}{2S_n+1}a_{S_n-\frac{1}{2}}\right)^2,$$

$$3\frac{S_n(S_n+1)}{(2S_n+1)^2}(a_{S_n+\frac{1}{2}}-a_{S_n-\frac{1}{2}})^2,$$

$$\frac{S_n(S_n+1)}{(2S_n+1)^2}(a_{S_n+\frac{1}{2}}-a_{S_n-\frac{1}{2}})^2,$$

and

$$\left(\frac{S_n+1}{2S_n+1}a_{S_n+\frac{1}{2}}+\frac{S_n}{2S_n+1}a_{S_n-\frac{1}{2}}\right)^2+\frac{2}{3}\frac{S_n(S_n+1)}{(2S_n+1)^2}(a_{S_n+\frac{1}{2}}-a_{S_n-\frac{1}{2}})^2.$$

The actual cross sections are these quantities multiplied by functions of the neutron energy which involve only properties of the hydrogen molecule.

The experiments of both Dunning[3] and Stern[4] and their collaborators show that the scattering cross section of *ortho*-H_2 at liquid-air neutron temperatures ($T=100°$K) is much larger than the corresponding *para*-H_2 cross section. It has already been pointed out[1] that this result is in agreement with the theoretical expectations for a virtual singlet state. Assuming a neutron spin of $\frac{3}{2}$, the theoretical value of the ratio $\sigma_{ortho}/\sigma_{para}$, at an energy of $3kT/2=0.012$ ev, is 3.11 for a virtual quintet state and 1.09 for a real quintet state. In either case, the two cross sections are quite comparable in magnitude, in contradiction with experiment. On the basis of these experiments the conclusion must be drawn that the intrinsic angular momentum of the neutron is, in reality, $\frac{1}{2}\hbar$.

The author wishes to express his deep gratitude to Professors Breit and Wigner for the benefit of stimulating conversations on this and other subjects.

JULIAN SCHWINGER*

University of Wisconsin,
Madison, Wisconsin,
November 17, 1937.

* Tyndall Fellow of Columbia University.

[1] J. Schwinger and E. Teller, Phys. Rev. **52**, 286 (1937).
[2] E. Fermi, Ricerca Scient. **7**, 13 (1936).
[3] J. R. Dunning, F. G. Brickwedde, J. H. Manley and H. J. Hoge, to be published shortly.
[4] J. Halpern, J. Estermann, O. C. Simpson and O. Stern, Phys. Rev. **52**, 142 (1937).

Does the Formula for the Rydberg Constant Require Revision?

Values of h/e with estimated error limits as determined by eight different methods are shown in the accompanying chart.[1] My purposes here are (1) to re-emphasize the inescapability of the discrepancy[2] between results III and VIII and (2) to consider which of the two is more likely to be correct. Recently von Friesen,[3] emphasizing method V, has ignored under generous error limits this discrepancy in an article which, I have learned from conversations and correspondence, gave many physicists a false sense of security.

To assign uncritically such discrepancies to errors of measurement as von Friesen seems to do is to ignore the possibility of obtaining precise information for the revision or refinement of theories and concepts. These, one cannot too often insist, are no more secure than their experimental foundations.

(1) Since the assignment of error limits is so controversial we refer the reader directly to our experimental results,[4] for the "isochromats" determining the threshold voltages of excitation of two different x-ray wave-lengths (continuous spectrum). These wave-lengths refer to the peak of the spectral "window" selected by the two-crystal monochromator, the window shapes being shown to correct voltage scale for both cases. I wish to emphasize the positions of the points W_1 and W_2 where the thresholds would have to be to make this experiment agree with VIII. Even with von Friesen's liberal error limits on e, the positions W_1 and W_2 cannot have uncertainties exceeding ± 12 and ± 6 volts, respectively (smallest divisions of voltage scale, Fig. 14, 10 volts).

The observed isochromat is a resultant of the true shape of the continuous spectrum and the shape of the "window" curve of the monochromator. If the former were an oblique featureless straight line terminating at the axis of abscissae then the integrated effect of its intenser regions shining through the remote "tail" of the "window" might indeed give the apparent shift of the isochromat toward lower voltages. *The humps K_2 on both isochromats make this explanation untenable and furnish the most clinching evidence for the discrepancy.*[5] These can only correspond to similar prominences on the true continuous spectrum and they must appear on the isochromat at that voltage at which such features of the continuous spectrum coincide with the *peak* of the "window" of the monochromator. Both conclusions follow because the window curve is everywhere so smooth save at its peak. The positions of K_2 and W therefore establish the reality of the discrepancy quite objectively.

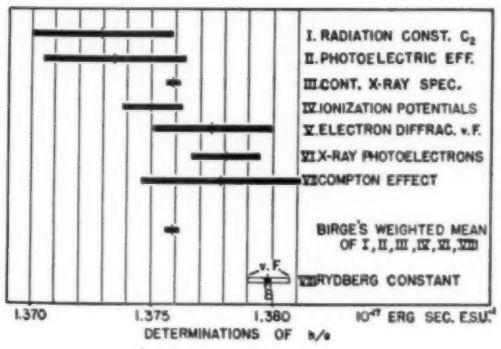

FIG. 1.

(2) Five of the six less precise methods plotted above have error limits overlapping III while only two overlap VIII. Any reasonably weighted mean of the six lies far closer to III than VIII. *This suggests that the Rydberg formula may require revision.* Such revision of theory must of course leave the series formula $(1/n^2 - 1/m^2)$ intact. It may be only a coincidence that if a constant multiplier $(1-\alpha^{-1})$ is joined to the present Rydberg formula the discrepancy vanishes (α being of order 137). Or perhaps the action quantum (like mean free path in kinetic theory) may be at present too vaguely defined and may require different values for different purposes.

JESSE W. M. DUMOND

California Institute of Technology,
Pasadena, California,
November 17, 1937.

[1] I have to thank Dr. K. Overhage who plotted all of this diagram save point V from Birge's most recent data. I have added V from von Friesen's article, reference 3.
[2] R. T. Birge, Phys. Rev. **52**, 241 (1937); DuMond and Bollman, Phys. Rev. **51**, 400 (1937).
[3] S. von Friesen, Proc. Roy. Soc. **A160**, 424 (1937).
[4] Fig. 14, Phys. Rev. **51**, 416 (1937).
[5] Humps K_2 were not previously observed for reasons discussed in our paper, reference 2. The substantial agreement of our results with those of others strongly supports the reality of the discrepancy. For this see Kirkpatrick and Ross, Phys. Rev. **51**, 529 (1937).

Stability of Neon and Carbon with Respect to α-Particle Disintegration

Kalckar, Oppenheimer and Serber in a recent article[1] have proposed as an explanation for the experimentally observed stability of compound nuclei Ne^{20}, C^{12} against α-decay by small $l-s$ coupling. The smallness of coupling would mean that the energy of coupling is small compared with the separation of energy levels, but it is well known that the distance between energy levels in heavy nuclei is very small and in the above elements is surely much less than the energy of $l-s$ coupling. Therefore such an explanation of the anomalous stability seems untenable.

I should like to point out that there is no need to look for special explanations, because the observed phenomenon can be explained by the fundamental conservation laws which, as is well known in wave mechanics, include also the conservation of parity. As already pointed out by Fermi for atoms it can sometimes occur that a decay which is energetically possible cannot take place because of this conservation law. Let us assume for instance that the state in question is an odd state with angular momentum zero and the states of the disintegration particles are even states with momenta also zero. Then it is easy to see that no states of relative motion can satisfy both the law of conservation of angular momentum and parity.

L. LANDAU

Moscow Institute for Physical Problems,
Academie of Sciences of USSR,
November 14, 1937.

[1] Phys. Rev. **52**, 279 (1937).

Light of the Night Sky

Last spring, during the preparation of a high pressure auroral tube, a number of afterglow spectrograms were obtained of the stage of the clean-up in which the cyanogen bands were very strong, the so-called cyanogen stage. Some ten new members of the tail bands in the CN violet $^2\Sigma \rightarrow {}^2\Sigma$ system were observed, all of them between λ3000 and λ3400. We have made the hypothesis that the tail bands, all of which originate on levels with $v = 10$ or higher, were enhanced in the cyanogen glow in a manner analogous to the enhancement of the green sequence of the first-positive group of nitrogen in the auroral glow. A comparison was then made between the wave-lengths of the tail band heads as given by Jenkins, and the list of unidentified night sky radiations of Gauzit.[1] The agreement, which is quite satisfactory, is indicated in Table I.

TABLE I. *Comparison of lines in the CN tail bands with unidentified lines in the light from the night sky.*

CN Tail Bands	Night Sky
4085	4083
4035	4036
3992	3990
3954	3950
3921	3921
3895	3891
3697	—
3666	3660
3632	3633
3505	3501
3470	3471
3438	3446

Rough measurements indicate that the ten new members agree with other night sky radiations. Thus the night sky excitation appears to produce selectively the tail bands of cyanogen.

JOSEPH KAPLAN

University of California at Los Angeles,
November 29, 1937.

[1] Gauzit, J. de phys. **5**, 527 (1934).

Origin of Cosmic Rays

The paper "Cosmic Rays on the Pacific," [1] reports the failure to observe an excess of intensity of the radiations in the Northern Hemisphere required by the extra-galactic theory of the origin of cosmic rays. Instead of abandoning the theory, however, the authors cling to it with the explanation that either the sun's motion with the rotation of the galaxy is only a small fraction of the 300 kilometers per second estimated by the astronomers, or that the rays are trapped within the galaxy and share its motion. Certain seasonal changes are also described which, to quote the authors, "indicate that the origin of the change is atmospheric rather than astronomical, . . . such atmospheric conditions might for example include the electric potential gradient, or the Heaviside layer." This latter idea, of changes in the intensity of the radiations being caused by the earth's electric field, appears to be moving in the direction of the suggestion advanced by this writer[2] to the effect that the radiations themselves are caused by an extension of the earth's field, not merely *changes* in their intensity, and that they originate not by some mysterious process in outer space, but in the outer reaches of our own atmosphere simply as a result of the acceleration of ions in the electric field.

It is generally conceded that the primary radiations do consist largely of high speed electrified particles. The most logical place then in which to seek their origin is not in thermal processes of the interiors of remote stars, nor in the primeval explosions postulated by Lemaitre but simply in an accelerating electric field. The earth's electric field has been measured up to a height of only 10 kilometers, a distance most minute compared with the dimensions of the earth. It has been found to decrease up to these heights, of course, but a reduction of field strength is to be expected in regions of increasing conductivity. If the field increases again after passing through the regions of high conductivity, as seems to be indicated by the auroral and other data referred to in the paper by Holmes, it could conceivably amount to the 10^8 or 10^{10} volts required. If these values do not seem quite high enough, there exists the possibility, or rather the probability, of still higher fields on the giant planets Jupiter and Saturn, which might account for the extremely high energy particles occasionally observed. Repeated reports of, and subsequent denials of, the extremely small sidereal effect could then be attributed to the changing relative positions of Earth, Saturn and Jupiter. Such a simple origin would also explain the fact that a slight sidereal effect is noted in the plane of the ecliptic but not the northern excess at right angles to the plane. Such an origin would also be consistent with the other two effects reported in the paper, namely the steady poleward increase of intensity after passing the knee, and the decrease in intensity when the earth is nearest the sun, since the outer electric field would then be smaller due to increased ionization and consequent conductivity.

M. C. HOLMES

Department of Physics,
West Virginia University,
Morgantown, West Virginia,
November 13, 1937.

[1] Compton and Turner, Phys. Rev. **52**, 799 (1937).
[2] M. C. Holmes, "A Terrestrial Origin for Cosmic Rays," J. Frank. Inst. **223**, 495 (1937).

Radioactive Isotopes of Element 43

Professor E. O. Lawrence kindly gave to one of us a molybdenum target which had been bombarded for many months with deuterons in the Berkeley cyclotron. The target arrived on January 6th, 1937 and the measurements which we report started on February 24th, 1937. All short-lived radioactive substances have thus escaped detection.

The molybdenum sample was analyzed chemically and it has been shown that its radioactivity is due to radioactive isotopes of element 43.[1] The following investigation is made on a sample precipitated together with Re by sulphuretted hydrogen and on a sample precipitated by means of nitron. Other samples prepared from other re-

actions or deposited electrolytically show the same absorption curves for the activity, taking into account the absorption by the substance itself, but we did not follow their radioactivity over a long period of time.

In Fig. 1 we report (curve *a*) the decay curve of the activity measured with an ionization chamber closed by two Al foils of 1μ thickness. The sample was wrapped in a 2.8 mg/cm² Al foil. All radiations had to pass the foils of the ionization chamber and the wrapping of the sample.

This decay curve is apparently fairly closely exponential, but from absorption measurements it is easily shown that it does not correspond to the curve for a single substance.

In Fig. 2 we give the absorption curves of the radiations. Curve *a* is taken on February 24, 1937 and curve *b* is taken on the same sample on November 11, 1937. They are drawn with different scales in order to have the same ordinate with an Al absorber of 2.8 mg/cm.[1] They show that the radiation emitted alters its composition with time. On the other hand there is a short-lived radiation which has, in our samples, a very small activity compared with the long period ones and it is difficult to obtain the periods of the different components of the total activity just by subtracting from the total activity the activity with the longest period, etc., according to the standard procedure.

We have therefore taken absorption curves of the total radiation in Al foils at different times. We have analyzed

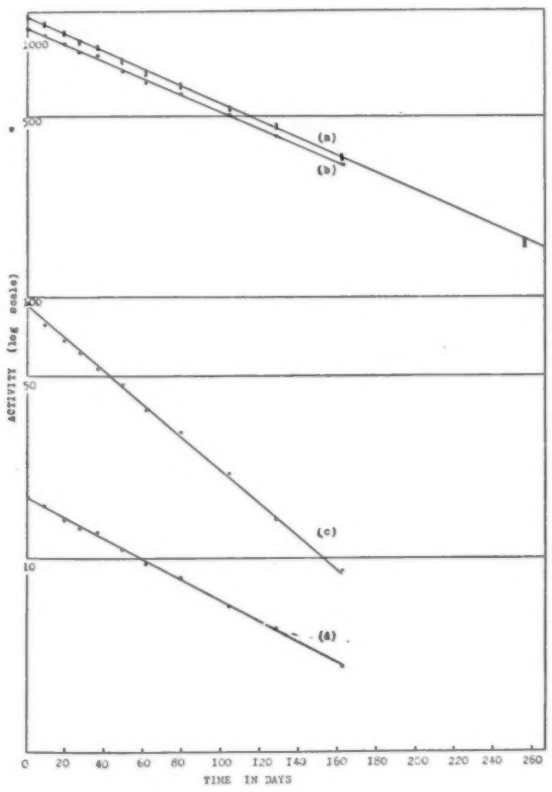

FIG. 1. (*a*) Decay curve of the activity of radioactive isotopes of element 43. (*b*), (*c*), and (*d*) Plot of the amplitude of the three component activities as a function of time.

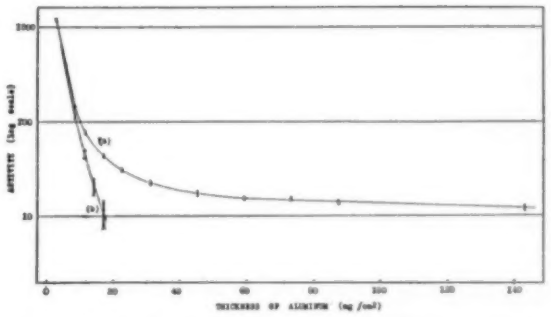

FIG. 2. Absorption curves of radiations from radioactive isotopes of element 43. Curve *a* is taken on February 24, 1937 and curve *b* is taken on November 11, 1937.

these curves in exponentials and we have plotted the amplitude of the components as a function of time (Fig. 1 curves *b*, *c*, *d*). This process is open to question for many reasons, but we could not find a better one applicable to our case. The experimental curve is very accurately reproduced by the sum of three components. Its equation according to our measurements is

$$y=1082\exp(-491x-t/130)+100\exp(-90x-t/72)+16.7\exp(-2.6x-t/118)$$

y=activity; x, absorber thickness in g/cm² Al; t, the time in days.

Thus we find 3 components with half-value periods of 90.50 and 80 days and half-value thickness of 1.4; 7.65; 264 mg/cm² Al, respectively.

Of course it is hard to be sure that there are only these three activities or to trust very much in the exactness of the half-value periods especially of the latter two. The period of the hardest component could very well be the same as the period of the softest one.

Molybdenum has seven stable isotopes all with the comparable abundances and it is impossible to assign the masses of the radioactive nuclei formed most probably by the usual reaction:

$$A_Z^M+D_1^2=B_{Z+1}^{M+1}+n_0^1.$$

The radiation emitted is mainly due to electrons as shown by magnetic deflection experiments; there is also a γ-radiation; the third (harder) component is chiefly due to it. One may suggest tentatively that this component is due to γ-rays accompanying the disintegration corresponding to the softest component.

Our warmest thanks are due to Professor E. O. Lawrence and to the staff of the Radiation Laboratory (Berkeley) which by their invaluable gift made this investigation possible.

B. N. CACCIAPUOTI
E. SEGRÈ

Royal University,
Palermo, Italy,
November 17, 1937.

[1] C. Perrier, E. Segrè, J. Chem. Phys. 5, 712 (1937).

On Sidereal Diurnal Variation in Cosmic-Ray Intensity

In their investigation of the apparent effect of galactic rotation upon the intensity of cosmic rays, Compton and Getting[1] stressed the importance of testing the reality of the apparent 24-hour sidereal wave indicated by their discussion of one year's data obtained by Hess and Steinmaurer[2] on the Hafelekar, Austria. Illing[3] from additional data at this station, and Schonland, Delatizky, and Gaskell[4] from data at Capetown, found sidereal curves somewhat similar to the theoretical curve of Compton and Getting, which has an amplitude about 0.05 percent of the total intensity and maximum near 21^h. Comparison of their curves for separate years does not lend support for the reality of the average.

Although rigorous statistical methods are available[5, 6] for determining the reality of geophysical periodicities, these have not been applied heretofore to cosmic-ray data except in the case of the solar diurnal variation.[7] Analyzing data for 595 days obtained with a Compton-Bennett[8] precision recording cosmic-ray meter at the Magnetic Observatory of the United States Coast and Geodetic Survey near Cheltenham, Maryland, we find an apparent 24-hour sidereal wave with amplitude about 0.03 percent of the total intensity and with maximum near 22^h. To test whether this wave is statistically significant we utilize the amplitudes of the 24-hour *solar* wave which were obtained for each of 273 days in our analysis of the solar diurnal variation.[7] For each day the calculated amplitude of the 24-hour sidereal wave will be practically indentical with that for the solar wave—only the phase will differ. We assume that the distribution of amplitudes for the remaining 322 days (out of 595) is similar to that obtained for the 273 days. Following Bartels[5] we find that, *if the phases associated with the 595 single amplitudes are completely random*, the probability of obtaining an average 24-hour sidereal wave with amplitude at least as great as that which we actually found is about one in fifty.

Those experienced in applying these tests would not take this to indicate more than the slightest suspicion of statistical reality for the observed 24-hour sidereal wave which, even if statistically real, might be due to other causes[5] than an actual sideral variation.

If a 24-hour sidereal wave actually exists in these data, the observations for 595 days are statistically inadequate to establish the fact. This conclusion is emphasized by analysis of data for 396 days from a Compton-Bennett meter at the Huancayo Magnetic Observatory of the Department of Terrestrial Magnetism. These data indicate an apparent 24-hour sidereal wave, the statistical significance of which has not been tested, with amplitude about 0.06 percent of the total intensity and with maximum near 5^h. Since this maximum differs by 7 hours, out of a possible 12, from that for the Cheltenham data, it is evident that the apparent sidereal wave at each station cannot be a true sidereal one.

Compton and Getting[1] found from the data of Hess and Steinmaurer[2] that the amplitude of the apparent 24-hour sidereal wave was nearly ten times their estimate of its probable error. Their exact procedure in obtaining this estimate was not given. Estimates of the probable errors in geophysical data are especially misleading. If based on the departures of observed points from a fitted wave, they are invariably too small unless the departures for successive points are *statistically independent*. Tests on cosmic-ray data from Cheltenham indicate that such departures are *not* independent. Our conclusions regarding the reality of the 24-hour sidereal wave are based on a method of analysis[5] which takes account of this.

It is surely one of the most constructive recent developments in physics that such powerful tools have been evolved for evaluating the real or illusory nature of such interesting periodicities.

S. E. FORBUSH

Department of Terrestrial Magnetism,
Carnegie Institution of Washington,
Washington, D. C.,
November 30, 1937.

[1] A. H. Compton and I. A. Getting, Phys. Rev. **47**, 817–821 (1935).
[2] V. Hess and R. Steinmaurer, Berlin, Sitz. Ber. Akad. Wiss. 521–542 (1933).
[3] W. Illing, Terr. Mag. **41**, 185–191 (1936).
[4] B. F. J. Schonland, B. Delatizky, and J. P. Gaskell, Nature **138**, 325 (1936).
[5] J. Bartels, Terr. Mag. **40**, 1–60 (1935).
[6] J. Bartels, Sitz. Ber. Akad. Wiss. 504–522 (1935).
[7] S. E. Forbush, Terr. Mag. **42**, 1–16 (1937).
[8] A. H. Compton, E. O. Wollan and R. D. Bennett, Rev. Sci. Inst. **5**, 415–422 (1934).

The Maximum Energy Obtainable from the Cyclotron

It is the purpose of this note to show that a very serious difficulty will arise when the attempt is made to accelerate ions in the cyclotron to higher energies than obtained thus far. This difficulty is due to the relativistic change of mass which has the effect of destroying either resonance or focusing. Since the resonance condition is extremely sensitive, quite small changes of mass, of the order of less than one percent, will have serious effects.

For exact resonance, the magnetic field H^0 must be given by

$$\omega = zeH^0/Mc, \tag{1}$$

where ω is the frequency of the electric field and ze is the charge of the ion. M is the relativistic mass

$$M = M_0(1+E/M_0c^2), \tag{2}$$

M_0 being the rest mass and E the ion energy. As the energy increases with increasing distance from the source, the *resonance field* H^0 *increases* also. At first sight it would seem natural to make the actual field equal to H^0 everywhere. Unfortunately, such a field while maintaining resonance will yield extremely small intensities because practically all the ions will be defocused and thus be lost from the beam (cf. below). Therefore it is necessary to choose a field H^1 which is not exactly the resonance field. At the νth acceleration the ion will then be off resonance by a phase difference

$$\Delta\theta_\nu = \pi \int_0^{n_\nu} (H^0/H - 1)dn. \tag{3}$$

Here H^0 and H are functions of the distance r from the source, r being proportional to n^2. If the phase shift at any point reaches π, an ion which is originally in phase to be accelerated by the electric field, will now be decelerated.

Therefore $\Delta\theta_\nu$ must always remain very small compared to π (let us say, $<\pi/6$).

Besides the resonance, the most important feature governing the intensity of the emergent beam is the focusing. As will be shown in a subsequent paper,[2] the focusing in the first part of the path is due to the electric field accelerating the ions, and in the second part is due to the magnetic field. The focusing depends on the quantity

$$Q=-\pi^2\frac{d\log H}{d\log r}+\pi\frac{\tan\theta}{\nu}, \tag{4}$$

where θ is the phase of the electric field at the time of the νth acceleration of the ion, $\theta=0$ corresponding to maximum dee voltage. When Q is positive, focusing of the ions results which is the better the larger Q. When Q is negative, the ions are strongly defocused and the beam intensity at the exit slit is reduced by a factor

$$\exp-\int_{\nu_0}^{N}|Q(\nu)|^{\frac{1}{2}}d\nu, \tag{5}$$

where N is the total number of accelerations and ν_0 is that value of ν at which Q becomes zero.

For large ν (large r) the first term in (4) (magnetic focusing) will be predominant and must therefore not be negative. This means that, at least for large r, the magnetic field must not increase with r. It is just in these regions where an increase is required by the resonance condition (1). Therefore we see that either the resonance or the focusing is destroyed by the relativistic change of mass irrespective of the special choice of the magnetic field.

It is interesting to estimate quantitatively the effects concerned. First we shall assume that the magnetic field is chosen equal to the resonance field. Assuming that ν_0 (cf. (5)) is small compared to N which is true for high energies (see below), we find for the beam intensity

$$\exp\left[-(2\pi N/3)(2E_0/M_0c^2)^{\frac{1}{2}}\right]$$
$$=\exp\left[-2^{\frac{1}{2}}(\pi/3)E_0^{\frac{1}{2}}(M_0c^2)^{-\frac{1}{2}}(V\varepsilon)^{-1}\right], \tag{6}$$

where V is the accelerating potential and E_0 the final energy of the ion. For protons of 20 MV and $V=100$ kv, this gives e^{-80}.

If we want to avoid this magnetic defocusing and at the same time preserve exact resonance, we must therefore make the critical ν_0 at least equal to N. For a phase $\theta=45°$, this gives for the maximum energy obtainable

$$E_m=(M_0c^2V\varepsilon/2\pi)^{\frac{1}{2}}. \tag{7}$$

Somewhat higher energies may, of course, be obtained by sacrificing exact resonance. In order to obtain best results, very careful design of the magnetic field is necessary. In the outer regions ($\nu>$ about ν_0), the magnetic field should be homogeneous or, perhaps, even decrease slowly. In the inner regions, a moderate increase is permissible. At the boundary of the two regions ($\nu\sim\nu_0$) the field should be slightly too large for resonance so that the ions will, in the outer region, first gain phase compared to the electric field and will only afterwards start losing phase. If we consider a loss of phase $\Delta\theta_N\sim\pi/6$ permissible, it will be possible to reach energies roughly twice as high as E_m (cf. (7)). With a dee voltage of 50 kv, this would permit the production of protons of about 5.5 MV, deuterons of 8 MV and α-particles of 16 MV. It will be noticed that these limits are very close to the highest energies actually obtained at present. Thus it appears that the cyclotron cannot be made to give much higher energies than those obtained thus far.

The only way to obtain higher energies seems to be to increase the voltage on the dees. But even this will increase the energy limit only moderately, i.e. just as the square root of the dee voltage. Therefore it seems useless to build cyclotrons of larger proportions than the existing ones. With a magnetic field of 18,000 gauss, an accelerating chamber of 37 cm radius will suffice to produce deuterons of 11 MV energy which is the highest obtainable with as much as 100 kv dee voltage. Pole pieces of 34″ diameter will be ample for such an accelerating chamber. For a field of 15,000 gauss which has some advantage for the calculation of the necessary "shimming," poles of 40″ diameter will be sufficient.

Note added December 4: We have found it possible to devise a magnetic field which gives, at 50 kv dee voltage, 12 MV protons, 17 MV deuterons or 34 MV α-particles with small but measurable intensities. These energies we believe to be the maximum obtainable. A homogeneous field, 0.6 percent greater than the resonance field at the center, will give protons of 10.5 MV, deuterons of 15 MV and α-particles of 30 MV with somewhat greater intensity.

H. A. Bethe
M. E. Rose

Cornell University,
Ithaca, New York.
November 24, 1937.

[1] H denotes the vertical component of the magnetic field.
[2] M. E. Rose, Phys. Rev., to appear shortly.

On the Scattering Cross Section of Fast Neutrons by Hydrogen

Recently we have measured[1] the scattering of 2.4 Mev neutrons by carbon and by paraffin and obtained as scattering cross section of hydrogen $(2.1\pm0.2)\times10^{-24}$ cm^2. This value is in apparent agreement with theory if one uses the formula given by Eq. (26) in the report of Bethe-Bacher.[2] Dr. E. Feenberg has kindly drawn our attention to the fact that the corrected scattering formula, where the finite range of nuclear forces is taken into account,[3] gives a somewhat higher value, namely 2.5×10^{-24}. A similar difference exists between the experimental value $(1.8\pm0.4)\times10^{-24}$ found by Booth and Hurst[4] for the scattering cross section of 2.9 Mev neutrons by hydrogen and the corrected theoretical value (2.34×10^{-24}). It thus appears from these data that a small, but real discrepancy exists between the theoretical and the experimental results.

Rudolf Ladenburg
Morton H. Kanner

Palmer Physical Laboratory,
Princeton University,
Princeton, N. J.,
November 27, 1937.

[1] Ladenburg and Kanner, Phys. Rev. **52**, 911 (1937).
[2] Bethe and Bacher, Rev. Mod. Phys. **8**, 117 (1936).
[3] See E. Wigner, Zeits. f. Physik **83**, 253 (1933) and especially Eq. (4) in the paper of Schwinger and Teller, Phys. Rev. **52**, 287 (1937).
[4] Booth and Hurst, Proc. Roy. Soc. **A161**, 248 (1937).

Possible Origin of the *X* Particle

Anderson, Neddermeyer, Street and Stevenson have recently reported evidence for the existence of an X particle of mass between the proton and the electron. In 1925 Bothe[1] considered the possibility of the Compton effect taking place in two stages. In the first stage the photon was absorbed by the electron and then later emitted in a direction different from the original direction. In both stages energy and momentum were conserved. The conservation principles required that at the end of the first stage the rest mass of the electron must be greater than its normal rest mass.

Taking a hint from the first stage of Bothe's process we consider the following process: A particle of rest mass m_1, traveling with velocity $\beta_1 c$ is struck by a photon $h\nu_1$. Part of the photon is absorbed so that the rest mass of the particle is changed to m_2 and its velocity to $\beta_2 c$ and a photon $h\nu_2$ is left over. For simplicity we suppose the photons $h\nu_1$ and $h\nu_2$ and the particle before and after the collision to be traveling in the same direction. Conservation of energy gives

$$h\nu_1+m_1c^2/(1-\beta_1^2)^{\frac{1}{2}}=h\nu_2+m_2c^2/(1-\beta_2^2)^{\frac{1}{2}} \quad (1)$$

and conservation of momentum gives

$$h\nu_1/c+m_1\beta_1c/(1-\beta_1^2)^{\frac{1}{2}}=h\nu_2/c+m_2\beta_2c/(1-\beta_2^2)^{\frac{1}{2}}. \quad (2)$$

We introduce $\alpha_1=h\nu_1/m_0c^2$, $\alpha_2=h\nu_2/m_0c^2$, $p_1=m_1/m_0$ and $p_2=m_2/m_0$, where m_0 is the rest mass of the ordinary electron. From (1) and (2) we obtain

$$p_1[(1-\beta_1)/(1+\beta_1)]^{\frac{1}{2}}=p_2[(1-\beta_2)/(1+\beta_2)]^{\frac{1}{2}}. \quad (3)$$

This relation means that the process we have supposed cannot occur unless there is a change of rest mass of the particle.

For brevity and simplicity we shall assume that an ordinary electron at rest partially absorbs the photon so that $p_1=1$ and $\beta_1=0$. We then obtain

$$p_2=[1+2(\alpha_1-\alpha_2)]^{\frac{1}{2}} \text{ and } \beta_2=(\alpha_1-\alpha_2)/(1+\alpha_1-\alpha_2). \quad (4)$$

When Street and Stevenson's recent value[2] of 130 for p_2 is put into (4), we obtain $\alpha_1-\alpha_2=8450$ and $\beta_2=1-1.18\times10^{-4}$. The loss of energy of the original photon was 4306 Mev. A photon with at least this energy was necessary to produce Street and Stevenson's particle from an ordinary electron at rest. On absorbing an energy of 4306 Mev from the photon the particle had a kinetic energy of 4240.5 Mev and a mass energy of 66 Mev. The mass energy of the original electron was 0.5 Mev. The kinetic energy of the particle was gradually lost by ionization along the path through the counter tubes, lead filter and intermediate air in the experiment. By the time the particle had reached the cloud chamber it had a kinetic energy of about 6 Mev and had preserved its rest mass of 130 m_0. It is conceivable that the particle may lose mass energy while producing ions. Also it may lose mass by emitting radiation. In this case the process of (1) and (2) is reversed. On this theory there is no special reason why the particle should have the mass 130 m_0 since the mass of the particle depends upon the energy of the original photon.

It has probably occurred to various physicists that Street and Stevenson's value of 130 for p_2 is not far from Eddington's mysterious 137. One is tempted to postulate that after the absorption of energy from the photon the particle which was originally an ordinary electron at rest develops a fixed mass of 137 m_0. Then, in virtue of (3), β_2 and the total energy of the particle is also fixed. A photon with energy of at least 4790 Mev is necessary.

G. E. M. Jauncey

Wayman Crow Hall of Physics,
Washington University,
St. Louis, Missouri,
December 1, 1937.

[1] Bothe, Zeits. f. Physik **34**, 819 (1925).
[2] Street and Stevenson, Phys. Rev. **52**, 1004 (1937).

The Band Spectrum of Antimony Chloride

The band spectrum attributed to the molecule SbCl, in the region λλ4200−5600, has been excited by means of active nitrogen. The spectrum consists of two (sub) systems of bands (designated A_1 and A_2) degraded toward the red end of the spectrum. The wave numbers of the heads of 28 bands are tentatively represented by the formulas:

$$A_1\colon \nu_1=19{,}146.1+367.7u'-2.61u'^2-483.3u''+1.43u''^2,$$
$$A_2\colon \nu_2=21{,}896.6+364.2u'-2.19u'^2-492.7u''+4.46u''^2.$$

The electronic separation, $\delta\nu_e$, the system origin, ν_e, and the vibrational coefficients, ω_e and $\chi_e\omega_e$, for these two systems are compared with the corresponding values for the band systems of other monohalides of group $V(b)$ elements. With increasing number of electrons and mass of a molecule the expected trend is observed; namely, a decrease in the values of ν_e, ω_e, and $\chi_e\omega_e$, and an increase in the value of $\delta\nu_e$.

I. Hudes

New York University,
Washington Square College,
New York, N. Y.,
November 29, 1937.

On Supraconductivity

In answer to a letter[1] by Wick about the diamagnetism of supraconductive bodies, F. London tries to show that the parallelism, claimed by Wick to exist between a metal which can be supraconductive and the system liquid gas (as described according to van der Waals) is misleading.[2] In his argument he points out that on the basis of Wick's suggestion above the transition line the neighborhood of the other (supraconductive) phase ought to make itself perceptible, as in the case of a nearly saturated vapor.

When, some time ago, I elaborated Langevin's old viewpoint of the existence of a separate supraconductive phase,[3] I had in mind experimental evidence suggesting an intimate connection between the two phases. For simplicity of argument I did not then stress this evidence. But as the matter is being discussed again, it might be useful to point out that measurements on thermoelectricity as well as on heat conductivity seem to indicate supraconductivity several degrees above the transition line.

When the temperature is lowered the thermoelectric force per degree decreases approximately linearly to the

(zero) value, which it reaches at the transition temperature, and which is the same for all supraconductors.[4] Also the heat conductivity of lead becomes extremely sensitive to a magnetic field a few degrees above the transition temperature.[5] Perhaps also the observation of "latent heat" above the transition line[6] and some of the mysterious relaxations in the transition[7] might be brought into harmony with Wick's view. This conception also describes satisfactorily the astonishing fact[8] that at the transition temperature the entropy as well as the free energy of the two phases are equal. Thus several experimental arguments suggest the existence of an unknown intimate relationship between the two phases.

I do not venture to take a standpoint in the theoretical controversy, but admitting that Wick's idea may easily lead to unjustified speculations, one must not forget that also London's very elegant treatment has not yet found any direct quantitative confirmation or refutation.

C. J. GORTER

Natuurkundig Laboratorium der Rijks-Universiteit,
Groningen, Germany,
November 9, 1937.

[1] G. C. Wick, Phys. Rev. **52**, 526 (1937); cf. Th. de Donder, Bull. Cl. d. Sc. Acad. roy. de Belgique (1926), p. 854.
[2] F. London, Phys. Rev. **52**, 886 (1937).
[3] C. J. Gorter, Arch. Teyler **7**, 378 (1933); Nature **132**, 931 (1933); cf. C. J. Gorter and H. Casimir, Physica **1**, 305 (1934).
[4] G. Borelius, W. H. Keesom, C. H. Johansson and J. O. Linde, Leiden Comm. 217*c*.
[5] H. Bremmer and W. J. de Haas, Leiden Comm. 243*a*; Physica **3**, 672 (1936).
[6] W. H. Keesom and J. A. Kok, Leiden Comm. 230*e* and 232*a*; Physica **1**, 503 and 595 (1934).
[7] W. H. Keesom and P. H. van Laer, Leiden Comm. 240*c*; Physica **3**, 173 (1936). J. W. Rjabinin and L. W. Schubnikov, Physik. Zeits. Sowjetunion **6**, 557 (1934). K. Mendelssohn and R. B. Pontius, Physica **3**, 327 (1936). W. J. de Haas and O. A. Guinau, Leiden Comm. 241*b*, Physica **3**, 534 (1936).
[8] C. J. Gorter and H. Casimir, Physik. Zeits. **35**, 963 (1934).

Author Index to Volume 52

References with (A) are to abstracts of papers presented at meetings of the American Physical Society. References with (L) are to Letters to the Editor.

Adams, N. I., Jr. (see Page, Leigh)—647

Albertson, Walter. Extension of the analysis of the spectrum of neutral samarium, Sm I—644

——— **and George R. Harrison.** Preliminary analysis of the first spark spectrum of cerium—Ce II—1209

Allen, Harriet W. Electron temperatures and mobilities in rare gases—707

——— (see Allis, W. P.)—703

Allen, Mildred. Effect of tension on the electrical resistance of single tetragonal tin crystals—1246

Allis, W. P. (see Tonks, Lewi)—710

——— **and Harriet W. Allen.** Theory of the Townsend method of measuring electron diffusion and mobility—703

Allison, Samuel K. On the generalization of the notation for the double crystal x-ray spectrometer—884(L)

Almy, G. M. (see Kinzer, G. D.)—814

Altar, William (see Condon, E. U.)—254(A)

Alvarez, Luis W. Nuclear K electron capture—134(L)

Anderson, Paul A. New charcoal trap for oil vapors—257(A)

——— Volta potential between barium and magnesium. An experimental test of the relation between work functions and volta potential—253(A)

Bacher, R. F. Scattering of neutrons by iron—248(A)

——— **and D. H. Tomboulian.** Electric quadrupole moment of In^{115}—836

Bacon, Ralph H., Edgar N. Grisewood and Carel W. van der Merwe. β-ray spectrum of Mn—668(L)

Baldes, E. J. (see Herrick, J. F.)—244(A)

Ballard, Stanley S. Some applications of spectroscopy to agriculture—253(A)

Bancroft, George H. Intensity variation of L series x-ray lines with the tube voltage—6

Bardeen, J. Conductivity of monovalent metals—246(A), 688

Barkas, Walter H. Interpretive remarks bearing on the metrical field associated with heavy particles—1074(L)

Barker, E. F. Perpendicular vibration bands of NH_3—250(A)

Bayley, D. S. and H. R. Crane. Beta-ray spectra of Li^8 and B^{12}—604

Beams, J. W. (see Snoddy, L. B.)—739

Bellamy, J. C. (see Parkinson, D. B.)—75, 247(A)

Benson, A. N. and R. A. Sawyer. Nuclear moment of barium—1127

Bernet, E. J. (see Herb, R. G.)—379(L)

Bernstein, Seymour (see Holley, Clifford)—525(L)

Bethe, H. A. and M. E. Rose. Maximum energy obtainable from the cyclotron—1254(L)

——— **and F. H. Spedding.** Absorption spectrum of $Tm_2(SO_4)_3 \cdot 8H_2O$—454

Beyer, H. (see Powers, P. N.)—38(L)

Birge, R. T. Comments on the letter by Sten von Friesen—886(L)

——— On the values of fundamental atomic constants—241(L)

Bitter, F. (see Tarasov, L. P.)—353

Bloch, F. (see Bradbury, N. E.)—256(A), 1023

——— **and A. Nordsieck.** Note on the radiation field of the electron—54

Bonner, Lyman G. and Robert Hofstadter. Infrared absorption spectra and approximate force constants of propene and allene—249(A)

Bonner, T. W. Neutron-proton scattering and the disintegration of deuterium by deuterons—685

——— (see Stephens, W. E.)—527(L), 1079

Bowen, I. S. Low terms in Cr III, Cr IV, Mn IV and Fe V—1153

——— **R. A. Millikan and H. V. Neher.** Influence of the earth's magnetic field on cosmic-ray intensities up to the top of the atmosphere—80

Bowls, Woolford E. Townsend coefficient in pure nitrogen—253(A)

Bradbury, N. E. and F. Bloch. Deuteron source for nuclear research—256(A)

———, **F. Bloch, H. Tatel and P. A. Ross.** Scattering and absorption cross sections of neutrons in cobalt—1023

Bramley, Arthur. Hard component of cosmic radiation—248(A)

Brammer, Forest E. (see Ruark, Arthur E.)—322, 885(L)

Breit, G. (see Share, S.)—546

——— **and J. R. Stehn.** On the comparison of proton-proton and proton-neutron interactions—396

Brickwedde, F. G. (see Dunning, J. R.)—1076(L)

Brosi, A. R. and William D. Harkins. Abundance ratio of the isotopes in natural or isotopically separated carbon—472

Brown, William Fuller, Jr. Domain theory of ferromagnetics under stress: Part I—325

Broxon, James W. (see Merideth, George T.)—252(A)

——— **and George T. Merideth.** High pressure ionization currents at high and low temperatures—252(A)

Brubaker, Gordon (see Pollard, Ernest)—762(L)

Bundy, F. P. Attempt to observe the spectrum of doubly excited helium—452

——— Excitation functions of the auroral bands of N_2^+ and the comet-tail bands of CO^+, excited by electron impact—698

Cacciapuoti, B. N. and E. Segrè. Radioactive isotopes of element 43—1252(L)

Carroll, H. (see Powers, P. N.)—38(L)

Carroll, Thomas. Magnetic rotation spectra of diatomic molecules—822

Cartmel, W. B. Is the null result inherent in the interferometer or the motion?—250(A)

——— Second-order null result of the Michelson-Morley-Miller experiment—250(A)

Cashman, R. J. Effect of temperature on photoelectric emission—512
——— Temperature effects in photoelectric emission—246(A)
Čerenkov, P. A. Visible radiation produced by electrons moving in a medium with velocities exceeding that of light—378(L)
Chapman, Seville. Carrier mobility spectra of spray electrified liquids—184
Ch'en, Shang-Yi (see Ny, Tsi-Ze)—1158
Chodorow, Marvin I. and Millard F. Manning. Energy bands in the body-centered lattice—731
Clark, G. L. (see Dunn, C. G.)—1167
——— **and C. G. Dunn.** X-ray and magnetic analyses of deformed silicon steel rings—1170
Clay, J. Ionization by gamma-rays and cosmic rays in gases at high pressure and high collecting fields—143
Cohen, V. W. (see Ellett, A.)—509
—— **and A. Ellett.** Velocity analysis by means of the Stern-Gerlach effect—502
Cohn, Byron E. and S. C. Lind. Luminescence and color excited by radium in zinc borate glasses which contain manganese—254(A)
Colby, M. Y. (see Daniels, F. B.)—1200(L)
Cole, A. C. (see Varney, Robert N.)—526(L)
Cole, K. S. (see Curtis, H. J.)—244(A)
Collins, J. R. Near infrared absorption band of liquid water at 1.79 μ—88
Compton, A. H. and R. N. Turner. Cosmic rays on the Pacific Ocean—799
Condon, E. U., William Altar and Henry Eyring. Theory of optical activity—254(A)
Cork, J. M. (see Kraus, J. D.)—763
——— (see Lawson, J. L.)—531
——— (see Pool, M. L.)—41(L), 239, 380(L)
——— (see Stewart, D. W.)—901
Crane, H. R. High potential apparatus for nuclear disintegration experiments—11
——— (see Bayley, D. S.)—604
——— (see Gaerttner, E. R.)—582
——— (see Turin, J. J.)—63, 247(A), 610
Curtis, H. J. and K. S. Cole. Alternating current impedance of *nitella*—244(A)

Daniels, F. B. and M. Y. Colby. Contact potential of cleavage face of zinc crystal cleaved in vacuum—1200(L)
Dempster, A. J. Isotopic constitution of tungsten—1074(L)
Dennison, D. M. (see Randall, H. M.)—160
Depp, Wallace A. (see Reich, Herbert J.)—245(A)
Dieke, G. H. and Margaret N. Lewis. Bands of HD and D_2 ending on the $2p^1\Sigma$ state—100
Dietrich, J. R. (see Snoddy, L. B.)—739
Djanab, Kamal (see Stephens, W. E.)—1079
Doermann, F. W. (see Halpern, O.)—937
Duffendack, O. S., H. Lifschutz and M. M. Slawsky. Production, characteristics and reliability of Geiger-Müller counters—1231
DuMond, Jesse W. M. Theory of the use of more than two successive x-ray crystal reflections to obtain increased resolving power—872
——— Does the formula for the Rydberg constant require revision?—1251(L)
——— **and Harry A. Kirkpatrick.** Direct spectrum of the structure and shift of the Compton line with helium gas as the scatterer—419
Dunn, C. G. (see Clark, G. L.)—1170
——— **and G. L. Clark.** Magnetic field of a symmetrical bundle of parallel wires carrying equal currents—1167
Dunning, J. R. (see Powers, P. N.)—38(L)
———, **F. G. Brickwedde, J. H. Manley and H. J. Hoge.** Interaction of neutrons with normal and parahydrogen —1076(L)
Dunnington, Frank G. Determination of e/m for an electron by a new deflection method. II—475

Eastman, E. D. Indication of a genetic relation between indium and tin—1226
Ellett, A. (see Cohen, V. W.)—502
——— **and V. W. Cohen.** Velocity analysis of potassium atoms scattering by magnesium oxide—509
Elsasser, Walter M. On quantum measurements and the role of the uncertainty relations in statistical mechanics —987
Estermann, I. (see Halpern, J.)—142(L)
———, **O. C. Simpson and O. Stern.** Magnetic moment of the proton—535
Evans, Robley D. and Clark Goodman. Alpha-particle counting and geologic ages—255(A)
Eyring, Henry (see Condon, E. U.)—254(A)
——— (see Hirschfelder, Joseph)—246(A)

Fairbrother, F. (see Livingood, J. J.)—135(L)
Feenberg, E. Further remarks on the saturation property of nuclear forces—667(L)
——— Note on the Thomas-Fermi statistical method—758
Forbush, S. E. On sidereal diurnal variation in cosmic-ray intensity—1254(L)
Fox, Francis E. Ultrasonic interferometry of liquid media—973
Fox, G. W. and H. T. Hurley. Diffraction patterns of silicon iron crystals oscillating magnetostrictionally—1077(L)
Fox, J. G. and G. Herzberg. Analysis of a new band system of the C_2 molecule—638
Froman, D. K. (see Stearns, J. C.)—254(A)
——— **and J. C. Stearns.** Cosmic-ray shower production curves on Mt. Evans—382(L)
——— **and J. C. Stearns.** Effects of time and meteorological factors on the intensities of cosmic-ray primaries and showers—255(A)
Furry, W. H. On fluctuations in size of multiplicative showers—247(A)
——— On fluctuations phenomena in the passage of high energy electrons through lead—569

Gabel, Joseph W. and R. V. Zumstein. The $^1\Sigma_1^* - {}^1\Sigma_1$ band system of ionized zinc deuteride—726
Gaerttner, E. R. and H. R. Crane. Experiments on the gamma-radiation from lithium and fluorine bombarded with protons—582

Gardner, M. E. Recombination of ions in pure oxygen as a function of pressure and temperature—252(A)
——— (see Varney, Robert N.)—526(L)
Germer, L. H. Electron diffraction studies of cuprous oxide—959
Gerö, L., G. Herzberg and R. Schmid. On the Cameron bands ($^3\Pi - {}^1\Sigma$) of carbon monoxide—467
Gibson, G. E. (see Seaborg, G. T.)—408
Ginsburg, Nathan (see Randall, H. M.)—160
Goeppert-Mayer, M. and Albert May. Erratum: Some lattice sums involved in the calculation of elastic constants—242(L)
Goodman, Clark (see Evans, Robley D.)—255(A)
Goodrich, Max. Electron scattering in helium—259
Gordy, Walter and Philip C. Martin. Infrared absorption of HCl in oxygenated solvents—1075(L)
Gorter, C. J. On supraconductivity—1256(L)
Grahame, D. C. (see Seaborg, G. T.)—408
Green, G. K. (see Kruger, P. Gerald)—247(A), 773
Green, J. B. Zeeman effect of the rare gases—736
Greenfield, E. W. Determination of fiber to void ratio of wood pulp paper by electrical methods—245(A)
Grisewood, Edgar N. (see Bacon, Ralph H.)—668(L)
Grover, Horace. Thermionic emission of positive ions from molybdenum—982
Gwathmey, E. (see Halpern, O.)—944

Hafstad, L. R. (see Roberts, R. B.)—247(A)
Halpern, J., I. Estermann, O. C. Simpson and O. Stern. Scattering of slow neutrons by liquid ortho- and para-hydrogen—142(L)
Halpern, O. and F. W. Doermann. Wide-angle interference of multipole radiation—937
——— **and E. Gwathmey.** Effect of similarity of particles on gas kinetic quantities with application to nuclear spins—944
——— **and M. H. Johnson, Jr.** Magnetic scattering of slow neutrons—52
——— **and M. H. Johnson.** On scattering of neutrons by magnetic dipoles—248(A)
Harkins, William D. Nuclear exclusion principle and the neutron-proton pattern—39(L)
——— (see Brosi, A. R.)—472
Harrington, E. L. (see Thiessen, G. J.)—256(A)
Harris, Wilbur T. (see Turner, Louis A.)—626, 630
Harrison, George R. (see Albertson, Walter E.)—1209
Hart, Harold M. Coexistence of dia- and paramagnetism in single crystals of antimony-tin alloys—130
Harvey, G. G. Simple derivation of the formula for the total scattering of x-rays from a general crystal—248(A)
Havens, R. J. (see Rollefson, R.)—249(A)
Haworth, E. E. Energy of lattice distortion in cold worked permalloy—613
Haxby, R. O. (see Shepherd, W. G.)—247(A), 674
——— (see Williams, J. H.)—247(A), 390, 1031
Hayner, Lucy J. (see Kurrelmeyer, Bernhard)—952
Heatley, A. H. Collector theory for ions with Maxwellian and drift velocities—235
Henderson, G. H. and G. C. Laurence. Range of the α-particles from thorium—46
Henderson, W. J. (see Ridenour, Louis N.)—139(L), 889
——— **and Louis N. Ridenour.** Artificial radioactivity produced by alpha-particles—40(L)
Hendricks, S. B. (see Maxwell, L. R.)—968
Henshaw, C. L. Normal energy distribution of photoelectrons from thin potassium films as a function of temperature—854
Herb, R. G. (see Parkinson, D. B.)—75, 247(A)
——— **and E. J. Bernet.** Maximum voltage of Wisconsin electrostatic generator as a function of air pressure—379(L)
Herrick J. F. and E. J. Baldes. Thermo-stromuhr for measuring blood flow—244(A)
Herring, Conyers. Accidental degeneracy in the energy bands of crystals—365
——— Effect of time-reversal symmetry on energy bands of crystals—361
Herzberg, G. (see Fox, J. G.)—638
——— (see Gerö, L.)—467
Herzfeld, Karl F. Second virial coefficient of argon—374
Hicks, Bruce. Shape of the Compton line for helium and molecular hydrogen—436
Hicks, Victor (see Sidhu, Surain S.)—667
Hill, E. L. (see Shepherd, W. G.)—674
Hirschfelder, J. O. and J. F. Kincaid. Application of the virial theorem to approximate molecular and metallic eigenfunctions—658
———, **David Stevenson and Henry Eyring.** Theory of liquid structure—246(A)
Hodgdon, Robert E. (see Lacount, Reginald G.)—98
Hoffman, J. G. and M. Stanley Livingston. Neutron absorption limit in cadmium—1228
Hofstadter, Robert (see Bonner, Lyman C.)—249(A)
Hoge, H. J. (see Dunning, J. R.)—1076(L)
Hoisington, L. E. (see Hudson, C. M.)—664(L)
Hollenberg, A. V. Hyperfine structure of the resonance lines of rubidium—139(L)
Holley, Clifford and Seymour Bernstein. Grating space of barium-copper-stearate films—525(L)
Holmes, M. C. Origin of cosmic rays—1252(L)
Holzer, R. E. (see Workman, E. J.)—256(A)
Houston, W. V. Surface photoelectric effect—1047
——— Viscosity of air—751
Hudes, I. Band spectrum of antimony chloride—1256(L)
Hudson, C. M. (see Parkinson, D. B.)—75, 247(A)
———, **L. E. Hoisington and L. E. Royt.** Dielectric strengths CCl_2F_2 air and SO_2 air mixtures—664(L)
Hughes, A. L. and S. S. West. Scattering of fast electrons in hydrogen—43
Hughes, D. S. and P. E. Lloyd. Pressure effects of homogeneous K vapor in absorption—1215
Hulswit, W. H., Jr. and B. J. Spence. Effect of containing tubes on ultrasonic velocities in benzene—256(A)
Humphreys, R. F. (see Watson, William W.)—318
Hurley, H. T. (see Fox, G. W.)—1077(L)

Hurst, D. G. (see Laslett, L. Jackson)—1035
Hustrulid, A. (see Kusch, P.)—840, 843
——— (see Tate, John T.)—249(A)

Ichimiya, T. (see Nishina, Y.)—1198
Iskenderian, Haig P. Paramagnetic measurements at low fields with the Rankine balance—1244

Jauncey, G. E. M. Possible origin of the *X* particle—1256(L)
——— **and E. M. McNatt.** Electron asymmetry in the atoms of zinc crystals—257(A)
Jenkins, F. A. and George D. Rochester. Spectrum of SnF—1135
——— **and George D. Rochester.** Extension of the spectrum of AgCl—1141
Jesse, William P. Experiments on the variation of the atomic structure factor of nickel with x-ray wave-length—443
Johnson, M. H., Jr. (see Halpern, O.)—52, 248(A)
Johnson, R. P. (see Koller, Lewis R.)—519
Johnson, Thomas H. Vertical cosmic-ray intensity up to 43.5 mm Hg—255(A)

Kalckar, F., J. R. Oppenheimer and R. Serber. Note on nuclear photoeffect at high energies—273
———, **J. R. Oppenheimer and R. Serber.** Note on resonances in transmutations of light nuclei—279
Kamen, Martin (see McMillan, Edwin)—375
Kanne, W. R. Disintegration of aluminum by polonium alpha-particles—266
——— On the preparation of polonium sources—380(L)
Kanner, Morton H. (see Ladenburg, Rudolf)—911; 1255(L)
Kaplan, Joseph. Light of the night sky—1252(L)
——— Preparation of auroral afterglow tubes—254(A)
——— Production of ions in the auroral glow—257(A)
Kemmer, N. Field theory of nuclear interaction—906
Kincaid, J. F. (see Hirschfelder, J. O.)—658
King, Robert B. (see Russell, Henry Norris)—456
Kinzer, G. D. and G. M. Almy. Emission spectrum of diatomic arsenic. II—814
Kirkham, Don. Variation of the initial susceptibility with temperature, and the variation of the magnetostriction and reversible suceptibility with temperature and magnetization in nickel—1162
Kirkpatrick, Harry A. (see DuMond, Jesse W. M.)—419
Kirkpatrick, Paul. Double scattering of polarized x-rays—1201
——— (see Smick, A. E.)—256(A)
Koller, Lewis R. and R. P. Johnson. Visual observations on the Malter effect—519
Knerr, Henry W. Electric spectrum of liquid water from five to twenty centimeters—1054
Knauss, Harold P. and Myron S. McCay. Temperature determinations from band spectral data—1143
Kraus, J. D. and J. M. Cork. Radioactive isotopes of palladium and silver from palladium—763
Kruger, P. Gerald and G. K. Green. Gamma-ray spectrum of B^{10}—247(A), 773
——— **and H. S. Pattin.** Extreme ultraviolet spectra of scandium VI, scandium VII and other elements isoelectronic with phosphorus I and sulphur I—621
——— **and L. W. Phillips.** Deep terms in the spectra of Sc VIII and Sc IX—97
——— **and S. G. Weissberg.** Extreme ultraviolet series of Cr VI, Mn VII and Fe VIII—314
———, **W. E. Shoupp and F. W. Stallmann.** Scattering of protons by neutrons—678
Kuhn, H. Pressure shift of spectral lines—133(L)
Kurrelmeyer, Bernhard and Lucy J. Hayner. Shot effect of secondary electrons from nickel and beryllium—952
Kusch, P. (see Tate, John T.)—249(A)
———, **A. Hustrulid and John T. Tate.** Dissociation of HCN, C_2H_2, C_2N_2 and C_2H_4 by electron impact—843
———, **A. Hustrulid and John T. Tate.** Dissociation processes produced in $SbCl_3$, $AsCl_3$ and PCl_3 by electron impact—840

Lacount, Reginald G. and Robert E. Hodgdon. Interferometer wave-lengths in the secondary spectrum of hydrogen—98
Ladenburg, Rudolf and Morton H. Kanner. On the neutrons from the deuteron-deuteron reaction—911
——— **and Morton H. Kanner.** On the scattering cross section of fast neutrons by hydrogen—1255(L)
Lagsdin, J. B. (see Wyckoff, Ralph W. G.)—254(A)
Landau, L. Stability of neon and carbon with respect to α-particle disintegration—1251(L)
Landshoff, Rolf. Quantum mechanical calculation of the lattice energy of NaCl—246(A)
Lang, R. J. (see Russell, Henry Norris)—456
Langer, Lawrence M. (see Mitchell, Allan C. G.)—137(L)
Laporte, Otto. Absorption coefficients for thermal neutrons. Remarks on the preceding paper of C. T. Zahn—72
——— (see Mack, J. E.)—254(A)
——— **and J. E. Mack.** Spectral series in neutral tungsten, WI, and limitations upon the possibility of determining spectroscopic ionization potentials—249(A)
Laslett, L. Jackson. Long period positron activity: Na^{22}—529
——— **and D. G. Hurst.** Energy losses of fast electrons—1035
Laurence, G. C. (see Henderson, G. H.)—46
Lawson, J. L. (see Stewart, D. W.)—901
——— **and J. M. Cork.** Radioactive isotopes of indium—531
Lewis, Margaret N. (see Dieke, G. H.)—100
Libby, W. F. and Earl A. Long. Production and properties of low temperature neutrons—592
Lifschutz, H. (see Duffendack, O. S.)—1231
Lind, S. C. (see Cohn, Byron E.)—254(A)
Little, Edward M. Liquid *vs.* vapor temperature—255(A)
Livingood, J. J. and G. T. Seaborg. Radioactive antimony isotopes—135(L)
———, **F. Fairbrother and G. T. Seaborg.** Radioactive isotopes of manganese, iron and cobalt—135(L)
Livingston, M. Stanley (see Hoffman, J. G.)—1228
Lloyd, P. E. (see Hughes, D. S.)—1215

Loeb, Leonard B. Ionic recombination in the ionosphere—40(L), A correction—136(L)
London, F. On a letter of Wick's about superconductivity—886(L)
Long, Earl A. (see Libby, W. F.)—592

Mack, J. E. (see Laporte, O.)—249(A)
——— **and Otto Laporte.** Structure of the arc spectrum of tungsten, WI.—254(A)
Manley, J. H. (see Dunning, J. R.)—1076(L)
Mann, W. B. Nuclear transformations produced in copper by alpha-particle bombardment—405
Manning, Millard F. (see Chodorow, Marvin I)—731
Margenau, Henry (see Warren, Dana T.)—1027
——— **and Dana T. Warren.** Normal states of nuclear three- and four-body systems—790
——— **and William W. Watson.** Pressure shifts of krypton lines—384(L)
Martin, Philip C. (see Gordy, Walter)—1075(L)
Mason, R. C. Breakdown of vacuum spark gaps—126
——— Reflection coefficient of mercury—248(A)
Maxwell, L. R., S. B. Hendricks and V. M. Mosley. Interatomic distances of the alkali halide molecules by electron diffraction—968
May, Albert. Lattice energies and transition temperatures of caesium chloride and ammonium chloride—339
——— (see Goeppert-Mayer, M.)—242(L)
McCay, Myron S. (see Knauss, Harold P.)—1143
McCormick, W. W. and R. A. Sawyer. First spark spectrum of tin: Sn II—249(A)
McDonald, John C. Grain orientation in rolled magnesium alloys—886(L)
McKeehan, L. W. Magnetic interaction and resultant anisotropy in unstrained ferromagnetic crystals—18
——— Errata: Magnetic quadruple field and energy in cubic and hexagonal crystals and magnetic interaction and resultant anisotropy in unstrained ferromagnetic crystals—527(L)
McMillan, Edwin, Martin Kamen and Samuel Ruben. Neutron-induced radioactivity of the noble metals—375
McNatt, E. M. (see Jauncey, G. E. M.)—250(A)
McNish, A. G. On the ultraviolet light theory of magnetic storms—155, Errata—762(L)
Merideth, George T. (see Broxon, James W.)—252(A)
——— **and James W. Broxon.** Preliminary report on recombination of ions in air at high pressures—252(A)
Merrill, Paul W. Unidentified interstellar lines—761(L)
Michels, Walter C. Accommodation coefficients of the noble gases and the specific heat of tungsten—1067
Millikan, R. A. (see Bowen, I. S.)—80
Mitchell, Allan C. G. Sargent curves for artificially radioactive substances—1
——— **and Lawrence M. Langer.** Energy of the gamma-rays of radioindium and radiomanganese—137(L)
——— **and R. N. Varney.** Neutron scattering cross section as a function of energy—282
More, Kenneth R. and Alice H. Parker. Band spectrum of TiCl—1150
Morgan, Karl Z. and W. M. Nielsen. Shower production under thick layers of various materials—564
Morgan, J. E. (see Nielsen, W. M.)—568
Mosley, V. M. (see Maxwell, L. R.)—968
Motz, Lloyd and William Rarita. Photoelectric effect of H^2—271
Mueller, Hans. Intensity and polarization of the light diffracted by supersonic waves in solids—223

Nahmias, M. E. Further search for transmutations with possible emission of negative protons—525(L)
——— On the distribution of the lifetimes of radio elements—666(L)
Neher, H. V. (see Bowen, I. S.)—80
Newman, Morris. Short time lag of spark breakdown—652
Nielsen, W. M. (see Morgan, Karl Z.)—564
——— **and J. E. Morgan.** Note on the production of showers in various materials—568
Nier, Alfred O. Isotopic constitution of osmium—885(L)
——— Mass-spectrographic study of the isotopes of Hg, Xe, Kr, Be, I, As, and Cs—933
Nilikantan, P. Temperature variation of the magnetic anisotropy of ammonium nitrate—383(L)
Nishina, Y., M. Takeuchi and T. Ichimiya. On the nature of cosmic-ray particles—1198
Nordsieck, A. Low frequency radiation of a scattered electron—59
——— (see Bloch, F.)—54
Norton, K. A. Space and surface waves in radio propagation—132(L)
Ny, Tsi-Zé and Shang-Yi Ch'en. Pressure effects of rare gases on the second doublet of rubidium principal series—1158
——— **and San-Tsiang Tsien.** Band spectra and energy of dissociation of the rubidium molecule—91

Ochiai, K. Collision of proton and deuteron—1221
O'Conor, John S., S. J. Beta-ray spectrum of radium E—303
Oppenheimer, J. R. (see Kalckar, F.)—273, 279
Overhage, Carl J. F. Normal energy distribution of photoelectrons from sodium—1039

Page, Leigh, and N. I. Adams, Jr. Electromagnetic waves in conducting tubes—647
Parker, Alice H. (see More, Kenneth R.)—1150
Parkinson, D. B., R. G. Herb, J. C. Bellamy and C. M. Hudson. Range of protons in aluminum and in air—75, 247(A)
Pattin, H. S. (see Kruger, P. Gerald)—621
Paul, Fred W. Absorption spectra of manganese and silver in the Schumann region—923
Phillips, L. W. (see Kruger, P. Gerald)—97
Pickering, W. H. Production of cosmic-ray showers at great depths—1131
Pielemeier, W. H. Acoustical detection of purely mechanical vibrations in quartz plates—244(A)
——— Supersonic dispersion in air—244(A)
Plumley, Harold J. Contact potentials for metals immersed in a dielectric and conduction of electricity by liquid dielectrics—140(L)

Pollard, Ernest and Gordon Brubaker. Maximum energy of the protons from the bombardment of boron by alpha-particles—762(L)
Pool, M. L., J. M. Cork and R. L. Thornton. Evidence for the simultaneous ejection of three neutrons from elements bombarded with fast neutrons—41(L)
———, **J. M. Cork and R. L. Thornton.** Positron-electron emitting isomer in radio-silver—380(L)
———, **J. M. Cork and R. L. Thornton.** Survey of radioactivity produced by high energy neutron bombardment —239
Poritsky, H. (see Suits, G. C.)—136(L)
Powers, P. N., H. Carroll, H. Beyer and J. R. Dunning. Sign of the magnetic moment of the neutron—38(L)
Primakoff, H. On the relation of proton-deuteron to neutron-deuteron scattering—1000

Quimby, S. L. and Sidney Siegel. Elastic constants of crystalline sodium at 80°K—665(L)

Randall, H. M., D. M. Dennison, Nathan Ginsburg and Louis R. Weber. Far infrared spectrum of water vapor—160
Rarita, William (see Motz, Lloyd)—271
Reich, Herbert J. and Wallace A. Depp. Dynamic characteristic curves of glow-discharge tubes—245(A)
Ridenour, Louis N. (see Henderson, W. J.)—40(L)
——— **and W. J. Henderson.** Artificial radioactivity produced by alpha-particles—139(L), 889
Risser, J. R. Neutron-induced radioactivity of long life in cobalt—768
Roberts, R. B., L. R. Hafstad and L. H. Rumbaugh. Delayed alpha-particles from Li^7 bombarded by deuterons—247(A)
Robinson, Howard A. Additions to certain spectra of sulphur, potassium and calcium—724
——— **and George H. Shortley.** Coupling of p electron configurations—713
Rochester, George D. (see Jenkins, F. A.)—1135, 1141
Rogers, F. T., Jr. Note on the absolute determination of magnetic field strength—381(L)
Rollefson, R. and R. J. Havens, Index of refraction of methane in the infrared—249(A)
Rose, M. E. (see Bethe, H. A.)—1254(L)
Ross, P. A. (see Bradbury, N. E.)—1023
Rouse, Arthur G. Large angle scattering and energy loss of potassium ions scattered by heavy monatomic gases—1238
Royt, L. E. (see Hudson, C. M.)—664(L)
Ruark, Arthur E. and Forest E. Brammer. Efficiency of counters and counter circuits—322: Erratum—885(L)
Ruben, Samuel (see McMillan, Edwin)—375
Rukavichnikov, V. N. First USSR cyclotron—1077(L)
Rumbaugh, L. H. (see Roberts, R. B.)—247(A)
Russell, Henry Norris, Robert B. King and R. J. Lang. Third spectrum of cerium (Ce III)—456

Sambursky, S. Static universe and nebular red shift---335
Sampson, J. B. Energy levels of neon and argon—1157
Sawyer, R. A. (see Benson, A. N.)—1127
——— (see McCormick, W. W.)—249(A)
Schelkunoff, Sergei A. Electromagnetic waves in conducting tubes—1078(L)
Schiff, L. I. On the capture of thermal neutrons by deuterons—242(L)
——— Scattering of neutrons by deuterons—149
Schmid, R. (see Gerö, L.)—467
Schwinger, Julian. On the spin of the neutron—1250(L)
——— **and E. Teller.** Scattering of neutrons by ortho- and parahydrogen—286
Seaborg, G. T. (see Livingood, J. J.)—135(L)
———, **G. E. Gibson and D. C. Grahame.** Inelastic scattering of fast neutrons—408
Seely, Samuel. Variation of the diamagnetism of water with temperature—662(L)
——— **(see Zinn, Walter H.)**—919
Segrè, E. (see Cacciapuoti, B. N.)—1252(L)
Serber, R. (see Kalckar, F.)—273, 279
Shankland, Robert S. Compton effect with gamma-rays—414
Share, S. and G. Breit. Relativistic effects for the deuteron —546
——— **and J. R. Stehn.** Effects of long range forces on neutron-proton scattering—48
Shepherd, W. G. (see Williams, J. H.)—247(A), 390, 1031
———, **R. O. Haxby and E. L. Hill.** Search for protons from Li bombarded by Ra C′ α-particles—674
———, **R. O. Haxby and J. H. Williams.** Gamma-rays from B and Be under proton bombardment and from Li under bombardment—247(A)
Shockley, W. Empty lattice test of the cellular method in solids—866
Shortley, George H. (see Robinson, Howard A.)—713
Shoupp, W. E. (see Kruger, P. Gerald)—678
Sidhu, Surain S. and Victor Hicks. Space lattice and "super-lattice" of pyrrhotite—667(L)
Siegel, Sidney. (see Quimby, S. L.)—665(L)
Siegert, A. J. F. Note on the interaction between nuclei and electromagnetic radiation—787
Simpson, O. C. (see Estermann, I.)—535
——— (see Halpern, J.)—142(L)
Sixtus, K. J. Coercive force in single crystals—347
Skinner, Selby M. Thin-film lubrication of non-planar surfaces of finite width—244(A)
Slater, J. C. Nature of the superconducting state. II—214
——— Theory of ferromagnetism: Lowest energy levels—198
Slawsky, M. M. (see Duffendack, O. S.)—1231
Smick, A. E. and Paul Kirkpatrick. Fringe systems produced by passage of x-rays through plane slits—256(A)
Smith, Noyes D. Molecular spectrum of hydrogen in mixtures of hydrogen and helium—728
Snavely, Benjamin L. Secondary processes of ionization in mercury vapor—174
Snell, Arthur H. Radioactive isotopes of bromine: Isomeric forms of bromine 80—1007
Snoddy, L. B., J. R. Dietrich and J. W. Beams. Propagation of potential in discharge tubes—739

Spedding, Frank H. Sharp absorption lines for use as a comparison spectra in stellar photography—137(L)
——— (see Bethe, H. A.)—454
Spees, A. H. (see Zahn, C. T.)—524(L)
Spence, B. J. (see Hulswit, W. H., Jr.)—256(A)
Spencer, Roy C. Theorem on the effect of vertical divergence—761(L)
Stallmann, F. W. (see Kruger, P. Gerald)—678
Starr, Merle A. Ionization in cosmic-ray tracks—253(A)
Stearns, J. C. (see Froman, Darol K.)—255(A), 382(L)
——— **and D. K. Froman.** Frequency of cosmic-ray showers produced in different metals—254(A)
Stehn, J. R. (see Breit, G.)—396
——— (see Share, S. S.)—48
Stephens, W. E. and T. W. Bonner. Disintegration of boron by deuterons—527(L)
———, **Kamal Djanab and T. W. Bonner.** Neutrons from the disintegration of nitrogen by deuterons—1079
Stephenson, S. T. Focusing x-ray ionization spectrometer —255(A)
Stern, O. (see Estermann, I.)—535
——— (see Halpern, J.)—142(L)
Stevenson, David (see Hirschfelder, Joseph)—246(A)
Stevenson, E. C. (see Street, J. C.)—1003(L)
Stewart, D. W., J. L. Lawson and J. M. Cork. Induced radioactivity in strontium and yttrium—901
Straus, H. A. Magnetic focusing of ion beams—128
Street, J. C. (see Young, R. T., Jr.)—552
——— **and E. C. Stevenson.** New evidence for the existence of a particle of mass intermediate between the proton and electron—1003(L)
Stueckelberg, E. C. G. On the existence of heavy electrons —41(L)
Suits, C. G. High pressure arc phenomena—245(A)
——— **and H. Poritsky.** Interpretation of high pressure arc data—136(L)
Swann, W. F. G. Electrodynamic force equation in its bearing upon the evidence for the existence of a new cosmic-ray particle—387

Takeuchi, M. (see Nishina, Y.)—1198
Tarasov, L. P. and F. Bitter. Precise magnetic torque measurements on single crystals of iron—353
Tate, John T. (see Kusch, P.)—840, 843
———, **A. Hustrulid and P. Kusch.** Products of dissociation of ethylene by electron impact—249(A)
Tatel, H. (see Bradbury, N. E.)—1023
Teller, E. (see Schwinger, Julian)—286
Thein, Louis P. Photoelectric sensitization of aluminum—245(A)
Thiessen, G. J. and E. L. Harrington. Use of twin sources in experimental studies of thermal neutrons—256(A)
Thompson, Julian L. Solar diurnal variation of cosmic-ray intensity as a function of latitude—140(L)
Thornton, R. L. (see Pool, M. L.)—41(L), 239, 380(L)
Tomboulian, D. H. (see Bacher, R. F.)—836
Tonks, Lewi and W. P. Allis. Plasma electron drift in a magnetic field with a velocity distribution function—710
Torrey, H. C. Erratum; The sign of the magnetic moment of the K^{39} nucleus—30
Tsien, San-Tsing (see Ny, Tsi-Zé)—91
Turin, J. J. and H. R. Crane. Absorption of high energy electrons, Part I—63: Part II—610
——— **and H. R. Crane.** Energy loss of high energy beta-rays in lead—247(A)
Turner, Louis A. Stepwise fluorescence in mercury-nitrogen mixtures. The 3650 line—632
——— **and Wilbur T. Harris.** Determination of rotational quantum numbers in single *Q* branches—630
——— **and Wilbur T. Harris.** Ultraviolet bands of magnesium hydride—626
Turner, R. N. (see Compton, A. H.)—799

Valasek, Joseph. X-ray spectroscopic data in regard to the electronic energy bands in potassium and sodium chloride—250(A)
van der Merwe, Carel W. (see Bacon, Ralph H.)—668(L)
Van Vleck, J. H. On the anisotropy of cubic ferromagnetic crystals—1178
——— On the magnetic susceptibilities of Ti, V, and Cr alums—246(A)
Varney, R. N. (see Mitchell, Allan C. G.)—282
———, **Milton E. Gardner and A. C. Cole.** Ionization of mercury vapor by positive potassium ions—526(L)
von Friesen, Sten. On the values of fundamental atomic constants—886(L)

Walke, Harold J. New radioactive isotope of potassium—663(L)
——— Induced radioactivity of scandium—669
——— Induced radioactivity of titanium and vanadium—777
——— Radioactive isotopes of scandium from calcium and potassium by alpha-particle bombardment—400
Wannier, Gregory H. Structure of electronic excitation levels in insulating crystals—191
Warren, Dana T. (see Margenau, Henry)—790
——— **and Henry Margenau.** Note on the validity of methods used in nuclear calculations—1027
Watson, William W. (see Margenau, Henry)—384(L)
——— **and R. F. Humphreys.** Ultraviolet spectra of BeH and BeH^+—318
Wayland, Harold. Ionization of neon, krypton and xenon by bombardment with accelerated neutral argon atoms —31
Weber, Louis R. (see Randall, H. M.)—160
Weissberg, S. G. (see Kruger, P. Gerald)—314
Weisskopf, V. Statistics and nuclear reactions—295
West, S. S. (see Hughes, A. L.)—43
Wheeler, John Archibald. Molecular viewpoints in nuclear structure—1083
——— On the mathematical description of light nuclei by the method of resonating group structure—1107
——— Wave functions for large arguments by the amplitude-phase method—1123
Whitaker, Martin D. Magnetic scattering of neutrons—384(L)
Wick, G. C. Diamagnetism of superconducting bodies—526(L)

Williams, H. J. Magnetic properties of single crystals of silicon iron—747

——— Variation of initial permeability with direction in single crystals of silicon-iron—1004(L)

Williams, J. H. (see Shepherd, W. G.)—247(A)

———, **R. O. Haxby and W. G. Shepherd.** Disintegration of Be by protons and deuterons—247(A)

———, **Robert O. Haxby and William G. Shepherd.** Disintegration of beryllium and the masses of the beryllium isotopes—1031

———, **William G. Shepherd and Robert O. Haxby.** Disintegration of lithium by deuterons—390

Williams, R. M. (see Winans, J. G.)—250(A) 930

Winans, J. G. and R. M. Williams. Collisions of the second kind and sensitized fluorescence of tin and mercury atoms—250(A)

——— **and R. M. Williams.** Sensitized fluorescence of tin—930

Workman, E. J. and R. E. Holzer. Multiple camera for lightning studies—256(A)

Wyckoff, Ralph W. G. and J. B. Lagsdin. Design and performance of quantity heads for the air-driven ultracentrifuge—254(A)

Young, L. A. Proton's magnetic moment—138(L)

Young, R. T., Jr. Cosmic-ray measurements with a small ionization chamber. II. Comparison of small bursts at different altitudes and their variations with thickness of shield—559

——— **and J. C. Street.** Cosmic-ray measurements with a small ionization chamber. I. Variation with altitude and latitude of the total ionization for various shields—552

Zahn, C. T. Absorption coefficients for thermal neutrons—67

——— **and A. H. Spees.** Ratio of e/m for *primary* beta-rays from radium E—524(L)

Zener, Clarence. Internal friction in solids. I. Theory of internal friction in reeds—230

Zinn, Walter H. Low voltage positive ion source—655

——— **and Samuel Seely.** Neutron generator utilizing the deuteron-deuteron reaction—919

Zumstein, R. V. (see Gabel, Joseph W.)—726

Analytic Subject Index to Volume 52

References with (A) are to abstracts of papers presented at meetings of the American Physical Society. References with (L) are to Letters to the Editor.

Absorption (see also **Scattering of electrons, neutrons, and ions; X-ray, absorption**)
- Of electrons in Pb and C, L. J. Laslett, D. G. Hurst—1035
- Of high energy electrons, J. J. Turin, H. R. Crane—63; 247(A), 610
- Range of protons in Al and air, D. B. Parkinson, R. G. Herb, J. C. Bellamy, C. M. Hudson—75; 247(A)
- Of thermal neutrons, C. T. Zahn—67; O. Laporte—72

Accommodation coefficient
- Of noble gases, W. C. Michels—1067

Acoustics
- Detection of vibrations in quartz plates, W. H. Pielemeier—244(A)
- Diffraction by supersonic waves in solids, H. Mueller—223
- Supersonic dispersion, W. H. Pielemeier—244(A)
- Ultrasonic interferometry in liquids, F. E. Fox—973
- Ultrasonic velocities in tubes, W. H. Hulswit, Jr., B. J. Spence—256(A)

Astrophysics
- Sharp lines for comparison in stellar photography, F. H. Spedding—137(L)
- Static universe and red shift, S. Sambursky—335

Atmospheric electricity (see **Meteorology**)

Atomic and molecular beams
- Velocity of K atoms scattered by MgO, A. Ellett, V. W. Cohen—509
- Velocity by Stern-Gerlach effect, V. W. Cohen, A. Ellett—502

Atomic form factors
- Of Ni, variation with wave-length, W. P. Jesse—443

Aurora
- Afterglow tubes, J. Kaplan—254(A) 257(A)

Biophysics
- Impedance of *nitella*, H. J. Curtis, K. S. Cole—244(A)
- Measuring blood flow, J. F. Herrick, E. J. Baldes—244(A)

Collisions of second kind
- In Sn and Hg, J. G. Winans, R. M. Williams—250(A); 930

Compton effect (see **X-rays, diffraction, scattering**)

Conductivity, electrical (see **Electrical conductivity; Discharge of electricity in gases**)

Constants, physical, standards
- Atomic constants, R. T. Birge—241(L); 886(L); S. von Friesen—886(L)
- Values of h/e; Rydberg constant, J. W. M. DuMond—1251(L)

Contact potentials
- Of Ba and Mg; work function, P. A. Anderson—253(A)
- Of Zn, change in vacuum, F. B. Daniels and M. Y. Colby—1200(L)
- In liquid dielectrics, H. J. Plumley—140(L)

Cosmic radiation
- Diurnal variation; latitude, J. L. Thompson—140(L)
- Electrodynamic force equation; new particle, W. F. G. Swann—387
- Fluctuation phenomena, W. H. Furry—247(A); 569
- Frequency of showers, J. C. Stearns, D. K. Froman—254(A)
- γ-ray ionization currents in air, J. W. Broxon, G. T. Merideth—252(A)
- Hard component, A. Bramley—248(A)
- Intensities near top of atmosphere, I. S. Bowen, R. A. Millikan, H. V. Neher—80
- Ionization in gases, high pressure and high fields, J. Clay—143
- Ionization tracks, M. A. Starr—253(A)
- Nature of particles, Y. Nishina, M. Takeuchi, T. Ichimiya—1198
- Particle of mass between proton and electron, E. C. G. Stueckelberg—41(L); J. C. Street, E. C. Stevenson—1003(L); G. E. M. Jauncey—1256(L)
- Primaries and showers, intensities, D. K. Froman, J. C. Stearns—255(A)
- Records from Vancouver to Sydney, A. H. Compton, R. N. Turner—799
- Shower-production under thick layers, K. Z. Morgan, W. M. Nielsen—564
- Showers at great depths, W. H. Pickering—1131
- Showers curves on Mt. Evans, D. K. Froman, J. C. Stearns—382(L)
- Showers in various materials, W. M. Nielsen, J. E. Morgan—568
- Sidereal diurnal variation, S. E. Forbush—1254(L)
- Small bursts, variation with thickness of shield, R. T. Young, Jr.—559
- Terrestrial origin, M. C. Holmes—1252(L)
- Total ionization for various shields, R. T. Young, Jr., J. C. Street—552
- Vertical intensity, T. H. Johnson—255(A)

Crystal structure
- Lattice and "superlattice" of pyrrhotite, S. S. Sidhu, V. Hicks—447(L)

Crystalline state
- Anisotropy of cubic ferromagnetic crystals, J. H. Van Vleck—1178
- Anisotropy in ferromagnetic crystals, L. W. McKeehan—18; 527(L)
- Deformed silicon steel, x-ray and magnetic analyses, G. L. Clark, C. G. Dunn—1170
- Electronic energy bands in KCl and NaCl, J. Valasek—250(A)
- Electronic levels in insulating crystals, G. H. Wannier—191
- Energy bands in body-centered lattice, M. I. Chodorow, M. F. Manning—731

Energy bands of crystals, C. Herring—361; 365
Energy of lattice distortion, F. E. Haworth—613
Grain orientation in rolled Mg alloys, J. C. McDonald—886(L)
Lattice energies of CsCl and NH_4Cl, A. May—339
Lattice energy calculation, R. Landshoff—246(A)
Magnetic properties of Fe crystals; initial permeability, H. J. Williams—747; 1004(L)
Resistance and tension of Sn crystal, M. Allen—1246
Superconducting state, J. C. Slater—214
Susceptibility, magnetostriction in Ni, D. Kirkham—1162
Test of cellular method in solids, W. Shockley—866

Dielectrics and dielectric properties
Dielectric strengths of CCl_2F_2 and SO_2, C. M. Hudson, L. E. Hoisington, L. E. Royt—664(L)
Discharge of electricity in gases
Collection of ions, A. H. Heatley—235
Dynamic characteristics of tubes, H. J. Reich, W. A. Depp—245(A)
Electron diffusion and mobility, W. P. Allis, H. W. Allen—703
Electron temperatures and mobilities, H. W. Allen—707
High pressure arc, C. G. Suits, H. Poritsky—136(L); C. G. Suits—245(A)
Plasma electron drift, L. Tonks, W. P. Allis—710
Propagation of potential in tubes, L. B. Snoddy, J. R. Dietrich, J. W. Beams—739
Recombination at high pressures, G. T. Merideth, J. W. Broxon—252(A)
Recombination in oxygen, M. E. Gardner—252(A)
Time lag of spark, M. Newman—652
Townsend coefficient in N_2, W. E. Bowls—253(A)
Discharge of electricity in high vacuum (see also **Thermionic emission; High voltage tubes and machines**)
Breakdown of spark gaps, R. C. Mason—126
Disintegration of nucleus (see also **Radioactivity**)
α-particles from Li^7, R. B. Roberts, L. R. Hafstad, L. H. Rumbaugh—247(A)
Of Al by He^4, W. R. Kanne—266
Of Be; masses of Be isotopes, J. H. Williams, R. O. Haxby, W. G. Shepherd—274(A); 1031
β-rays from Li^8 and B^{12}, D. S. Bayley, H. R. Crane—604
Of B by H^2, W. E. Stephens, T. W. Bonner—527(L)
Of B, energy of H^1, E. Pollard, G. Brubaker—762(L)
Capture of neutrons by deuterons, L. I. Schiff—242(L)
Of Cu by He^4, W. B. Mann—405
Of deuterium by H^2, T. W. Bonner—685
Ejection of three neutrons, M. L. Pool, J. M. Cork, R. L. Thornton—41(L)
γ-radiation from Li and F, E. R. Gaerttner, H. R. Crane—582
γ-ray of B^{11}, P. G. Kruger, G. K. Green—247(A); 773
γ-rays from B and Be, W. G. Shepherd, R. O. Haxby, J. H. Williams—247(A)
Of Li by H^2, J. H. Williams, W. G. Shepherd, R. O. Haxby—390
Negative protons; search for, M. E. Nahmias—525(L)
Neutrons from H^3-H^2 reaction, R. Ladenburg, M. H. Kanner—911
Of N by H^2, W. E. Stephens, K. Djanab, T. W. Bonner—1079
Of noble metals, E. McMillan, M. Kamen, S. Ruben—375
Resonances in transmutations, F. Kalckar, J. R. Oppenheimer, R. Serber—279
Search for H^1 from Li, W. G. Shepherd, R. O. Haxby, E. L. Hill—674
Dissociation
Of HCN, C_2H_2, C_2N_2 and C_2H_4 by electrons, P. Kusch, A. Hustrulid, J. T. Tate—249(A); 843
Of $SbCl_3$, $AsCl_3$ and PCl_3 by electrons, P. Kusch, A. Hustrulid, J. T. Tate—840
Dissociation, heat of (see also **Molecular structure and constants**)
Of Rb_2, Ny Tsi-Zé, Tsien San-Tsiang—91

Elasticity
Constants of crystalline Na at 80°K, S. L. Quimby, S. Siegel—665(L)
Erratum: Calculation of elastic constants, M. Goeppert-Mayer, A. May—242(L)
Internal friction in solids, C. Zener—230
Electrical conductivity and resistance
Diamagnetism of superconducting bodies, G. C. Wick—526(L); F. London—886(L)
Of liquid dielectrics, H. J. Plumley—140(L)
Of monovalent metals, J. Bardeen—246(A); 688
Superconducting state, J. C. Slater—214
Supraconductivity and diamagnetism, C. J. Gorter—1256(L)
Of Sn crystals under tension, M. Allen—1246
Electromagnetic theory
Space and surface waves, K. A. Norton—132(L)
Waves in conducting tubes, L. Page, N. I. Adams, Jr.—647; S. A. Schelkunoff—1078(L)
Electron diffraction (see also **Electrons, scattering of**)
In cuprous oxide, L. H. Germer—959
Interatomic distances of alkali halides, L. R. Maxwell, S. B. Hendricks, V. M. Mosley—968
Electrons
Existence of heavy electrons, E. C. G. Stueckelberg—41(L); J. C. Street, E. C. Stevenson—1003(L)
Electrons, scattering of
Of high energy, J. J. Turin, H. R. Crane—63; 247(A); 610
In H_2, A. L. Hughes, S. S. West—43
Electrons, secondary
Shot effect from Ni and Be, B. Kurrelmeyer, L. J. Hayner—952
E/m
Determination by a new deflection method, F. G. Dunnington—475
E/m for β-rays from RaE, C. T. Zahn, A. H. Spees—524(L)
Equations of state
Second virial coefficient of A, K. F. Herzfeld—374

Errata
Efficiency of counters and counter circuits, A. E. Ruark, F. E. Brammer—322; 885(L)
"Magnetic quadrupole field and energy in cubic and hexagonal crystals" and "Magnetic interaction and resultant anisotropy in strained ferromagnetic crystals," L. W. McKeehan—18; 527(L)
The sign of the magnetic moment of K^{39} nucleus, H. C. Torrey—30
Some lattice sums involved in the calculation of elastic constants, M. Goeppert-Mayer, A. May—242(L)
On the ultraviolet theory of magnetic storms, A. G. McNish—155; 762(L)
Errors of measurements
Atomic constants, R. T. Birge—241(L); 886(L); S. von Friesen—886(L)
Evaporation
Reflection coefficient of Hg, R. C. Mason—248(A)

Fluorescence
In Hg−N_2 mixtures, L. A. Turner—632
Of Sn and Hg, J. G. Winans, R. M. Williams—250; 930

Gamma-rays (see **Radioactivity**)
Geophysics
Geologic ages and α-particle counting, R. D. Evans, C. Goodman—255(A)

High voltage tubes and machines
Cyclotron with homogeneous field, V. N. Rukavichnikov—1077(L)
Dielectric strengths of CCl_2F_2 and SO_2, C. M. Hudson, L. E. Hoisington, L. E. Royt—664(L)
Maximum energy from cyclotron, H. A. Bethe, M. E. Rose—1254(L)
Transformer system at Michigan, H. R. Crane—11
Voltage of Wisconsin generator; air pressure, R. G. Herb, E. J. Bernet—379(L)
Hyperfine structure (see also **Nuclear moments and spin**)
Of Rb resonance lines, A. V. Hollenberg—139(L)

Instruments (see **Methods and instruments**)
Insulators
Fiber in wood pulp, E. W. Greenfield—245(A)
Ionization by particles (see also **Ionization potentials**)
In Hg vapor, secondary processes, B. L. Snavely—174
Of Hg by K^+, R. N. Varney, M. E. Gardner, A. C. Cole—526(L)
Of Ne, K, and Xe by A atoms, H. Wayland—31
Ionization potentials
Appearance potentials of ions in HCN, C_2H_2, C_2N_2 and C_2H_4 by electron impact, P. Kusch, A. Hustrulid, J. T. Tate—249(A); 843
Appearance potentials of ions in $SbCl_3$, $AsCl_3$ and PCl_3 by electron impact, P. Kusch, A. Hustrulid, J. T. Tate—840
Ionization by radiation (see **Photoionization**)
Ionosphere (see also **Meteorology**)
Ionic recombination corrections, L. B. Loeb—40(L); 136(L)
Magnetic storms, ultraviolet light theory, A. G. McNish—155; 762(L)
Ions, mobility
In electrified sprays, S. Chapman—184
Isotopes
Abundance ratio of C^{12} and C^{13}, A. R. Brosi, W. D. Harkins—472
Of Hg, Xe, Kr, Be, I, As, and Cs, A. O. Nier—933
Of Os, A. O. Nier—885(L)
Transition of Sn^{115} to In^{115}, E. D. Eastman—1226
Tungsten 180, A. J. Dempster—1074(L)

Kinetic theory of gases
Liquid *vs.* vapor temperature, E. M. Little—255(A)
Similarity of particles, transport phenomena, O. Halpern, E. Gwathmey—944

Liquids
Grating space of barium-copper-stearate films, C. Holley, S. Bernstein—525(L)
Theory of liquid structure, J. Hirschfelder, D. Stevenson, H. Eyring—246(A)
Thin-film lubrication, S. M. Skinner—244(A)
Luminescence
Excited by radium in glasses, B. E. Cohn, S. C. Lind—254(A)
Malter effect, visual observations, L. R. Koller, R. P. Johnson—519
Radiation by electrons moving in a medium with velocities exceeding c/n, P. A. Čerenkov—378(L)

Magnetic fields
Of bundle of parallel wires, C. G. Dunn, G. L. Clark—1167
Magnetic properties
Analyses of deformed silicon steel, G. L. Clark, C. G. Dunn—1170
Anisotropy of NH_4NO_3, temperature variation, P. Nilikantan—383(L)
Anisotropy in crystals, L. W. McKeehan—18; 527(L)
Anisotropy of cubic ferromagnetic crystals, J. H. Van Vleck—1178
Coercive force in single crystals, K. J. Sixtus—347
Coexistence of dia- and paramagnetism, H. M. Hart—130
Of crystals of Fe, initial permeability, H. J. Williams—747; 1004(L)
Diamagnetism of superconducting bodies, G. C. Wick—526(L); F. London—886(L)
Diamagnetism of water, temperature variation, S. Seely—662(L)
Domain theory; stress, W. F. Brown, Jr.—325
Initial susceptibility, magnetostriction, variation with temperature, D. Kirkham—1162
Paramagnetic measurements at low fields, H. P. Iskenderian—1244
Susceptibilities of Ti, V, and Cr alums, J. H. Van Vleck—246(A)

Theory of ferromagnetism, J. C. Slater—198
Torque measurements on crystals of Fe, L. P. Tarasov, F. Bitter—353
Velocity analysis by Stern-Gerlach effect, V. W. Cohen, A. Ellett—502
Mechanics, quantum—general
Capture of neutrons by deuterons, L. I. Schifi—242(L)
Low frequency radiation of electron, A. Nordsieck—59
Methods used in nuclear calculations; validity of, D. T. Warren, H. Margenau—1027
Nuclear effect at high energies, F. Kalckar, J. R. Oppenheimer, R. Serber—273
Photoelectric cross section of H^2, L. Motz, W. Rarita—271
Radiation field of electron, F. Bloch, A. Nordsieck—54
Scattering of neutrons by deuterons, L. I. Schiff—149
Shape of Compton line, B. Hicks—436
Virial theorem, molecular and metallic eigenfunctions, J. O. Hirschfelder, J. F. Kincaid—658
Wave functions for large arguments, J. A. Wheeler—1123
Mechanics, quantum—of solid bodies
Conductivity of monovalent metals, J. Bardeen—246(A); 688
Electronic levels in insulating crystals, G. H. Wannier—191
Energy bands in body-centered lattice, M. I. Chodorow, M. F. Manning—731
Energy bands of crystals, C. Herring—361; 365
Test of cellular method in solids, W. Shockley—866
Theory of ferromagnetism, J. C. Slater—198
Mechanics, statistical
Quantum measurements and role of uncertainty relations, W. M. Elsasser—987
Meteorology
Camera for lightning studies, E. J. Workman, R. E. Holzer—256(A)
Ions in afterglow, J. Kaplan—254(A), 257(A)
Magnetic storms, ultraviolet light theory, A. G. McNish—155; 762(L)
Methods and instruments
Afterglow tubes, J. Kaplan—254(A)
Air-driven ultracentrifuge, W. G. Wyckoff, J. B. Lagsdin—254(A)
α-Particle counting, R. D. Evans, C. Goodman—255(A)
Blood flow measurements, J. F. Herrick, E. J. Baldes—244(A)
Camera for lightning studies, E. J. Workman, R. E. Holzer—256(A)
Charcoal trap for vapors, P. A. Anderson—257(A)
Collection of ions, A. H. Heatley—235
Cyclotron with homogeneous field, V. N. Rukavichnikov—1077(L)
Deuteron source, N. E. Bradbury, F. Block—256(A)
Dielectric strengths of CCl_2F_2 and SO_2, C. M. Hudson, L. E. Hoisington, L. E. Royt—664(L)
Efficiency of counters and counter circuits; A. E. Ruark, F. E. Brammer—322; 885(L)
Fiber in wood pulp, E. W. Greenfield—245(A)
Focusing x-ray spectrometer, S. T. Stephenson—255(A)
G-M counters, reliability of, O. S. Duffendack, H. Lifschutz, M. M. Slawsky—1?31
Magnetic field of bundle of wires, C. G. Dunn, G. L. Clark—1167
Magnetic field strength determination, F. T. Rogers, Jr.—381(L)
Magnetic focusing of ions, H. A. Straus—128
Maximum energy from cyclotron, H. A. Bethe, M. E. Rose—1254(L)
Neutron generator, W. H. Zinn, S. Seely—919
Po sources, W. R. Kanne—380(L)
Positive ion source, W. H. Zinn—655
Sharp lines for comparison in stellar photography, F. H. Spedding—137(L)
Spectroscopy in agriculture, S. S. Ballard—253(A)
Temperature from band spectra, H. P. Knauss, M. S. McCay—1143
Thin-film lubrication, S. M. Skinner—244(A)
Twin sources of thermal neutrons, G. J. Thiessen, E. L. Harrington—256(A)
Mobility of ions (see **Ions, mobility**)
Molecular structure and constants (see also **Spectra, molecular**)
Double bond C force constant, L. G. Bonner, R. Hofstadter—249(A)
Interatomic distances of alkali halides, L. R. Maxwell, S. B. Hendricks, V. M. Mosley—968

Nucleus (see also **Disintegration of Nucleus**)
Stability, α-particle disintegration, L. Landau—1251(L)
Neutrino (see also **Radioactivity**)
Electrodynamic force equation; existence of neutrino, W. F. G. Swann—387
Neutrons
Absorption coefficients, C. T. Zahn—67; O. Laporte—72
Absorption limit in Cd, J. G. Hoffman, M. S. Livingston—1228
From H^2-H^2 reaction, R. Ladenburg, M. H. Kanner—911; 1255(L)
Generator utilizing H^2-H^2 reaction, W. H. Zinn, S. Seely—919
Inelastic scattering, G. T. Seaborg, G. E. Gibson, D. C. Grahame—408
Magnetic moment, sign, P. N. Powers, H. Carroll, H. Beyer, J. R. Dunning—38(L)
Magnetic scattering, M. D. Whitaker—384(L)
From $N-H^2$ reaction, W. E. Stephens, K. Djanab, T. W. Bonner—1079
Properties at low temperature, W. F. Libby, E. A. Long—592
Proton-proton and proton-neutron interactions, G. Breit, J. R. Stehn—396
Scattering cross section, A. C. G. Mitchell, R. N. Varney—282
Scattering by ortho- and parahydrogen, J. Schwinger, E. Teller—286; J. R. Dunning, F. G. Brickwedde, S. H. Manley, H. J. Hoge—1076(L)
Spin of, J. Schwinger—1250(L)
Twin sources of thermal neutrons, G. J. Thiessen, E. L. Harrington—256(A)

Nuclear moments and spin (see also **Hyperfine structure**)
Of Ba, A. N. Benson, R. A. Sawyer—1127
Erratum: Magnetic moment of K^{39}, H. C. Torrey—30
Magnetic moment of H^1, L. A. Young—138(L); I. Estermann, O. C. Simpson, O. Stern—535
Methods used in nuclear calculations; validity of, D. T. Warren, H. Margenau—1027
Of neutron, J. Schwinger—1250(L)
Quadrupole moment of In^{115}, R. F. Bacher, D. H. Tomboulian—836
Similarity of particles, O. Halpern, E. Gwathmey—944
Nucleus (see also **Disintegration of nucleus**)
Binding energies by statistical method, E. Feenberg—758
Exclusion principle, neutron-proton pattern, W. D. Harkins—39(L)
Field associated with heavy particles, W. H. Barkas—1074(L)
Field theory of interaction, N. Kemmer—906
K electron capture, L. W. Alvarez—134(L)
Light nuclei described by resonating group structure, J. A. Wheeler—1107
Molecular viewpoint, J. A. Wheeler—1083
Normal states, three- and four-body systems, H. Margenau, D. T. Warren—790
Nuclei and electromagnetic radiation; interaction, A. J. F. Siegert—787
Proton-proton and proton-neutron interactions, G. Breit, J. R. Stehn—396
Relativistic effects for H^2, S. Share, G. Breit—546
Saturation property of nuclear forces, E. Feenberg—667(L)
Statistics and nuclear reactions, V. Weisskopf—295
Wave functions for large arguments, J. A. Wheeler—1127

Optical constants and properties
Diffraction by supersonic waves in solids, H. Mueller—223
Index of methane in infrared, R. Rollefson, R. J. Havens—249(A)
Spectrum of water; absorption and refraction 5 to 20 cm waves, H. W. Knerr—1054
Optical theory
Interference of multipole radiation, O. Halpern, F. W. Doermann—937
Optical activity, theory of, E. U. Condon, W. Altar, H. Eyring—254(A)

Photoelectric effect and properties; cells
Cross section of H^2, L. Motz, W. Rarita—271
Effect of temperature, R. J. Cashman—246(A); 512
Energy distribution of electrons from *K* films, C. L. Henshaw—854
Energy distribution from Na, C. J. F. Overhage—1039
Nuclear effect at high energies, F. Kalckar, J. R. Oppenheimer, R. Serber—273
Sensitization of Al, L. P. Thein—245(A)
Surface effect, W. V. Houston—1047
Photoionization
γ-ray ionization in air, J. W. Broxon, G. T. Merideth—252(A)
Ionization in gases, high pressure and high fields, J. Clay—143
Plasmoidal discharges (see **Discharge of electricity in gases**)
Protons
Proton-proton and proton-neutron interactions, G. Breit, J. R. Stehn—396

Quantum mechanics (see **Mechanics, quantum**)

Radiation
Of electron, F. Bloch, A. Nordsieck—54
From electrons moving in a medium with velocities exceeding c/n, P. A. Čerenkov—378(L)
Radio
Space and surface waves, K. A. Norton—132(L)
Radioactivity (see also **Disintegration of nucleus**)
β-ray from Mn^{56}, R. H. Bacon, E. N. Grisewood, C. W. van der Merwe—668(L)
β-rays of RaE, J. S. O'Conor, S. J.—303
Of Br; isomeric forms, A. H. Snell—1007
Of Co, J. R. Risser—768
Distribution of lifetimes, M. E. Nahmias—666(L)
Of element 43, B. N. Cacciapuoti, E. Segrè—1252(L)
Of Ga^{68} and Ga^{66}, W. B. Mann—405
γ-rays of Rd In and Rd Mn, A. C. G. Mitchell, L. M. Langer—137(L)
Of In, J. L. Lawson, J. M. Cork—531
Induced in Cr, Co, Zn, Cu and As, W. J. Henderson, L. N. Ridenour—40(L); 139(L); 889
Induced by high energy neutrons, M. L. Pool, J. M. Cork, R. L. Thornton—239
Isotopes of Sb, J. J. Livingood, G. T. Seaborg—135(L)
Isotopes of Mn, Fe, and Co, J. J. Livingood, F. Fairbrother, G. T. Seaborg—135(L)
Isotopes of Pd and Ag, J. D. Kraus, J. M. Cork—763
Luminescence excited in glasses, B. E. Cohn—254(A)
Of noble metals; neutron-induced, E. McMillan, M. Kamen, S. Ruben—375
Po sources, W. R. Kanne—380(L)
Positron-electron emitting isomers, M. L. Pool, J. M. Cork, R. L. Thornton—380(L)
Of K^{42}, H. J. Walke—663(L)
Range of α-particles, G. H. Henderson, G. C. Laurence—46
Sargent curves, A. C. G. Mitchell—1
Of Sc^{42} and Sc^{44}, H. Walke—400; 669
Of Na^{22}, L. J. Laslett—529
Of Sr and Y, D. W. Stewart, J. L. Lawson, J. M. Cork—901
Of Ti and V, H. Walke—777
Range of particles
Of α-particles from Th, G. H. Henderson, G. C. Laurence—46
Of protons in Al and air, D. B. Parkinson, R. G. Herb, J. C. Bellamy, C. M. Hudson—75; 247(A)

Relativity
Null result of the Michelson-Morley experiments, W. B. Cartmel—250(A)
Relativistic effects for H^2, S. Share, G. Breit—546

Scattering of electrons, neutrons, and ions (see also **Electrons, scattering of; Electron diffraction**)
Collision of H^1 and H^2, K. Ochiai—1221
Electrons in He, M. Goodrich—259
Fast electrons in H_2, A. L. Hughes, S. S. West—43
Of high energy electrons, J. J. Turin, H. R. Crane—63; 610
Inelastic scattering of neutrons, G. T. Seaborg, G. E. Gibson, D. C. Grahame—408
Long range forces and neutron-proton, S. S. Share, J. R. Stehn—48
Magnetic scattering of neutrons, O. Halpern, M. H. Johnson, Jr.—52
Neutron scattering cross section as a function of energy, A. C. G. Mitchell, R. N. Varney—282
Of neutrons in Co, N. E. Bradbury, F. Bloch, H. Tatel, P. A. Ross—1023
Of neutrons by deuterons, L. I. Schiff—149
Of neutrons by Fe, R. F. Bacher—248(A)
Of neutrons; cross sections, R. Ladenburg, M. H. Kanner—911; 1255(L)
Of neutrons in liquid ortho- and parahydrogen, J. Halpern, I. Estermann, O. C. Simpson, O. Stern—142(L); J. R. Dunning, F. G. Brickwedde, S. H. Manley, H. J. Hoge—1076(L)
Of neutrons, magnetic, M. D. Whitaker—384(L)
Of neutrons by magnetic dipoles, O. Halpern, M. H. Johnson—248(A)
Of neutrons by ortho- and parahydrogen, J. Schwinger, E. Teller—286
Of neutrons by protons, T. W. Bonner—685
Of K ions in heavy gases, A. G. Rouse—1238
Proton-deuteron and neutron-deuteron scattering, H. Primakoff—1000
Of protons by neutrons, P. G. Kruger, W. E. Shoupp, P. W. Stallmann—678

Secondary electrons (see **Electrons, secondary**)

Shot effect
Of electrons from Ni and Be, B. Kurrelmeyer, L. J. Hayner—952

Solid state (see **Crystalline state**)

Specific heat
Of W, W. C. Michels—1067

Spectra, absorption
Of CO; Cameron bands ($^3\Pi - {}^1\Sigma$), L. Gerö, G. Herzberg, R. Schmid—467
Of HCl in solvents; infrared, W. Gordy, P. G. Martin—1075(L)
Of Mn and Ag in Schumann region, F. W. Paul—923
Of propene and allene, L. G. Bonner, R. Hofstadter—249(A)
Of Rb_2, Ny Tsi-Zé, Tsien San-Tsiang—91
Of $Tm_2(SO_4)_3 \cdot 8H_2O$, H. A. Bethe, F. H. Spedding—454
Of water at 1.79 μ, J. R. Collins—88

Spectra, atomic
Levels of Ne and A, J. B. Sampson—1157
Of Ce II, W. E. Albertson, G. R. Harrison—1209
Of Ce III, H. N. Russell, R. B. King, R. J. Lang—456
Coupling of p configurations, H. A. Robinson, G. H. Shortley—713
Of Cr III, Cr IV, Mn IV and Fe V, I. S. Bowen—1153
Of Cr VI, Mn VII and Fe VIII; ultraviolet, P. G. Kruger, S. G. Weissberg—314
Of He, doubly excited, F. P. Bundy—452
Levels of Ne and A, calculated, J. B. Sampson—1157
Of Rb, pressure effects, Ny Tsi-Zé, Ch'en Shang-Yi—1158
Of Sm I, W. Albertson—644
Of Sc VI and Sc VII, P. G. Kruger, H. S. Pattin—621
Of Sc VIII and Sc IX, P. G. Kruger, L. W. Phillips—97
Of S, K, and Ca, H. A. Robinson—724
Of Sn II, W. W. McCormick, R. A. Sawyer—249(A)
Of W I, O. Laporte, J. E. Mack—249(A); 254(A)

Spectra, general
Applications in agriculture, S. S. Ballard—253(A)
Interferometer wave-lengths of H_2, R. G. Lacount, R. E. Hodgdon—98
Light of night sky, J. Kaplan—1252(L)
Magnetic rotation spectra of molecules, T. Carroll—822
Pressure effects in K vapor, D. S. Hughes, P. E. Lloyd—1215
Pressure shift, H. Kuhn—133(L)
Pressure shifts of Kr lines, H. Margenau, W. W. Watson—384(L)
Sharp lines for comparison in stellar photography, F. H. Spedding—137(L)
Spectrum of water; absorption and refraction 5 to 20 cm waves, H. W. Knerr—1054
Temperature from band spectra, H. P. Knauss, M. S. McCay—1143
Unidentified interstellar lines, P. W. Merrill—761(L)

Spectra, molecular (see also **Molecular structure and constants**)
Of NH_2 vibration bands, E. F. Barker—250(A)
Of As_2, G. D. Kinzer, G. M. Almy—814
Of BeH and BeH^+, ultraviolet, W. W. Watson, R. F. Humphreys—318
Of C_2, J. G. Fox, G. Herzberg—638
Determination of rotational quantum numbers, L. A. Turner, W. T. Harris—630
Far infrared of water vapor, H. M. Randall, D. M. Dennison, N. Ginsburg, L. R. Weber—160
Of H_2 in He, N. D. Smith—728
Of HD and D_2, G. H. Dieke, M. N. Lewis—100
Of MgH, ultraviolet, L. A. Turner, W. T. Harris—626
Of N_2^+ and CO^+, excitation functions, F. P. Bundy—698
Of AgCl, F. A. Jenkins, G. D. Rochester—1141
Of SbCl, I. Hudes—1256(L)
Of SnF, F. A. Jenkins, G. D. Rochester—1135
Of TiCl, K. R. More, A. H. Parker—1150
Of ZnH^+, J. W. Gabel, R. V. Zumstein—726

Standards (see **Constants, physical**)

Statistical mechanics (see **Mechanics, statistical**)

Superconductivity (see **Electrical conductivity and resistance**)

Thermionic emission of electrons; Emitting surfaces
Contact potential of Ba and Mg, P. A. Anderson—253(A)
Thermionic emission of positive ions
From Mo; work function, H. Grover—982

Work function (see **Thermionic emission; Photoelectric effect**)

Viscosity
Of air, W. V. Houston—751

X-rays, diffraction, scattering, reflection, refraction and polarization
Compton effect; time lag, R. S. Shankland—414
Electron asymmetry in Zn, G. E. M. Jauncey, E. M. McNatt—256(A)
Fringe, systems, plane slits, A. E. Smick, P. Kirkpatrick —256(A)
Grating space of barium-copper-stearate films, C. Holley, S. Bernstein—525(L)
Patterns from magnetostriction oscillators, G. W. Fox, H. T. Hurley—1077(L)
Radiation doubly scattered, P. Kirkpatrick—1201
Shape of Compton line, B. Hicks—436
Structure and shift of Compton line, J. W. M. DuMond, H. A. Kirkpatrick—419
Total scattering from a crystal, G. G. Harvey—248(A)
X-rays, emission (see also **X-rays, spectra and spectroscopy, etc.**)
Intensity variation with tube voltage, G. H. Bancroft—6
X-rays, spectra and spectroscopy, wave-length measurements (see also **X-rays, emission**)
Two crystal reflections, resolving power, notation, J. W. M. DuMond—872; S. K. Allison—884(L)
Vertical divergence, R. C. Spencer—761(L)
X-rays, tubes, apparatus
Focusing x-ray spectrometer, S. T. Stephenson—255(A)

Zeeman effect
Of rare gases, J. B. Green—736

DEC 27 1937

THE PHYSICAL REVIEW

VOLUME 52 *Second Series* NUMBER 12

DECEMBER 15, 1937

Published for the

AMERICAN PHYSICAL SOCIETY

by the

AMERICAN INSTITUTE OF PHYSICS
Incorporated

LANCASTER, PA., AND NEW YORK, N. Y.

CONTENTS

PHYS. REV. 52 (1937) DECEMBER 15

Double Scattering of Polarized X-Rays . . . . . PAUL KIRKPATRICK 1201

Preliminary Analysis of the First Spark Spectrum of Cerium—Ce II . . . . . WALTER E. ALBERTSON AND GEORGE R. HARRISON 1209

Pressure Effects of Homogeneous K Vapor in Absorption . . D. S. HUGHES AND P. E. LLOYD 1215

Collision of Proton and Deuteron . . . . . K. OCHIAI 1221

Indication of a Genetic Relation Between Indium and Tin . . . . . E. D. EASTMAN 1226

Neutron Absorption Limit in Cadmium . . J. G. HOFFMAN AND M. STANLEY LIVINGSTON 1228

Production, Characteristics, and Reliability of Geiger-Müller Counters . . . . . O. S. DUFFENDACK, H. LIFSCHUTZ AND M. M. SLAWSKY 1231

Large Angle Scattering and Energy Loss of Potassium Ions Scattered by Heavy Monatomic Gases . . . . . ARTHUR G. ROUSE 1238

Paramagnetic Measurements at Low Fields with the Rankine Balance . HAIG P. ISKENDERIAN 1244

Effect of Tension on the Electrical Resistance of Single Tetragonal Tin Crystals . . . . . MILDRED ALLEN 1246

Letter to the Editor:

On the Spin of the Neutron . . . . . JULIAN SCHWINGER 1250
Does the Formula for the Rydberg Constant Require Revision? . . . . JESSE W. M. DUMOND 1251
Stability of Neon and Carbon with Respect to α-Particle Disintegration . . . . . L. LANDAU 1251
Light of the Night Sky . . . . . JOSEPH KAPLAN 1252
Origin of Cosmic Rays . . . . . M. C. HOLMES 1252
Radioactive Isotopes of Element 43 . . . . . B. N. CACCIAPUOTI AND E. SEGRÈ 1252
On Sidereal Diurnal Variation in Cosmic-Ray Intensity . . . . . S. E. FORBUSH 1254
Maximum Energy Obtainable from the Cyclotron . . . . . H. A. BETHE AND M. E. ROSE 1254
On the Scattering Cross Section of Fast Neutrons by Hydrogen . . . . . RUDOLF LADENBURG AND MORTON H. KANNER 1255
Possible Origin of the *X* Particle . . . . . G. E. M. JAUNCEY 1256
Band Spectrum of Antimony Chloride . . . . . I. HUDES 1256
On Supraconductivity . . . . . C. J. GORTER 1256

Author Index to Volume 52 1258

Analytic Subject Index to Volume 52 1266

LANCASTER PRESS, INC., LANCASTER, PA.